Ci-TCF Gene Function and Its Involvement in *Ciona intestinalis* Pigment Cell Differentiation

Thesis

Ci-TCF gene function and its involvement in *Ciona intestinalis* pigment cell differentiation

A thesis submitted to the Open University, UK for the degree of

DOCTOR OF PHILOSOPHY

By

FATEEMA PARVEEN

Sponsoring Establishment:

STAZIONE ZOOLOGICA ANTON DOHRN

NAPOLI, ITALY

November 2009

ProQuest LLC.
789 East Eisenhower Parkway
P.O. Box 1346
Ann Arbor, MI 48106 – 1346

This thesis work has been carried out in the laboratory of Dr Antonietta Spagnuolo,

at the Stazione Zoologica Anton Dohrn in Napoli, Italy

Director of studies: Dr. Antonietta Spagnuolo (Stazione Zoologica, Napoli, Italy)

External Supervisor: Dr. Detlev Arendt (EMBL, Heidelberg, Germany)

ABSTRACT

Transcription factors of T cell factor (TCF) family have been identified in a wide range of organisms, from hydra to mammals, where they play important roles during embryonic development. As a terminal nuclear component they mediate the canonical Wnt signaling cascade by their context dependent transcriptional regulatory properties. The TCF protein family in *Ciona intestinalis* is represented by a single member, named *Ci-TCF*, whose zygotic expression has been observed in pigment precursor cells as well as in palp precursors. Ascidians occupy a strategic position in the phylogeny and thus provide a useful model system to study developmental processes difficult to approach in more complex organisms.

I aimed to better clarify the role played by *Ci-TCF* specifically in pigment cell differentiation in *Ciona*. To this end I exploited targeted interference with *Ci-TCF* function. I used an enhancer specific for pigment cell lineage to drive the expression of a dominant negative form of *Ci-TCF*. From this study it was possible to deduce that *Ci-TCF* is effectively involved in the terminal differentiation of pigment cells in sensory organs.

Simultaneously, my project was also focused on the regulatory factors controlling the precise spatio-temporal activation of *Ciona TCF* gene in pigment lineage. Analysis of the *cis*-regulatory region of *Ci-TCF* gene was performed through a series of constructs containing various *Ci-TCF* 5' promoter fragments fused to a reporter gene. This study allowed me to characterize a region of 400 bp in *Ci-TCF* enhancer element which was able to drive reporter gene expression in pigment cells of *Ciona*. In silico analysis of this *cis*-regulatory region revealed the possible involvement of Ets transcription factors governing the tissue specific expression of *Ci-TCF* at the right time. The data was further

confirmed by detailed *in vivo* and *in vitro* studies, through mutational assay and EMSA (Electrophoretic mobility shift assay), respectively. My study therefore led to the identification of Ets factors as the first upstream regulator of a *TCF* representative. Since Ets transcription factors are activated via MAP kinase pathway which is triggered by FGF signaling, the present study provides clues for a crosstalk between the Wnt and FGF signaling cascades during pigment cell differentiation in *Ciona intestinalis.* This finding is noteworthy, since up to now all the data on *TCFs* have concerned their function as effectors of Wnt signaling. No explanations have been reported so far as to why and how TCF factors are present at the right time and in the right place to play their role downstream from Wnt. So, my study gives a first answer to this question and represents a first step toward a better understanding of the regulation of *TCFs* expression.

LIST OF CONTENTS

LIST OF FIGURES

LIST OF TABLES:

LIST OF ABBREVIATIONS

aa	Amino acid
ANESEED	Ascidian Network for in Situ Expression and Embryological Data
A/P	anterior/posterior
AP	Alkaline phosphatase
APC	Adenomatous polyposis coli
ATP	Adenosine triphosphate
BCIP	5-bromo-4-chloroindol-3-indolyl phosphate
bFGF	basic Fibroblast Growth Factor
βγ	Beta gamma
BMP	Bone Morphogenetic Protein
bp	Base pair
BSA	Bovine serum albumin
°C	Celsius degree
CAD	Context-dependent activation domain
CBP	CREB binding protein
cDNA	Complementary DNA
CDS	Coding sequence
Ci	Curie
CIAP	Calf Intestinal Alkaline Phosphatase
cm	centimetre
CNS	Central Nervous System
CRD	Context-dependent Regulatory Domain
CTP	Cytidine triphosphate
DAG	diacylglycerol
dATP	Deoxyadenosine triphosphate
DBD	DNA binding domain
dCTP	Deoxycytidine triphosphate
Dct	dopachrome tautomerase gene
DEPC	Diethylpyrocarbonate
dGTP	Deoxyguanosine triphosphate
Dig	Digoxigenin

DMSO	Dimethylsulfoxide
DNA	Deoxyribonucleic Acid
DNase	Deoxyribonuclease
dNTP	Deoxyribonucleoside triphosphate
DTT	Dithiothreitol
dTTP	Deoxytimidine triphosphate
D/V	Dorsal/Ventral
Dsh	Dishevelled
EBS	Ets binding site
EDTA	Ethylene-diaminetetraacetic acid
EMSA	Electrophoretic mobility shift assay
ERK	Extracellular signal-regulated kinase
et al.	et altera
EtBr	Ethidium Bromide
ETS/Ets	E twenty six
F	Forward
FACS	Fluorescence Activated Cell Sorting
FGF	Fibroblast growth factor
FGFR	Fibroblast growth factor receptor
Fig	Figure
Fz	Frizzled
GDP	Guanosine diphosphate
GFP	Green fluorescent protein
GSK3β	glycogen synthase kinase 3β
GTP	Guanosine triphosphate
HAT	Histone acetyltransferase
HDAC	Histone deacetylase-1
Hdl	Headless
HMG	High mobility group domain
HRP	Horseradish peroxidase
JNK	C-Jan N-terminal Kinase
Kb	Kilobase pairs
L	Liter
LB	Luria-Bertani broth

LEF	Lymphoid enhancer factor
LRP5/6	Low-density-lipoprotein-related protein 5/6
M	Molar
MAPK	Mitogen activated protein kinase
Mbp	Megabase pair
mCherry	Monomeric Cherry
MEK	Mitogen-activated protein kinase kinase
µF	Micro Farade
MFSW	Millipore-Filtered Sea Water
µg	Microgram
Mg	Milligram
Mitf	Microphthalmia transcription factor
µl	Microliter
ml	Milliliter
µm	Micrometer
mM	Millimolar
MOPS	3-(N-Morpholino) propanesulfonic acid- 4-Morpholinepropanesulfonic acid
mRNA	Messenger RNA
msecond	millisecond
NBT	Nitroblue tetrazolium
ng	Nanograms
NLS	Nuclear Localization Signal
nm	Nanometer
OU	Outer segment
PBS	Phosphate-buffered saline
PBT	Phosphate-buffered saline plus Tween 20 (0.1%)
PCP	Planar Cell Polarity
PCR	Polymerase chain reaction
pH	Potentium hydrogenii
PKC	Protein Kinase C
Pmol	Picomole
PNK	Polynucleotide kinase

PP2A	Protein phosphatase 2A
pTyr	Tyrosinase promoter
qPCR	Quantitative PCR
R	Reverse
R/L	Right/Left
RNA	Ribonucleic acid
RNase	Ribonuclease
RPE	Retinal Pigmented Epithelium
Rpm	Rotations per minute
RT	Room temperature
SDS	Sodium dodecyl sulphate
SSC	Standard saline citrate
TCF	T cell factor
TBE	Tris Borate EDTA
TLCs	Trunk lateral cells
Tris	Tris-(hydroxymethyl)aminoethane
tRNA	Transfer RNA
TLE	Transducin-like enhancer of split
TVCs	Trunk ventral cells
Tyr	Tyrosinase
Tyrp1	Tyrosinase Related Protein-1
Tyrp2	Tyrosinase Related Protein-2
U	Unit (enzymatic activity)
U0126	1,4-diamino-2,3-dicyano-1,4-bis[2-aminophenylthio]butadiene
UTP	Uridine triphosphate
UTR	Untranslated region
UV	Ultraviolet
V	Volt
WMISH	Whole Mount in Situ Hybridization
WRE	Wnt-response element
W.T.	Wild type

PREFACE

This thesis is the result of my PhD study which was conducted between January, 2007 to October, 2009 at the Cell and Developmental Biology Laboratory at the Stazione Zoologica Anton Dohrn in Naples.

The thesis contains five chapters. The first chapter, Chapter 1; is a general introduction to the topic of the thesis. Chapter 2 contains a detailed description of the materials and experimental procedures used during this study. Chapter 3 presents the evolutionary analysis of *TCF*/LEF protein family members from different organisms in brief. Chapter 4 describes the results of the experiments explaining the function of *Ci-TCF* in pigment cell formation during *Ciona intestinalis* development as well as the regulatory mechanism of *Ci-TCF* expression. Chapter 5 discusses and summarizes the results obtained and also includes future perspectives.

CHAPTER 1

INTRODUCTION

1.1. *Ciona intestinalis*, the model organism

The ascidian *Ciona intestinalis* is a marine invertebrate chordate belonging to the subphylum Urochordata or tunicata, which includes appendicularians and salps in addition to the ascidians. Urochordata, together with Vertebrata and Cephalochordata belong to the phylum Chordata.

Members of subphylum Urochordata show various degrees of morphological diversity. However, all of them posses the basic chordate features, notably a notochord and a dorsal tubular nerve cord, at least in one phase of their life cycle. Urochordates have been thought, for more than a century, to be the most basal chordate, occupying a key position in the evolutionary tree. Recent phylogenetic analyses of Delsuc and his co-workers, 2006 have revised this assessment and placed tunicates as the closest living relative of vertebrates, where the cephalochordates were previously positioned (Fig. 1 B) (Delsuc et al., 2006). In this light, cephalochordates are seen as the most basal extant chordate while, this issue is somewhat contentious and needs to be further verified. However, the contribution that studies on Urochordate representatives have provided to the understanding of chordate developmental mechanisms is invaluable.

Among the three classes of Urochordata, *C. intestinalis* belongs to the Ascidian class. Most of the chordate characteristics of this animal are exhibited clearly in the larval stage and gradually lost during metamorphosis.

The adult *Ciona sp.* is a simple vase like filter feeder and sessile animal. During their life cycle they produce the motile form only as the tadpole larva which displays its chordate affinities (Fig. 1A, C), a dorsal hollow nerve cord with underlying notochord, firstly discovered by Alexander Kowalenski in 1866. Since then the extremely simplified structure of *Ciona* tadpole fascinated embryologists and molecular biologists to study the chordate development mechanisms using *Ciona* as a model organism.

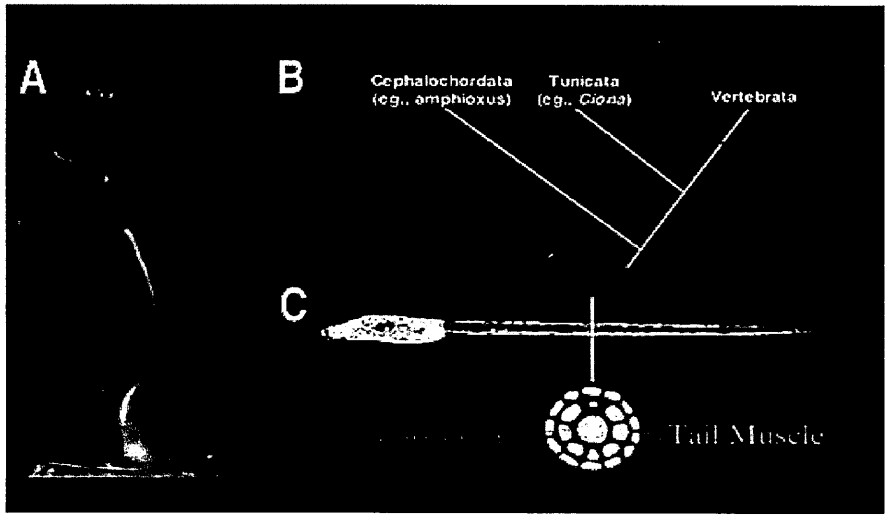

Figure 1.1. *Ciona intestinalis* and its chordate characteristics.
A: Adult *Ciona intestinalis*. B: Current chordate phylogeny. C: Cross section of the tail of *C. intestinalis* larvae representing the basic chordate features; a central notochord overlying with a hollow nervecord surrounded by tail muscule.{adapted from (Davidson et al., 2006)}.

1.1.1 *Ciona intestinalis* as a model

Ascidians were the first metazoan model organisms in which experimental embryology were carried out (Lemaire, 2009). Due to their simple developmental process they have been serving as classic experimental systems for the study of developmental mechanisms for more than a century {reviewed by (Satoh et al., 2003)}. Their unique position in the phylogenetic tree and their compact genome offer them as an elegant model system for the analysis of chordate developmental gene regulation for several reasons. *C.*

intestinalis gamete can be easily collected by surgical extraction. A single animal can produce thousand of embryos and their transparency makes them ideal for live imaging. During development *Ciona* embryos permit detailed visualization of differential gene expression by whole mount *in situ* hybridization. Development is fast, since they reach the larval stage within 18 hours after fertilization at 18°C (Fig.1.2).

The ascidian tadpole consists of only ~2,600 cells, which constitute a small number of organs including the epidermis, the central nervous system (CNS) with two sensory organs (otolith and ocellus), the endoderm, mesenchyme, trunk lateral cells (TLCs) and trunk ventral cells (TVCs), and the notochord and muscle in the tail (Fig.1.4.B). During ascidian embryogenesis the developmental fate is restricted early, between the 64/110 cell stage, when each blastomere is directed to a single specific type of tissue at the larval stage (Fig.1.3). Cloning and characterization of developmental genes indicate that each gene is expressed under discrete spatio-temporal pattern within their lineage (Di Gregorio and Levine, 1998; Satou and Satoh, 1999; Wada and Satoh, 2001; Yasuo and Satoh, 1993). Incorporation of foreign DNA into fertilized eggs is facilitated by introduction of plasmid DNA via an electroporation technique (Corbo et al., 1997). Thus it is possible to transform in a single round, hundreds or even thousands of embryos which develop almost synchronously. This method permits rapid screening of genomic DNA fragments linked to reporter genes with the aim to identify regulatory elements controlling tissue specific gene expression. Microinjection is also possible in fertilized eggs, by which novel functions of conserved chordate developmental genes can be discovered through specific misexpression or knockdown using morpholino antisense nucleotide. Moreover, RNA interference has been recently reported as an efficient tool as a mean of disrupting gene function in Ascidian embryo (Nishiyama and Fujiwara, 2008). The entire lifecycle takes less than three months which favors mutagenic studies and genetic screen in this model (Moody et al., 1999; Nakatani et al., 1999; Sordino et al., 2001). Artificial self-fertilization

allows identification of interesting mutant phenotypes that can be used to identify and map harmful alleles during *Ciona* embryogenesis (Sordino et al., 2008).

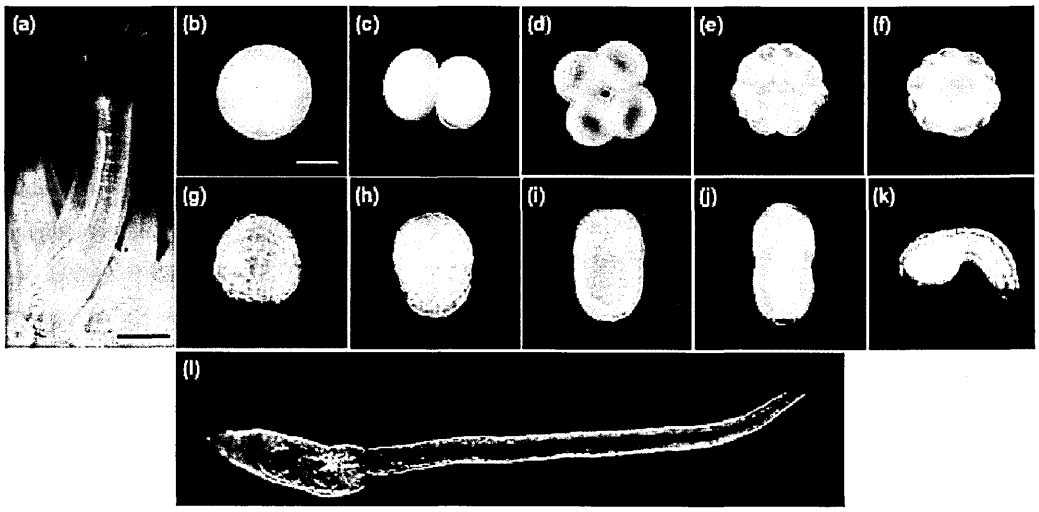

Figure 1.2. Embryogenesis of the sea squirt, *C. intestinalis*.
(A) Adults with incurrent and outcurrent siphons. The white duct is the sperm duct, while the orange duct paralleling it is the egg duct. (B to L) Embryogenesis. (B) Fertilized egg, (C) 2-cell embryo, (D) 4-cell embryo, (E) 16-cell embryo, (F) 32-cell embryo, (G) gastrula (about 150 cells), (H) neurula, (I to K) tailbud embryos, and (L) tadpole larva. Embryos were dechorionated to show their outer morphology clearly {Adapted from (Dehal et al., 2002)}.

1.1.2 Insight into *C. intestinalis* genome organization

Some of the tunicate members contain the smallest bilaterian genomes (Holland and Gibson-Brown, 2003). Up to now the whole genome has been fully sequenced for two tunicates, *C. intestinalis* and *Ciona savignyi*. The draft genome of *C. intestinalis*, sequenced by whole-genome shotgun method, was announced in December, 2002 (Holland and Gibson-Brown, 2003; Satoh et al., 2003). This is the third complete genome sequenced of an invertebrate, after *Caenorabhdetis eleganes* (*C. elegans* Sequencing Consortium, 1998) and *Drosophila* (Adams et al., 2000) genomes, and the first of a non-vertebrate in the deuterostome branch of Metazoa (Holland and Gibson-Brown, 2003). More genome sequences have been completed recently from two non-vertebrate

deuterostomes such as the sea urchin, *Strongylocentrotus purpuratus* (Sodergren et al., 2006) and amphioxus, *Branchiostoma floridae* (Putnam et al., 2008), and from two ascidian species, as *Ciona savignyi* (Vinson et al., 2005) and *Oikopleura dioica* (Seo et al., 2001). The increasing number of sequenced genomes provides a huge opportunity, through comparative analyses, to resolve a number of outstanding evolutionary questions. The total size of *C. intestinalis* genome is only ~153-159 Mb, one-twentieth the size of mouse genome, since the genome organization is very compact, containing one gene in every 5 kb of DNA on average (Dehal et al., 2002). Moreover, the ascidians diverged before the gene duplication event (Holland et al., 1994). The genome contains a total of 15,852 protein coding genes distributed over 14 chromosomes (Satoh et al., 2003). *C intestinalis* genome has been evolving very rapidly (Holland and Gibson-Brown, 2003), sometimes with a loss of intergenic regions together with entire genes, as in the case of some members of Hox gene family (Hox 7, Hox 8, Hox 9, Hox 11) (Spagnuolo et al., 2003). A comprehensive study of *Ciona* genome revealed that ascidians contain, in many cases, a single representative of multiple paralogous vertebrate genes (Dehal et al., 2002). This is the case for many of the gene families involved in developmental signaling and regulatory processes such as, *LEF/TCF* (Arce et al., 2006), *SMAD* or T-box genes (Satoh et al., 2003). This characteristic offers the unique oppurtunity to justify gene function without the genetic redundancy seen in many vertebraes.

Another important advantage of the compact *Ciona* genome is that key *cis*-regulatory DNAs tend to map near the core promoter, within the first 1.5 kb upstream of the transcription initiation site (Corbo et al., 1997; Imai et al., 2002; Takahashi et al., 1999). This feature of the ascidian genome, together with the electroporation method mentioned previously, has made them particularly useful in studies on the function and on the transcriptional regulation of developmental genes.

1.1.3. Development in Ascidian

Ascidians are hermaphrodites, i.e. each individual produces both gametes. This phenomenon provides a better opportunity of reproduction for this sedentary and pelagic mode of life, although some species are partially or totally sterile upon self-fertilization (Satoh, 1994). General time for life cycle depends on species which is in *Ciona* less than 3 months. Usually they develop in a relatively short time. Ascidian embryogenesis is very simple and easy to understand (Satoh, 2001). After fertilization an invariant and bilaterally symmetrical cleavage program starts which is quite rapid and the embryos develop in a stereotyped fashion {reviewed in (Lemaire, 2009)}. Each division in the embryo produces cells large enough to be recognizable. So, the developmental stages of early ascidian embryos are named according to the number of cell like 8-, 16-, 32-, 64-, and 110-cell stages, instead of the morula and blastula stages (Fig.1.2) (Satoh, 2001). Moreover, each blastomere is distinguishable with specific and predictable lineage and is named according to Conklin, 1905 which was a real boon to the embryologist. Gastrulation starts at only 110 cell stage within which cell fates of most blastomeres have already become restricted to a specific tissue type (Lemaire et al., 2008). So, each type of tissue can be traced back at the cell level in the early embryo (Fig.1.3).

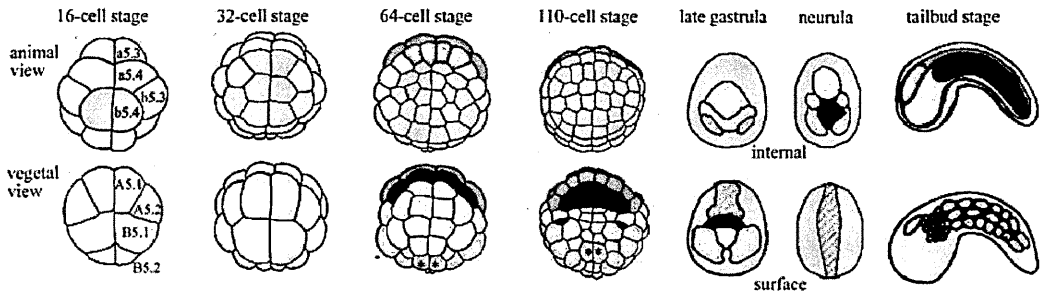

Figure 1.3. Developmental fates in the ascidian embryo. Schematic representation of ascidian embryos. Blastomeres whose developmental fate is restricted to one tissue are in color: yellow, endoderm; orange, mesenchyme; light blue, muscle; dark blue, notochord; green, epidermis; pink, nerve cord; red, nervous system, blastomeres marked with asterisks give rise to muscle and trunk ventral cells {Adapted from (Imai et al., 2004)} Mainly based on data obtained in *Halocynthia* by Nishida (Nishida, 1987).

Tadpole larva:

In about 24 hours of fertilization the non feeding swimming larvae hatch out at 18°C (Satoh, 1994) (Fig.1.4 A). *C. intestinalis* larva is composed of surprisingly low number of cells, approximately 2600, which constitute a small number of larval organs including the epidermis, central nervous system (CNS), notochord and tail muscle (Fig.1.4B). Beside that, rudiments of some adult organs such as, gut, mesodermal organs and gonads, are also present.

In *C .intestinalis*, the notochord is made up of 40 cells arranged in a single column which is surrounded by 30 muscle cells in tail region. There are ~800 epidermal cells, ~500 endodermal cells and ~900 mesenchymal cells, which later give rise to most of the adult tissues (Satoh, 1994), while the CNS contains less than 130 neurons and 230 glial cells (Imai *et al* 2007).

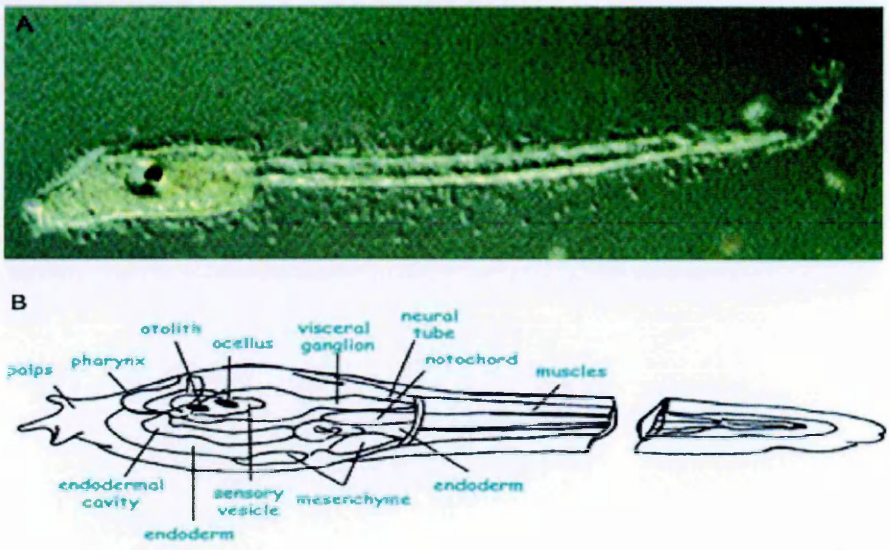

Figure 1.4. *Ciona intestinalis* larva. A: The swimming planktonic larva of the ascidian *C. intestinalis*. B: Graphic representation of the larval body territories showing different types of larval tissues. The larval CNS is formed by an anterior sensory vesicle, connected by a neck to the visceral ganglion, which proceeds as a neural tube extending along all the tail {Adapted from (Munro et al., 2006).

At the rostral end the larvae bear some adhesive papillae through which they attach themselves to a suitable substrate and start metamorphosis usually within few hours of hatching. It takes 2 or 3 months for the juvenile to become adult with reproductive capability depending on the temperature of the environment (Satoh 1994).

1.2.1. Pigment cells in Ascidians

The central nervous system of Ascidian tadpole is composed of an anterior sensory vesicle in the trunk, followed by a visceral ganglion and a caudal nerve cord. The sensory vesicle is a hollow cavity which on the basis of morphology and expression of marker genes has been considered the homolog of the vertebrate prosencephalon and mesencephalon (Wada et al., 1998). The large sensory vesicle of CNS contains two melanin containing pigmented structures, the anterior otolith or statocyte, and the posterior ocellus; both of them contribute to the swimming behaviour of the tadpole (Fig.1.5 A). The otolith lies on the ventral floor of the cerebral vesicle connected by a narrow stalk and functionally works as a gravity receptor, while the ocellus is positioned at the posterior right wall of the vesicle and is involved in light perception.

The otolith is a single-cell organ. Apart from the nucleus the cell body of otolith contains a large single spherical mass of pigment granule measuring about 10-15 μm in diameter (Sakurai et al., 2004). Electron microscopy showed that two dendrites connect the otolith body to the sensory cavity and through their deformation, caused by the movement of pigment granule into the cell body, they supply gravity information to the animal (Ohtsuki, 1991; Torrence 1986). The presence of relatively high concentration of metal elements such as, K, Ca, Zn in the otolith pigment mass also contributes to the gravity maintenance of the larvae. By laser ablation experiment Tusda and his coworkers, 2003 demonstrated that otolith controls the upward swimming behavior of the tadpole hence, working as a statocyte in gravity response (Tsuda et al., 2003).

Unlike the otolith, ocellus bears a more complex structure. It is a multicellular organ and is composed of three parts: a single cup-shaped pigment cell which, unlike otolith, contains around hundred tiny pigment granules, 3 lens cells, and about 30 photoreceptor cells in *C. intestinalis*. The number of photoreceptor cell varies depending on the species (Horie et al., 2005) (Fig. 1.5 B). Unlike the vertebrate melanosomes, the membrane bounded pigment granules of ascidian pigment cells lack elaborate fibrous matrix structures {Reviewed by (Sato and Yamamoto, 2001)}

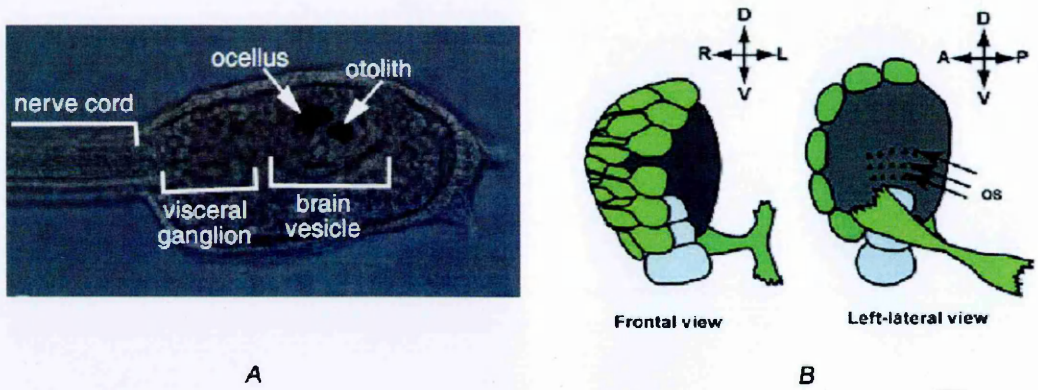

Figure 1.5. Sensory organs of *Ciona intestinalis*.
(A) The regional subdivisions of CNS of larva focusing the larval sensory organs a dapted from (Kusakabe and Tsuda, 2007). (B) Ocellus graphical representation. The ocellus sensory organ is composed of three parts: photoreceptor cells (green), pigment cell (gray), lens cells (pale blue). A: Frontal view. B: Left-lateral view. OS: photoreceptors' outer segments. Adapted from (Horie et al., 2005).

From highly magnified confocal microscopic image it was revealed that the cell bodies of the ocellus photoreceptor cells are grouped into two lobes and cover the ocellus pigment cell on the right-lateral side (Horie et al., 2005). The lens cells are located between photoreceptor cell and pigment cell.

The visual system is remarkably simple in ascidians but surprisingly it possesses some similarities to vertebrate eyes. The orientation of lens and photoreceptor cells in vertebrate RPE (Retinal Pigmented Epithelium, see later) is comparable with that of the ascidian light sensing organ. Moreover, the location and organization of the pigment cup of ocellus and the photoreceptor cells in the sensory vesicle are similar to those of the

retinal pigment epithelium (RPE) and photoreceptor cells in vertebrate retina (Horie et al., 2008). The angle of passing light through the lense cells in the vertebrate eye is controlled by the eye socket and the RPE provides the shield for the photoreceptor cells from light coming from inappropriate direction. In ascidian larva this function is achieved by the cup shaped pigment cell (ocellus) which surrounds the outer segment of the photoreceptor cells and thus restricts the traveling light intake to a single direction. In this way the larvae can sense the direction of light. Furthermore like vertebrate retinal photoreceptors, the photoreceptor cells of ocellus sensory organ are ciliary and hyperpolarized photoreceptors (Eakin and Kuda, 1971; Gorman et al., 1971).

1.2.2. Pigment cell in vertebrates

Pigmentation biology has been studied since the beginning of 18th century which has already provided useful information concerning the intersection of evolution, genetic and developmental biology (Hoekstra, 2006).

In vertebrates melanin is produced in specialized pigment cells and takes part in a variety of functions including visual acuity, camofluage, sexual display and protection from ultra violet (UV) radiation. Pigment cells are characterized by a specialized lysosome related organelle, melanosome. The pivotal function of melanosome is to biosynthesis and storage of melanin pigment. (Marks and Seabra, 2001)

In vertebrates the melanin producing cells are represented by three types of pigment cells that have distinct developmental origins.

The retinal pigment epithelium (RPE) is a multifunctional and indispensable component of the vertebrate eye, originates from the outer layer of the optic cup protruding from the developing diencephalon (Sato and Yamamoto, 2001).

The melanocytes or melanofores of the skin, hair follicle, inner ear, coroid, iris and the ciliary body originate from the neural crest (Sato and Yamamoto, 2001).

The 3rd type of pigment cell found in the pineal organ is formed from the dorsal part of the developing forebrain (Sato and Yamamoto, 2001).

The different types of pigment cells found in vertebrates play a variety of roles in organisms. For example, melanocytes of the skin, hair root or feather provide protection from UV radiation. Moreover, they are also involved in camofluage and mating coloration.

The RPE is a layer of pigment cells located between the endothelium of the choriocapillaris and the outer segments of photoreceptors. The RPE is a fundamental component of the vertebrate eyes where it exerts a number of important functions. It is assigned to absorb the straight light coming to the eye, preserving the overlying photoreceptor cells (Jeffery, 1997); it transports ions, water, and metabolites from the subretinal space to the blood (Hamann et al., 1998; Marmor, 1999; Miller and Edelman, 1990; Steinberg, 1985) and brings catabolites in the opposite direction. Furthermore, the RPE is involved in retinoid metabolism and in the renewal of the photoreceptors.

The inner ear of mammals contains melanocytes in the stria vascularis which is fundamental for hearing (Steel and Barkway, 1989). Some additional pigment bearing cells are also present in vertebrates such as the Harderian gland of eye (Sato and Yamamoto, 2001), some internal tissues in lung and skeletal muscle of reptiles and amphibians (Zuasti et al., 1998). Functions of these melanocytes are still remaining unclear.

1.2.3. Marker of pigment cell and gene regulatory network of pigment cell

1.2.3.1. Tyrosinase, the key enzyme for melanogenesis & *Mitf*, the pigment cell master gene

The characteristic phenotype of a pigment cell is given by the presence of melanin which is synthesized by the enzyme Tyrosinase. In all types of pigment cells the

Tyrosinase gene plays the key role for melanogenesis. In vertebrates three members of the tyrosinase-related family gene are involved in this process: Tyrosinase (*Tyr*), Tyrosinase related protein1 (*Tyrp1*) and Tyrosinase related protein2 (*Tyrp2*) which is also known as dopachrome tautomerase gene (*Dct*). The members of the tyrosinase-related gene family have been used as model to study pigment cell biology {for a review see (Murisier and Beermann, 2006)}. Studies on the genomic structure of the tyrosinase-related family indicate that they evolved from one ancestral tyrosinase gene that, through a first duplication, generated one tyrosinase-related gene, *Tyrp1* or *Tyrp2* (*Dct*). Then, the second *Tyrp* has been generated, most probably, from the primitive tyrosinase-related gene (Budd and Jackson, 1995; Sturm et al., 1995), given that *Tyrp1* and *Tyrp2* (*Dct*) are evolutionarily more closely related to each other than to tyrosinase. Studies on the transcriptional regulation of tyrosinase genes in vertebrate model systems, as fish and mouse, have brought to the identification of regulatory regions responsible for pigmented-lineage specific gene expression. Experiments of heterologous expression have also indicated that most of the molecular mechanisms controlling pigment cell-specific gene expression are conserved from fishes to mammals, given that promoters of fish are active in mouse and vice-versa. Furthermore, sequence analyses have revealed the presence of DNA motifs evolutionarily conserved amongst these promoters. One of them corresponds to the recognition sequence for the Microphthalmia transcription factor (Mitf) which is a key player in the establishment of the pigment cell lineage (Aksan and Goding, 1998; Hou et al., 2000). Mitf, which displays cell type-specific isoforms, is able to transactivate these *Tyr/Tyrp(s)* promoters in both melanocyte and RPE. On the other hand, specific DNA motifs have been highlighted in these promoters and have brought to the identification of Otx2 and Pax6 as RPE specific factors (Martinez-Morales et al., 2004) and of Sox10 (Jiao et al., 2004; Ludwig et al., 2004; Mollaaghababa and Pavan, 2003; Wegner, 2005) or Pax3 (Galibert et al., 1999) as melanocyte-lineage specific {reviewed by (Murisier and Beermann, 2006)}. Thus, by using the tyrosinase gene family as a model, it has been

possible to take the first step in the networks that govern pigment production in either melanocytes or RPE. Over the years much more has been learned about the molecular networks controlling pigment cell specification, mostly based on the genetic and molecular studies of Mitf. Some of them have indicated that in neural-crest-derived melanocytes, as in the RPE, the function of Mitf can be linked to components of the Wnt signalling cascade (see later).

1.3.1. The Wnt signaling transduction pathway

The Wnt signaling pathway is quite conserved evolutionarily and plays important roles in a remarkable variety of cellular processes, such as cell proliferation (Cadigan and Nusse, 1997; Miller et al., 1999), cell fate determination, embryonic patterning, (van Noort and Clevers, 2002) axis formation as well as organ development (Wodarz and Nusse, 1998); (Polakis, 2000). Most recently this pathway has been found playing a vital role in stem cell renewal (Yi and Merrill, 2007)

These extra-cellular signaling molecules can stimulate several intra-cellular cascades which can be grouped, broadly, in two different classes: the canonical or Wnt/β-catenin pathway and the non-canonical or β-catenin independent pathway, which is further sub divided into the Planar Cell Polarity and the Wnt/Ca^{2+} pathway (Habas and Dawid, 2005). Although both of them share some of the partner components, some participant molecules are unique for each of them. However, one of the major differences is the terminal signal transduction that is obtained by β-catenin-LEF/TCF bipartite protein complex in canonical Wnt signalling. In the last 2 decades enormous work has been published on Wnt signalling cascade and a huge amount of participant molecules have been identified involved in this pathway. So far the best understood is the canonical Wnt signalling pathway where the role of the most downstream nuclear mediator is played by LEF /TCF transcription factor; the gene of my interest. So, I present a very brief

description of both Wnt signalling pathways below, particularly focusing my attention on the canonical cascade.

1.3.1.1. The non-Canonical Wnt signaling pathway

The non-canonical pathway, less well characterized compared to the canonical, most likely functions independently of transcription. This pathway, whose participant components and their interaction show a huge diversity, contributes to a variety of functions, mostly related to cell motility, either during early embryogenesis (convergent extension), or during development (cytoskeletal reorganization) or during invasion and metastasis. Non-canonical pathway can be divided into two different types:

a) The Planar Cell Polarity (PCP) pathway

In the PCP pathway the Wnt signaling is conducted by interaction between Wnt factor and Fz receptor independent from a co-receptor LRP5/6 (He et al., 2004). Other co-receptors are not clearly defined though there are a number of putative candidates. Wnt-Fz interaction activates Dsh (Dishevelled) leading to the activation of the small GTPases Rho and Rac (Wallingford and Habas, 2005) in two parallel pathways. Signaling pathway operated by Rho finally activates myosin through a series activation process (Weiser et al., 2007) resulting in the modification and rearrangement of actin cytoskeleton. On the other hand activated Rac GTPase then stimulates JNK activity (Habas et al., 2003; Li et al., 1999b). Downstream effector of JNK remains poorly understood. Contribution of these two GTPases signaling pathways in transcribing any downstream gene has not emerged yet.

b) The Wnt/Ca^{2+} pathway

This pathway is mediated through a trimeric G protein. After stimulating by Wnt/Fz, G protein activates Dsh and downstream calcium influx. The release of

intracellular Ca^{2+} activates several calcium sensitive proteins including some kinases (Kuhl et al., 2000; Sheldahl et al., 2003). This active kinases contribute in this cascade by activating some other downstream effectors of Wnt/Ca pathway, and participate in a variety of functions such as regulating ventral cell fates in *Xenopus* embryos (Saneyoshi et al., 2002), promoting the tissue separation process during gastrulation (Winklbauer et al., 2001).

1.3.1.2. The Canonical Wnt signaling pathway

The most important event of this pathway is the stabilization and accumulation of β-catenin in cell cytoplasm and subsequent nuclear localization. According to the most accepted model of Wnt/β-catenin pathway, without stimulation, the cytoplasmic level of β-catenin is maintained low by a protein complex that includes Axin, adenomatous polyposis coli (APC), glycogen synthase kinase 3β (GSK3β), protein phosphatase 2A (PP2A) and casein kinase 1α (CK1α.) (Gordon and Nusse, 2006; He et al., 2004). Within this protein complex GSK3β and CK1α, phophorylate β-catenin, which is, in turn, subjected to ubiquitynilation and degradation (He et al., 2004; Liu et al., 2002) (Figure 1.6. A).

The activation of the canonical Wnt signaling pathway starts with the secretion of Wnt ligand and its binding to the specific transmembrane receptor, Frizzled (Fz). To mediate the signaling, co-receptors, as the low-density-lipoprotein-related protein 5/6 (LRP5/6), are also required (He, *et al* 2004). This interaction results in hyperphosphorylation and activation of Dsh (Dsh), by a number of kinases. The activated Dsh interferes with the enzyme activity of GSK3, thus inhibiting β-catenin phosphorylation (Li et al., 1999a). Moreover, the degradation of Axin is also achieved by Dsh, through the interaction of Dsh with FRAT and FZD (Li et al., 1999a; Tolwinski et al., 2003). The Inhibition of GSK3 activity and the degradation of Axin result in the

stabilization and accumulation of β-catenin in cytoplasm. Subsequently, this β-catenin translocates in the nucleus where it functions as a co activator of LEF/TCF transcription factor and activate target genes. Co-activators of other family members may also contribute in this complex (Figure 1.6 B).

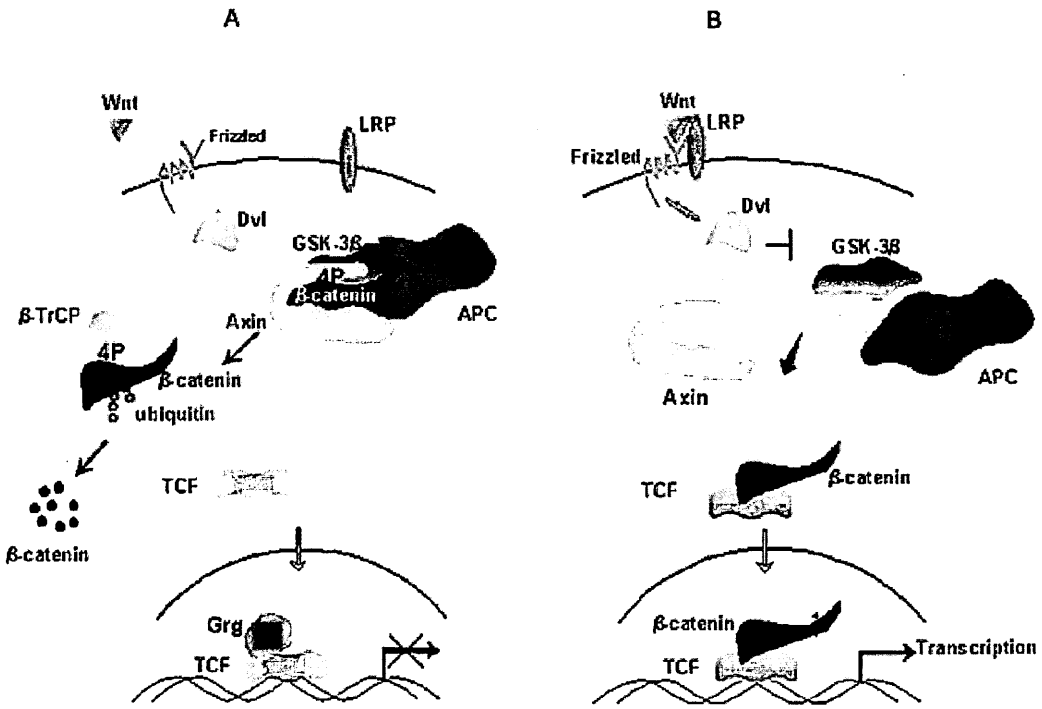

Figure 1.6. A simplified model of the canonical Wnt signaling cascade. These schemes depict the differences between a nonsignaling cell and its signaling counterpart. (A) and (B) with and without Wnt induction respectively {Adapted from (van Noort and Clevers, 2002)}.

LEF (Lymphoid enhancer factor)/TCF (T cell factor) are therefore one of the most important participants of the Wnt signalling pathway, since without LEF/TCF the co-activator β-catenin can not physically interact with the target DNA promoter {with some exceptions that suggest a β-catenin mediated nuclear activities without LEF/TCF transcription factor (Zorn et al., 1999)}.

1.3.2. The TCF/LEF family of transcription factors

The major breakthrough in the understanding of Wnt signalling came from the discovery of T-cell factor/lymphoid enhancer factor (TCF/LEF) proteins as the nuclear-binding partner of β-catenin. (Behrens et al., 1996; Molenaar et al., 1996; van de Wetering et al., 1997).

The TCF/LEFs belong to the high-mobility group (HMG)-box family of transcription factors, originally identified in the mammalian immune system (van de Wetering et al., 1991; Waterman et al., 1991). The TCF/LEFs act in a context-dependent manner, behaving as activator or repressor on the basis of their interaction with other cofactors.

The LEF/TCF transcription factor family contains small number of members. The vertebrate genome counts 4 members of this family. The vertebrate orthologues are known as LEF1, TCF1/ TCF7, TCF3 and TCF4 (Arce et al., 2006; Hurlstone and Clevers, 2002; van de Wetering et al., 1991; Waterman et al., 1991) except zebra fish where another orthologue, TCF3b, has been reported (Dorsky et al., 2003). On the other hand, invertebrate and non chordate species genomes investigated so far contain only one member of this protein family. The *Drosophila* TCF homologue is known as dTCF/ Pangolin, whereas the term POP1 was coined for nematode, *Caenorabhdetis eleganes*. The TCF homologue of tunicate *Ciona intestinalis*, the sister group of vertebrates is addressed as CiTCF.

1.3.2.1. Structure of TCF protein

Generally, the basic structures of all LEF/TCF family members are reasonably identical. All LEF/TCF proteins contain two principal domains to efficiently perform their function; an N-terminal β-catenin binding domain and a High Mobility Group (HMG) domain near the C terminal end. Usually the conserved amino terminal β-catenin binding

domain spans a region of around 50 amino acid (aa) through which TCF can interact with β-catenin allowing it to function as a transcriptional activator. This domain is vital for TCF otherwise the protein can not work as an activator. All LEF/TCFs bind β-catenin.

The HMG domain is highly conserved among species (~95-99% sequence identity) and is composed of around 88 aa including the NLS sequence (Nuclear Localization Signal) (Arce et al., 2006; Atcha et al., 2007). It is responsible for the physical interaction with target DNA promoter. All HMG boxes recognize a consensus sequence in the target promoters, the Wnt-response element (WRE: C/T-C-T-T-T-G-A/T-A/T), and bind to it (van Beest et al., 2000).

Another important function is offered by HMG domain upon binding with DNA. This physical interaction provides additional architectural supports by inducing a sharp bend, thereby helping in bringing distant transcription factors in proximity on the promoter. For example LEF-1 can produce a 130° bend upon binding with target DNA enhancer.

There are some additional domains found in some or all members of the TCF family:

The CRD (Context-dependent Regulatory Domain) domain (TLE in human), which is the most varied one, showing very low sequence similarity (15-20%). In general the CRD domain recruits the co-repressor Groucho (transducin-like enhancer of split) and thus aids in the repressor activity of TCF. Recently an auxiliary binding site for β-catenin has been discovered in CRD domain, which suggests a competitive interaction between β-catenin and Groucho/TLE (Daniels and Weis, 2005).

The C-terminal end of vertebrate LEF/TCFs are subjected to alternative splicing and thus give variations among the TCF proteins. For example E tail is produced as a result of alternative splicing from TCF gene and not from LEF1 which is probably too diverged to produce this domain. E tail is a non sequence specific DNA binding domain

and facilitates p300 interaction (Atcha et al., 2003; Atcha et al., 2007) and is found also in invertebrate chordate and non chordate TCF homologues.

E-tails are poorly conserved except for the 30-amino-acid motif which functions as a sequence-specific auxiliary DNA interaction domain. Moreover, the Wnt response elements require it for stable binding and subsequent β-catenin activation (Atcha et al., 2007).

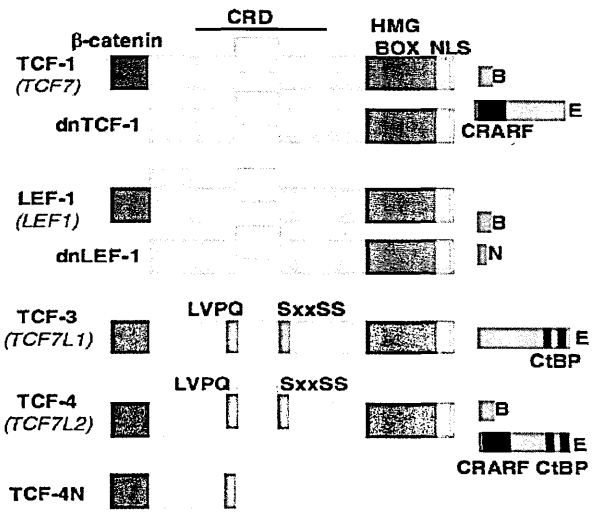

Figure 1.7. Schematic presentation of the structural organization of T-cell factor (TCF) proteins. Members of LEF/TCF protein familty in vertebrates: diversity is generated by alternative splicing and alternative promoter usage.. The b-catenin-binding domain (green) Context-dependent regulatory domain (CRD; grey/yellow), high-mobility group DNA-binding domain (HMG, red) and nuclear localization signal (NLS, orange). An internal exon in the CRD (yellow) is alternative in all members except for TCF-3, and the exon is flanked by small amino acid motifs (LVPQ, SxxSS; only in TCF-3 and TCF-4). Different C-termini in the E-tail, resulted from alternative splicing (blue; the most common tails are shown), and the CRARF domain (dark blue). The E-tail may also contain two CtBP-binding motifs (purple).HUGO nomenclature for the mammalian genes are given in parantheses; Taken from (Arce et al., 2006).

1.3.3. Binding partners of TCF

In spite of being the most downstream component of the Wnt/ β-catenin signaling pathway, in general, TCF can not contribute as classical transcription factor since its physical interaction with target DNA is not sufficient to regulate transcription. Transcriptional regulation of TCF family members is dependent upon the combinatorial

interactions between multiple proteins. The TCF protein modulates target gene regulation through protein-protein interactions.

The binding partners of the TCF family members are possible to describe in following two classes: ca-activators and co-repressors. Interaction between TCF and co-activator/repressor is fundamental for target gene regulation. From previous studies several proteins have been identified to physically interact with TCF.

1.3.3.1. The co-activators

Although all members of the TCF family proteins contain HMG DNA binding domain, it can not exert its transcriptional activation property until it gets a positive input from the Wnt signaling pathway. It has been already mentioned that all family members of TCF bind β-catenin through their N-terminal β-catenin-binding domain by which they can function as a classical transcriptional activator. β-catenin contains several domains among which the central domain is composed of 12 armadillo repeats that mediates the binding with TCF {reviewed in (Barker and Clevers, 2000)}. The Histone acetyltransferase (HAT) proteins CBP (CREB binding protein) and p300 have been found to aid in this process by directly interacting with β-catenin through armadillo repeat 10. This interaction locally acetylates nucleosomal histones thus promotes a conformational change of the chromatin. This change in turn might help other transcription factors and general transcriptional machineries to access to the target gene promotor and activate efficient transcription (Hecht et al., 2000; Takemaru and Moon, 2000). However, HAT activities of CBP and p300 are required for a subset of TCF target genes (Hecht et al., 2000). β-catenin also provides the necessary histone re-positioning machineries to its target gene loci and thus directly regulates nucleosome arrangements at Wnt-induced target genes {Reviewed by (Mosimann et al., 2009)}.

Another co-activator ALY has been found to interact with a unique member of the TCF family, LEF (Bruhn et al., 1997), because only this member contains a context-dependent activation domain (CAD) (Carlsson et al., 1993; Van de Wetering et al., 1996), which mediates the binding of ALY with LEF resulting into the transcriptional activation of target gene.

1.3.3.2. The co-Repressors

a) Groucho as a co-repressor

In the absence of Wnt signaling, TCF remains as a protein complex by interacting with several transcriptional repressors. As a consequence, the target promoter stays transcriptionally inert. Groucho is one of the potential co-repressor that cooperates with the conditional transcription factor TCF for inhibition of target gene expression. There are five Groucho homologue found in human (known as TLE for Transducin-like-enhancer of split) and mice genome.

All four members of mammalian TCFs can interact with each of these five Grg proteins (Brantjes et al., 2001). Except Grg5, the other four Grg/TLE members interact with histone deacetylase-1 (HDAC) which is responsible for chromatin condensation (Chen et al., 1999). In this way the co-repressor Grg contributes to target gene repression by TCF.

b) CtBP:

Another interesting scenario came from the study of Brannon and his co-workers in 1999 when they discovered the direct interaction between CtBP and XTCF-3 in repressing target gene in *Xenopus* embryos. It was later found that two consensus motifs (PSDLXS(K/R), present in the C-terminal domain of XTCF-3 and 4, interact with CtBP thereby, converting TCF proteins into repressors. Through a number of unrelated

transcription factors, CtBP contributes to short-range transcriptional repression within approximately 100bp (Zhang and Levine, 1999). The detailed molecular mechanism is a subject of intense investigation.

c) CBP:

In 1998 Waltzer and Beinz found another candidate co-repressor for TCF in *Drosophila*, histone acetylase dCBP, which was rather surprising since CBP functions as coactivator for lots of other transcription factors. In this particular case CBP connects with the HMG domain of TCF and acetylates a lysine residue (specifically K25) at the N-terminal β-catenin binding domain, thus interrupting the interaction with β-catenin and decreasing the level of transactivation. All family members of TCF cannot mediate repression through acetylation because this specific lysine is found to be absent from the N termini of TCF-1, TCF-3, Pop-1 {reviewed by (van Noort and Clevers, 2002)} as well as in Ci-TCF (our observation).

1.4. Biological role of TCF Proteins

TCF transcription factors are linked with diverse biological processes. They control the expression of genes critical for proper regulation of axis formation, cellular proliferation, differentiation, apoptosis, migration and oncogenic transformation. Major themes of TCF protein action include roles in tissue homeostasis, organogenesis (for example, eye, retina, head, limb) immunity and neuronal development. Disruption of these proteins often leads to embryonic lethality or cancer. Organisms and cells with mutations in a TCF locus display diverse phenotypes, strongly suggesting that individual the TCF proteins are able to direct distinct biological processes, despite their overlapping cellular distribution and similar DNA-binding properties.

1.4.1. TCF factors in Embryonic Development

Till now the role of TCF and the Wnt signaling pathway has been studied extensively in different laboratories all around the world which include almost all model organisms. Since TCF/LEF can work both as transcriptional activator and repressor, during embryogenesis proper balance between its regulatory function is a critical factor. The importance of this transcription factor family during development is highlighted by studies of functional knockout in different models.

Members of the TCF transcription factor family are expressed ubiquitously or tissue-specifically often in overlapping manner and contribute to a variety of embryonic developmental processes.

TCF has been found to be involved in axis determination in various organisms including both vertebrate and invertebrates, for example, *TCF3* has been demonstrated to be responsible for anterior posterior (AP) axis determination during early murine embryo development by its repressor activity. Partial or complete AP axis duplication wass obtained in *TCF* knockdown mice which also lack forebrain structure (Merrill et al., 2004). In *Xenopus* Wnt/TCF is crucial for embryonic axis determination and *XTCF3* is required to mediate the dorsalization of the embryonic axis (Roel et al., 2002). *XTCF3*$^{-/-}$ knock down causes disruption of axis formation which shows a dorso-anteriorized phenotype (Houston et al., 2002).

The anterior posterior axis of *C. elegans* (nematode) embryos is also specified by the repressor activity of *TCF* ortholog, *POP1* (Meneghini et al., 1999). Sea urchin orthologe of *TCF/LEF* member, *SpTCF* specifies the cell fates along the animal-vegetal axis of the embryo (Huang et al., 2000).

In Drosophila Pangolin /Pan (*dTCF*) is the most terminal element of Wnt/Wg pathway serving at the nuclear level. During embryonic development of the fly, the dorsoventral and/or anteroposterior axes are determined by Wg/pan transduction. This

event also regulates the ectoderm, mesoderm and endoderm specification in fruit fly embryos (Ahmed et al., 2002). Similar functions of this protein family have been described in other organisms too. For example, in sea urchin the expression of the endomesodermal regulatory genes require positive input from the Wnt/TCF signalling (Minokawa et al., 2005). In *Ciona* the Wnt/TCF signalling is suggested to be involved ectoderm pattering (Rothbacher et al., 2007) and in *Xenopus* embryos, both *XLEF1* and *XTCF3* regulate mesoderm induction (Liu et al., 2005).

Not only in the early embryogenesis, even later, the potential involvement of the LEF/TCF protein family has been reported in organogenesis of various organisms.

Contribution of *LEF/TCF* gene in head and brain development with some associated structures has been explored from the study in *Xenopus* and zebra fish. In *Xenopus, XTCF4* is required for normal midbrain and hindbrain development (Kunz et al., 2004)). In zebra fish two members of the *TCF* gene family, *TCF3a and TCF3b* contribute to head formation and brain patterning (Dorsky et al., 2003; Kim et al., 2000). In particular, *TCF3* (hdl) mutant embryos lack eye, forebrain, and part of the midbrain structures (Kim et al., 2000).

Another important function provided by *TCF/LEF* is postulated in pituitary growth and development in mouse, where *TCF4* acts as a crucial player in this process. Misregulation of this process can lead to pituitary tumor genesis (Brinkmeier et al., 2003).

Regulation by the *TCF/LEF* family members is also governed in some peculiar aspects of the central nervous system (CNS) development. In zebra fish *TCF3* is expressed through out the central nervous system and by its repressor activity on other genes it inhibits premature neurogenesis in spinal progenitors (Gribble et al., 2009). In mice, double knockdown of *TCF1* and *LEF1* either leads to early embryonic lethality (Galceran et al., 1999; Galceran et al., 2000) or these mice form excess neural ectoderm at the expense of paraxial mesoderm and have multiple neural tubes defects (Galceran et al., 1999; Takada et al., 1994). Together with their unique expression pattern, *TCF7* and *LEF1*

expression merge in different territories of the mouse embryo: in paraxial mesoderm, tail bud and limb bud and optic vesicle.

Establishment of embryonic nervous system controlled by *dTCF* mediated regulation is also suggested in fruit fly (Deb et al., 2008) which is also involved in adult appendages, such as the leg and different aspects of wing development including cell proliferation, wing margin specification, and wing self-refinement. (Schweizer et al., 2003).

Moreover, *LEF/TCF* involvement in mammalian immune system is also reported, actually, this is how these genes were first identified. Murine *TCF1* and *LEF1* are expressed in developing T cells in thymus (Van de Wetering et al., 1996) while *LEF1* is alone expressed in B cells in bone marrow (Travis et al., 1991). $TCF7^{-/-}$ mice have severe defect in T cell production (Galceran et al., 1999). Excluding this, *LEF1* is also involved in other aspects of organogenesis since, in $LEF1^{-/-}$ knockout mice various developmental abnormalities have been observed such as the failure to develop teeth, hair follicles, trigeminal nuclei, and mammary glands (Galceran et al., 1999).

Furthermore, LEF/TCF mediated Wnt signaling also plays essential roles in maintaining stem cells of the intestinal crypt cell, skin and haematopoietic stem cells {Reviewed by (Reya and Clevers, 2005)}. Recent observation of Faro and his co-workers postulated that, in zebrafish the intestine organogenesis needs *TCF4* mediated Wnt signalling (Faro et al., 2009).

Above all, *TCF/LEF* genes are also suggested to contribute in multiple aspects of retinal development: cell fate specification and/or differentiation, axon guidance as well as in retinal neuron homeostasis (Liu et al., 2006). It has been described quite recently that *TCF/LEF* activity is essential in cell fate maintenance in the developing RPE (retinal pigmented epithelium) through the direct regulation of *Mitf* and *Otx2* expression (Westenskow et al., 2009). *Mitf* regulation in neural crest derived melanocyte differentiation is also contributed by the Wnt/LEF1 signalling cascade (Schmidt and Patel,

2005). The promoter region of *Nacre*, a zebra fish homologue of *Mitf* which is crucial for melanocyte differentiation has been found to contain a LEF/TCF binding site which signifies the requirement of the Wnt signalling in pigment cell formation in zebrafish (Dorsky et al., 2000).

The findings of *TCF/LEF* involvement in RPE and melanocyte differentiation open up a new window to understand pigment cell formation in vertebrates although to deduce the detail mechanisms a very elaborate and deeper investigation is needed. Nevertheless, Ascidians can provide an elegant model organism to study pigment cell formation since some homologies has already been demonstrated with vertebrate pigment cells in terms of gene expression and function in pigment cell. Moreover, the presence of *TCF* in *C intestinalis* pigment cell precursors (explained later) sheds light on a possible involvement of the Wnt/TCF signaling cascade in pigment cell specification and /or differentiation in *C. intestinalis.*

1.5. Why study pigment cells in *C. intestinalis*?

To dissect the detail molecular mechanisms involved in pigment bearing cells in chordates, ascidians present themselves as the perfect system since they count 2 pigment cells and only in their larval stage. This may offer a significantly simpler study of a complex molecular mechanism.

Ascidians provide excellent model system in particular to understand the specification and differentiation of an individual cell type of tissue because from very early stage of embryogenesis; within 64/110 cell stage, the cell fate is determined and the cell lineage is predictable. Ascidians also offer to dissect the genetic cascade that effectively controls the overall mechanism of an organ formation due to the presence of lower number of vertebrate orthologue gene family. Thus, a complex gene regulatory network in vertebrates may be represented by a simple form in *C. intestinalis*. Moreover,

the regulatory region of a gene can be easily identified because of its close proximity to the coding sequence since it is already reported that the enhancer of a gene is positioned with in 1-2 kb upstream from the transcription start site (Corbo et al., 1997; Imai et al., 2002; Takahashi et al., 1999). This facilitates the identification and characterization of different tissue-specific enhancers responsible for particular gene expression pattern during embryonic development (Di Gregorio and Levine, 2002).

1.5.1. Pigment cell lineage in *Ciona intestinalis*

Cell lineage explains the history of cell divisions, the position of each cell in an embryo as well as the destiny of each cell regarding the different types of tissues they will form (Davidson, 1986); (Davidson, 1989). So, detailed knowledge of embryonic cell precursor lineages is obligatory to understand all the processes in embryonic development. Ascidian embryogenesis and cell lineage was first described in the late nineteenth century (Satoh, 1994). Conklin described a detailed cell lineage of two ascidians, *Styela partita* and *C. intestinalis* by observing the maternal factors in 1905, which was a pioneer work of embryology. His observations were later confirmed by vital-staining methods including the color chalk particles utilized by Ortolani. In this protocol the cells are marked with color chalk particles and the cell lineages are followed according to the destination of the chalk molecules in larva (Ortolani et al., 1979). Later, intracellular marking has been proved as an efficient technique for cell lineage study. By injecting horseradish peroxidase (HRP) as a tracer enzyme, specific cells of early embryonic blastomeres can be marked and further developmental fates of these cells can be established by histochemical detection of HRP (Nishida, 1987; Nishida and Satoh, 1983; Nishida and Satoh, 1985).

In recent days, cell lineage in ascidian embryos has been depicted in details by cell staining (Cole and Meinertzhagen, 2004), scanning electron microscopy (Nicol and Meinertzhagen, 1988),

The ability to form pigment cell is first committed to the left and right a4.2 cells at 8 cell blastomere stage when they receive an inductive signal from the anterior vegetal A-line blastomeres. The same A-line blastomere is specified to form the posterior nerve cord (Minokawa et al., 2001; Okada et al., 1997).

The major findings related to pigment cell lineage comes from the study on *Halocynthia roretzi* where by blastomeric recombination experiments it has been shown that, at early gastrula stage (110-cell), two symmetric descendants of the a4.2 blastomeres, the right and left a8.25 cells, start to be influenced by an inducing signal supplied by the underneath A-line blastomeres (Nishida, 1991). This inductive process lasts for all the gastrulating period.

By the mid-gastrula stage, the determination of a8.25 cells (bilateral pigment lineage cells at the eighth generation) as precursors of two pigment cells is accomplished. However, the developmental potential of the a8.25 pair of the 110 cell stage is not restricted to pigment cells, because it contains brain potential as well (Fig. 1.8 A). After 8^{th} division a8.25 pair divides to produce a9.49 and a9.50 cell pairs and the pigment cell fate separates from that of brain which is confined to a9.49 cell pair (Fig.1.8 B). These two cells (a9.49 pair) after final division at late neurula stage produce four cells: two smaller anterior (a10.98) and two larger posterior (a10.97). Among these cells the a10.97 pair inherits the pigment cell precursor potential.

At the onset of neural tube closure, these four cells migrate and intercalate with each other, lining up dorsally in a single row, along the anterior-posterior axis of the embryo. During this intercalation process each member of a10.97 has the equivalent chance to get the anterior or posterior position along the cell row (Fig. 1.8 D). At the tailbud stage differentiation of this a10.97 pair into two pigment cells occurs in a complementary manner (i.e. if the otolith cell is the left a10.97 cell, then the ocellus pigment cell is the right a10.97, and vice versa). This event is controlled by the positional information signals along the anterior-posterior axis of the embryo which induces the

posterior most cell of 10.97 pair to develop ocellus pigment cell while the anterioir most develops into otolith pigment cell (Darras and Nishida, 2001; Nishida and Satoh, 1989).

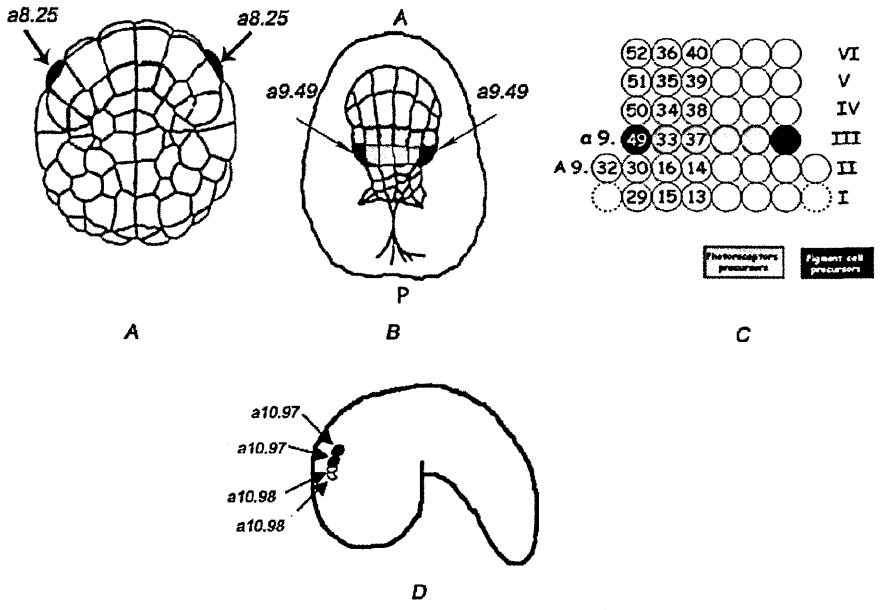

Figure 1.8. Sensory organs' pigment cell lineage in ascidian.

During gastrulation the specification of pigment cell precursors (a9.49 cell pair) starts: around the 110-cell stage (A, vegetal view, anterior is up), in a8.25 cell pair (blue) At the neural plates stage the decision is taken (B, dorsal view, anterior is up) which leads to the commitment of the a9.49 cell pair (in blue) derived from the a8.25 cell-division, as pigment cell precursors. At tailbud stage (D), the two a10.97 (in blue) and the two 10.98 cells, derived from the a9.49 blastomere division, migrate and intercalate with each other, lining up dorsally in a single row. Among these cells, the a10.97 couple inherits the pigment cell precursor potential. Positional information signals along the anterior-posterior axis of the animal determine the fate of the two a10.97 precursors in the larval otolith or ocellus sensory organ pigment cells. (Anterior is at the Left). C: Schematic view of the neural plate showing the pigment (blue) and photoreceptor cell (green) precursors.

Very little information is available concerning the genetics and molecular mechanisms involved in tunicate pigment cell development including the molecular pathways and factors responsible for pigment cell specification and fate determination. The little information obtained so far come from the study in ascidian *H. roretzi.*

Although during ascidian embryogenesis mosaic mode of development has been accounted significantly, determination of pigment precursor cells (a8.25) completely depends on the signal coming from the surrounding spinal cord precursor cells. During the specification and differentiation process of pigment cells in *H. roretzi* bFGF (Basic Fibroblst Growth Factor), BMP (Bone Morphogenic Protein) and an antagonist of BMP, CHORDIN has been found to play the fundamental roles (Darras and Nishida, 2001). The signal governed by FGF from the vegetal blastomere induces the neuralization of ectodermal cells during early cleavage. At the early gastrula stage BMP signal is provided by the A-line blastomere (A8.15, A8.16 pairs) positioned just below the row of a-line neural cells including the precursors of a8.25 pairs (Miya et al., 1997). This induction influences a8.25 cells to take up a pigment cell fate. From a10.97 cell pair at the tailbud stage the BPM/CHORDIN antagonism phenomenon determines the differentiation of ocellus and otolith. BMP induces the otolith pigment cell differentiation while suppression of BMP by CHORDIN is responsible for ocellus pigment cell differentiation. The manufacture of melanin is under control of Tyrosinase gene family which has been shown to be controlled by MITF (Microphthalmia associated transcription factor) (Yasumoto et al., 1997).

At present, further investigation is mandatory to demonstrate the mechanism for pigment cell development in ascidian sensory organ. The preliminary observation in *H. roretzi* is quite satisfactory but is far from being conclusive. Moreover, this information can not be used uniformly in all tunicate species because although there is a certain degree of conserved cell lineage pattern sometimes they do not share the developmental genetic pathways. This condition is very common in organisms between two different genera. For example, the expression pattern of *CiBMP* and *HrBMP* do not consign at 110-cell stage because unlike in *H. roretzi*, *CiBMP* is not expressed in A-line blastomere which means it can not work as a pigment cell inducer during the first inductive event. Concerning the second step of pigment cell fate determination at tail bud stage *Ci BMP* shows the same

expression pattern as *Hr BMP* (a10.97s and a10.98s) suggesting a possible role for *Ci BMP* in pigment cell determination.

1.5.2. Presence of common marker genes in both vertebrate and ascidian pigment cells

Not only in the physical properties but also at molecular level including pigment cell marker genes, homologies between ascidian and vertebrate pigment cells have been observed. Most of the published work available has been done on ascidian *Halocynthia roretzi.*

The vertebrate pigment cell markers Tyrosinase and Mitf are also expressed in the pigment cell lineage of *H. roretzi.* In *H. roretzi* two members of tyrosinase family genes have been identified. *HrTyr*, that codes for tyrosinase and *HrTyrp*, homologue of tyrosinase related protein (Tyrps) which shows more similarities with *Tyrp1* rather than Dct of vertebrate.

During pigment cell formation, the onset of *HrTyrp* expression coincides with the stage when the pigment precursor cells are fate restricted, that is at the early-mid-gastrula stage in a8.25 blastomeres. In contrast *HrTyr* expression starts a bit later {Reviewed in (Sato and Yamamoto, 2001)}. Additional expression of *HrTyrp* is also present in four neighboring cells (a8.17 and 18.19 pairs). These six *HrTyrp* positive cells later give rise to all parts of the brain including the two pigment cells. On the contrary the expression of *HrTyr* is very specific only to the pigment cell lineage and the expression begins at the early neurula stage in a9.49 pair positioned at the anterior neural plate. The expression of *HrTyrp* and *HrTyr* remains in a10.97 and a10.98 descendants of the a9.49 pair up to the late tailbud stage. The a10.97 pair differentiates into the otolith and ocellus pigment cells where *HrTyrp* and *HrTyr* expression persist up to the larval stage.

The expression pattern of the Tyrosinase gene family during chordate development presents comparable evolutionary constraints. The expression level of *HrTyrp* is always higher than *HrTyr* expression in both unpigmented and melanized cells; interestingly this pattern is also observed among mouse Tyrps (*Tyrp1 and Dct*) and *Tyr*. Both *HrTyrp* and vertebrate *Dct* are expressed in pigment precursor cells from very early stages during development. Moreover, both of their expression is not restricted to pigment cell lineage, since they have been detected also in non-pigment cell lineage such as the anterior end of the developing neural tube.

Similarly the *Mitf* homologue of *H roretzi, HrMitf* expression pattern has been also studied by Yajima and his co-workers (Yajima et al., 2003). The data indicate that maternal *HrMitf* signal is present throughout the cytoplasm in unfertilized eggs and becomes restricted to animal blastomeres up to the mid-gastrula stage. At the mid-neurula stage *HrMitf* transcript gets localized in the a9.49 blastomeres and is inherited by their four descendant cells, a10.97 and a10.98, reminding *HrTyr* and *HrTyrp* expression. However, in late tailbud stage the signal disappears. The expression of *HrTyr/HrTyrp* and *Hr Mitf* in pigment precursor cells indicates their importance in pigment cell development in ascidians. The expression of Tyrosinase gene has also been analysed in *C. intestinalis* by whole mount in situ hybridization (Caracciolo et al., 1997). The data indicate that *CiTyr* expression territories mirror *HrTyr* since *CiTyr* transcript is detected in the neural plate in a9.49 blastomeres, at the neural plate stage, and is maintained in the four descendant cells 10.97 and 10.98. The expression is then strongly preserved in the otolith and ocellus of the larvae.

The presence of *CiMitf* has been investigated in our laboratory previously (unpublished) by *in situ* experiment which indicate that the zygotic *CiMitf* mRNA is first detected in a row of six cells containing a9.49 blastomeres of the neural plate at neural plate stage. Later, at the neurula stage, the signal gets confined to the pigment precursor

cells, a9.49 blastomeres and persists in all four of their daughter cells a10.97 and a10.98 at tailbud stage (unpublished).

As previously mentioned, recent findings indicate that the Wnt signaling is involved in promoting melanocyte fate in neural crest cells (Dorsky et al., 1998; Dunn et al., 2005; Hari et al., 2002; Jin et al., 2001b). One of the mechanisms seems to be a direct activation of *Mitf*, since the LEF/TCF binding sites, present in the *Mitf* promoter, respond to β-catenin (Takeda et al., 2000; Widlund et al., 2002). Beside melanocytes, Wnt/ β-catenin signaling is involved also in mouse RPE differentiation, as demonstrated very recently by Westenskow and his co-werkers (Westenskow et al., 2009). The mechanism involves, here too, the activation of potential TCF/LEF sites present in the *Mitf* and *Otx2* enhancers. It appears therefore that the pigmentation program, both in the RPE and melanocytes, requires the presence of the TCF/LEF family members at the right time and in the right place to function as downstream effector of the Wnt/ β-catenin signaling. Thus far, however, a direct involvement of the TCF family members in pigmentation programs has been assessed only in very few cases in higher chordates (Lang *et al.*, 2005), since most of the experimental evidences concern the more generic "Wnt pathway" (Jin et al., 2001a; Lewis et al., 2004a), the use of TCF/LEF-responsive promoters (Dorsky et al., 2000: Dorsky et al., 2002) or the study of TCF/LEF responsive elements in the enhancers of the genes of interest (Dorsky et al., 2000; Westenskow, et al., 2009).

1.6. *TCF* in *Ciona intestinalis*

While higher organisms' genomes harbor four members of the LEF/TCF family of transcription factor, *Ciona* genome contains only one orthologue called *Ci-TCF*, confirmed by anlysis of the annotated genome (Arce et al., 2006).

The zygotic *Ci-TCF* expression starts quite late during development while early developmental stages proceeds with mRNA transcript of maternal *Ci-TCF*. With WMISH

experiment the expression profile of *Ci-TCF* during *Ciona* development has been studied extensively. The maternal transcript is present even in unfertilized eggs and this remains broadly distributed in all blastomeres up to the 32 cell stage (Fig. 1.9 A, B). The presence of mRNA of maternal *TCF* disappears at gastrula stage.

The zygotic staining is possible to detect at the late gastrula stage, first of all in the mesenchyme where it persists up to the tailbud stage (Fig.1.9 C). Signal in new territories is visible at the neurula stage in four cells localized anteriorly which corresponds to palp precursors (Fig. 1.9 D). Additional staining is also observed, very faintly, in two more cells of neural plate corresponding to the a9.49 pairs (Fig. 1.9 E) descendants of a8.25 pairs. These a9.49 pair blastomeres are the cells which after another division in tailbud stage give rise to the pigment cells of the ocellus and otolith organs, found in the sensory vesicle of *Ciona* tadpole.

At the tailbud stage *Ci-TCF* positive staining is localized in two out of four a9.49 descendants. An additional signal is also present in the brain vesicle. During the tailbud development the embryo exhibits the same expression pattern of *Ci-TCF* which disappears almost completely at the larval stage.

To understand better the lineage of the two a9.49 descendants positive to *Ci-TCF* signal, a double *in situ* hybridization experiment was conducted using *Ci-TCF* and Tyrosinase probes. Results obtained from this double *in situ* show the staining of *Ci-TCF* in the two posterior cells, the a10.97, fated to give rise to otolith and ocellus pigment cells (Fig. 1.9 H-J).

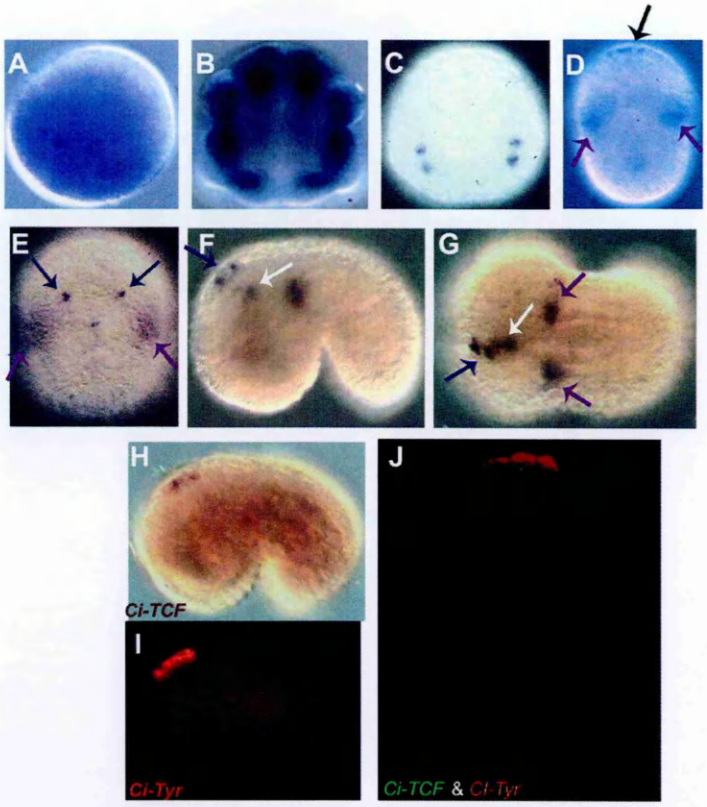

Figure 1.9. *Ci-TCF* expression profile. A–G: *Ciona* embryos hybridized with antisense probe for *Ci-TCF*. A: Unfertilized egg. B: 32 cell-stage embryo, vegetal view. C: Late gastrula, vegetal view. D-E: Neurula, vegetal view. D: A signal is visible in four cells localized anteriorly (black arrow), that correspond to the palp precursors, in the mesenchyme (purple arrow) and E: in the pigmented cell precursors (blue arrow). F-G: Early tailbud showing *Ci-TCF* localization in the brain vesicle (white arrow), in two cells on the dorsal side of the trunk (blue arrow) and in the mesenchyme (purple arrow). H-J: Double in situ hybridization with *Ci-TCF* (H) and *Ci-Tyr* (I) in the early tailbud embryos. The *Ci-TCF* positive cells correspond to the two posterior *Ci-Tyr* fluorescent blastomeres. J: Double *in situ* showing *Ci-TCF* positive cells in green and *Ci-Tyr* positive cells in red. Anterior is to the top (A–E, J), to the left (F–I).

1.6.1. *Ci-TCF* function in *Ciona intestinalis*

Injection of *Ci-TCF* "blocking translation" morpholino oligonucleotide (m*Ci-TCFbt*) provided the first indication of a potential role of *Ci-TCF* in pigment cell formation. It is important to note that injection of m*Ci-TCFbt* morpholino induces gross alteration in the overall brain vesicle organization and, really often, causes a very aberrant phenotype at the equivalent of larval stage. These malformations are related to an

interference with maternal *Ci-TCF*, which plays a fundamental role in early ectoderm patterning (Rothbacher et al., 2007). Therefore it has been very difficult, in each experiment, to finely dose the amount of morpholino able to interfere with the zygotic transcript without affecting the maternal transcript. This is the reason why it has not been possible to assess a precise amount, but instead a range of concentrations (between 0.2-0.06mM), able to interfere with zygotic *Ci-TCF*. The resulting phenotypes, at the larval stage, show morphological alterations in palps, sensory pigment cells and brain vesicle, just the territories where the endogenous *Ci-TCF* is expressed from neurula stage. Weakly affected larvae lack the palps and in most cases contain only one pigment cell morphologically some of which resembles with otolith and some ocellus (Fig. 1.10 B). In some larvae the head development is altered as well as a weird position of a pigmented region is observed that is, on the outermost external surface of the head (Fig. 1.10 C). In some larvae no pigment cell is present at all (Fig. 1.10 D). While, in 4 mismatch morpholino injected larvae no significant morphological alteration has been observed (Fig. 1.10 A).

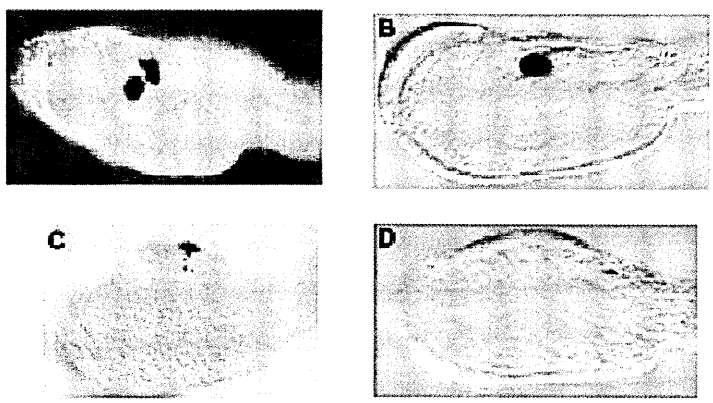

Figure 1.10. Interference with *Ci-TCF* function by morpholino injection. A: Control larva injected with 4 mismatch *Ci-TCF* morpholino (0,2mM). B-D: Phenotypes of larvae injected with *Ci-TCF* morpholino (0,2-0,06mM). B: No palps and one pigment cell. C: No palps, aberrant development of the brain and one pigment cell. D: No pigment cell.

For phenotypic clarification of the morphologically altered larvae, *in situ* hybridization was done with CNS specific marker, *Ci-Pans* (Alfano et al., 2007) and photoreceptor specific marker, *Ci-Opsin* (Kusakabe et al., 2001). The presence of signal for *Ci-Pans* in the CNS even in the strongly affected embryos indicates a certain grade of CNS differentiation. On the contrary, *Ci-Opsin* signal has been found reduced in many embryos but still the staining is detectable in the brain vesicle confirming the presence of cells with "photoreceptor properties" (data not presented).

These data suggest that *Ci-TCF* has a role in the development and/or differentiation of the pigment cells of *C. intestinalis.*

1.7. Aim of the thesis

From the previous findings in our laboratory, concerning the presence of *Ci-TCF* mRNA in the pigment cell precursors, a contribution of this gene in pigment cell formation, during *Ciona* embryogenesis appears possible. Further data obtained by morpholino injection supported this idea, since in the injected larvae phenotypic alterations were observed regarding the number and appearance of the pigment cells in the sensory vesicle.

Based on these previous results I started my PhD study with an aim to better define the function of *Ci-TCF* in pigment cell development. To this end, I exploited transgenesis experiments, through electroporation technique, an alternative approach to morpholino injection. A targeted interference of the endogenous *Ci-TCF* function, specifically in pigment cell precursors, was accomplished by introducing a dominant negative form of *Ci-TCF* under the control of the *pTyrosinase*, a pigment lineage enhancer.

At the same time efforts have been taken to deduce the molecular mechanisms presiding over *Ci-TCF* expression, by identifying putative factors involved in *Ci-TCF* expression in pigment precursor cells. Until now, the members of TCF family have been studied only as the downstream component of the Wnt signalling cascade. Thus, all the previous studies were directed towards the observation of the expression pattern of TCF proteins and understanding their possible function in various aspects of development in different organisms, including *Ciona*. No study has been conducted so far to identify the upstream regulators of this gene and the mechanism by which the TCF family members are expressed at the right time and in the right place to function as downstream effectors of Wnt signaling. So, the molecular mechanism regulating *TCF* expression remained unsolved.

To reach this goal the first priority was devoted to the isolation of the *cis*-regulatory elements of *Ci-TCF* that can efficiently recapitulate the endogenous *TCF* gene expression, then gradually decreasing the enhancer element, to obtain the minimal region which can drive *Ci-TCF* expression in pigment cell territories. Continuation of this study was followed by in silico analysis of the minimal promoter region to search for the putative transcription factor binding sites and analyzing them *in vitro* and *in vivo*.

CHAPTER 2

MATERIALS AND METHODS

2.1 Adult *Ciona sp.* and Gamete collection

Adult *Ciona intestinalis* were obtained from the Bay of Naples, Italy by the fishing service of Satzione Zoologica as well as from Roscoff bay, France. The animals were maintained in animal facility maintenance.

2.1.2 Gamete collection

Gametes were collected surgically from the gonoduct of adult individual separately in sterile condition and were stored at 18°C (eggs) or on ice (sperm) until use. The sperms were collected as dry as possible. The eggs were gently washed in seawater and let deposited at the bottom of a 15 ml test-tube by gravity sedimentation.

2.2. Transgenesis by electroporation

Introducing foreign DNA into cells of various model organisms has been facilitated by the invention of *in vivo* electroporation. This is a very effective and easy method to transfect DNA in *Ciona intestinalis* comparing to microinjection. The principal of this technique is to use electric pulse to create transient pores temporarily in the plasma membrane through which the negatively charged DNA molecules enter the cell.

Transfection of a gene into fertilized *Ciona* eggs permits to study the functional properties of the gene such as, gain of function, loss of function etc. Moreover, this method has also been used as a powerful tool to analyze regulatory region of a gene.

2.2.1 Chemical dechorionation

It is necessary to remove the surrounding chorion from *Ciona* eggs prior to electroporation. The most convenient way to get rid off this chorion is the chemical dechorionation which is performed in dechorionating solution [Thioglycolic acid (1%) and Proteinase E (0.05%) in MFSW (pH 10)]. The dechorionation process is done in a Petri dish containing a thin layer of 1% agarose in MFSW on the bottom. The eggs and the dechorionating solution are added to this plate. Then using a glass pipette the eggs are continuously shaken in the solution to remove the chorion and the follicular cells. When the eggs are deprived of the chorion they are washed several times to remove the residual solution.

2.2.2. *in vitro* fertilization

in vitro fertilization is done in the same Petri dish using few drops of diluted sperms collected from two or more individuals to avoid self-sterility problem. After 10 minutes, fertilized eggs are washed 2-4 times to eliminate the excess sperms.

2.2.3. Electrorporation

After fertilization the eggs were immediately transferred in a solution containing 0.77 M Mannitol and 50-100 µg of DNA. The electroporation was carried out in Bio-Rad Gene Pulser 0.4 cm cuvettes, using Bio-Rad Gene Pulser II with extension capability, at constant 50 V and 800 µF, in order to have a time constant of 14-20 mili seconds. After that the embryos were grown in MFSW at 18–20°C up to desired stages. They were further used or fixed to perform subsequent experiments.

2.3. Transformation in Bacteria

2.3.1. DNA digestion with restriction endonucleases

Plasmid DNA was digested with appropriate restriction endonuclease/s containing 5 units of enzymes/ 1μg of DNA in a final volume at least 20 times larger than the enzyme volume. In the presence of 1/10 volume of its respective buffer the mixture was incubated at least four hours/over night in a specific temperature suggested by the manufacturer's instruction.

2.3.2. DNA dephosphorylation

DNA dephosphorylation has been conducted as follows: a convenient amount of DNA has been incubated with 1U of Calf Intestinal Alkaline Phosphatase enzyme (CIAP) (Roche) per 1 pmol 5' ends of double stranded digested DNA, in 1X CIP dephosphorylation buffer (Roche), at 37° C for 30 minutes. After this time, a second aliquot of CIP as been added, and the reaction has been carried on for another 30 minutes, at 37°C.

2.3.3. DNA gel electrophoresis:

To check the length and the quality of DNA samples such as PCR products, genomic DNA, plasmid DNA and restriction digestions were run on 1% agarose gel (containing 0.5 μg Ethidium Bromide) prepared in 0.5 X TBE buffer (Tris Borate EDTA). Before loading into the well DNA samples were mixed with 6 X loading buffer. After running for appropriate time nucleic acid bands were observed under UV and pictures were taken using GelDoc 2000 (BioRad).

2.3.4. DNA extraction from agarose gel

DNA fragments from PCR product or enzymatic reaction of plasmid were extracted from gel using QIAGEN® QIAquick Gel Extraction Kit according to the manufacture's instruction.

2.3.5. DNA ligation

Each ligation reaction was carried out in 20 µl reaction mixture containing 1X T4 Ligase buffer (50 mM Tris-HCl pH 7.5, 10 mM $MgCl_2$, 10 mM dithiothreitol, 1 mM ATP, pH 7.5); and 1 µl of T4 DNA Ligase (New England Biolabs) at 1 unit/µl conc. The proportion of plasmid vector and insert DNA was usually kept 1:3, and the total amount of DNA was kept within 50-100 ng. T4 DNA ligase was used to catalyze the formation of a phosphodiester bond between juxtaposed 5'-phosphoryl and 3'-hydroxyl termini in duplex DNA. It is also able to repair single-stranded nicks in duplex DNA and joins both blunt-ended and sticky-ended restriction fragments of duplex DNA potentially.

2.3.6. Bacterial cell electroporation

This method permits introduction of foreign DNA in bacterial cells via circular plasmid. Briefly, circular plasmid containing the gene of interest and the competent bacterial cells (prepared by the Molecular Biology service of the 'Stazione Zoologica, Anton Dohrn', Naples) were placed in a 0.2cm electrocuvette. The electrocuvette was then subjected to an electric pulse at constant 1.7 KV using a Bio-Rad Gene Pulser™ electroporation apparatus. The transformed *E.coli* cells were allowed to recover for one hour at 37°C in 1ml LB medium (NaCl 10g/l, bactotryptone 10g/l, yeast extract 5g/l,). An aliquot was spread on a prewarmed LB solid medium (NaCl 10g/l, bactotryptone 10g/l, yeast extract 5g/l, agar 15g/l) in the presence of specific selective antibiotic grown at the same temperature overnight.

2.3.7. PCR screening

Transformed bacterial colony were checked for the right insert by PCR where half of each single colony was placed for PCR where as the rest half was grown in 3 ml of LB liquid medium in the presence of suitable antibiotic (50µg/ml) O/N shaking at 37C. The PCR reaction was set in a total volume of 20 µl ,the reaction mixture was as follows: 1X PCR buffer containing $MgCl_2$ (Boehringer Manneheim, Monza, Italy); 40 mM dNTP mix (dATP, dTTP, dCTP, dGTP); 20 pmol of each forward and reverse suitable oligonucleotides; and 1U Taq DNA polymerase (Roche; Biogem). PCRs were carried out with the following protocol:

First step (one cycle)

First denaturation: 5 minutes at 95°C.

Second step (repeated for 25 cycles)

Denaturation: 1 mintute at 94°C

Primer annealing: 1 minute at 45°C-65°C (according to the melting temperature of oligo)

Extension: at 72°C for a suitable time, (depends on the amplified fragment length that is 1min/kb).

By gel electrophoresis analysis, the samples presenting a band of expected size have been identified and plasmid DNA has been purified from the corresponding bacterial colonies.

2.3.8. DNA sequencing

The DNA sequences were obtained using Beckmen CEQ 2000XL NA analysis system Apparatus by the (SBM) Molecular Biology Service at the SZN.

2.4. Genomic and plasmid DNA isolation

2.4.1. Genomic DNA extraction

Genomic DNA from *C intestinalis* was extracted from adult specimens' sperm. The sperm was collected from the sperm-ducts with a scalpel and sucking them by a glass pipette. An aliquot of about 500 µl of fresh sperm was mixed with 500 µl of RSB (10 mM NaCl, 10 mM Tris pH 7.5, 25 mM EDTA pH 8.0). After the addition of Proteinase K, to the final concentration of 0.5 µg/µl, and 20X SDS, to the final concentration of 1.25X, the sample was incubated into a water-bath for 1 hour at 45°C. Then, 1 volume of phenol:chloroform:isoamyle alcohol (25:24:1) has been added to the sample, mixed and centrifuged for 20 minutes at 14000 rpm. The aqueous phase has been recovered and added to 1 volume of chloroform:isoamyle alcohol (24:1), mixed and centrifuged for 20 minutes at 14000 rpm. The supernatant has been recovered and the genomic DNA has been precipitated adding 2 volumes of ethanol 100% and 1/10 volumes of ammonium acetate 2.5M. The precipitated genomic DNA has been collected with a glass loop, washed two times in ethanol 80%, dried at R.T., and diluted in 500 µl of H_2O. Concentration and quality valuations have been obtained respectively by spectrophotometre and by gel electrophoresis, using, as length marker, 1X GeneRuler™ 1Kb DNA Ladder (Fermentas). The sample has been stored at 4°C for further use.

2.4.2. DNA mini and Maxi-Preparation

A single bacterial colony containing the plasmid DNA of interest was grown overnight in suitable volume of LB in the presence of appropriate antibiotic shaking at 37°C for plasmid DNA purification. The culture was then centrifuged at top speed to pellet the bacterial cell. The pellet was resuspended in respective buffer and manufacturer's handbook instructions were followed. For Mini-prep Qiagen and for Maxi-prep Qiagen and Sigma Maxi-Prep Kits were used. Before starting the protocol an aliquot of 750 µl of

the overnight culture was mixed with 250 µl of 100% sterile glycerol and stored at -80°C as stock.

2.4.3. Purification on CsCl of plasmid DNA

Plasmid DNA was resuspended in 1xTE and for each ml of DNA, 1.2 g of CsCl and 100 µl of EtBr (10 mg/ml) were added. The samples were then transferred in Beckman Quick Seal ultracentrifuge tubes and centrifuged in a VTi-65 rotor 16 hours at 55,000 rpm and at 25 °C in a Beckman L8-70M ultracentrifuge.

By this technique, circular plasmid DNA was separated by contaminant bacterial DNA and RNA. The separation occurred in virtue of different density acquired by plasmid DNA in the presence of EtBr compared to chromosomal DNA. Two distinct bands were formed on the gradient, the upper one contained nicked bacterial plasmid and chromosomal DNA, where as, the lower one corresponded to supercoiled plasmid DNA. The band containing the DNA of interest was collected using a 21-gauge needle.

The EtBr was removed by adding 1 volume of isoamyl alcohol and by centrifuging 10 minutes. The extraction was repeated several times until EtBr was eliminated from the alcoholic phase. Finally, removal of CsCl was obtained by precipitation of plasmid DNA. For precipitation, the sample was incubated on ice for 15 minutes after the addition of 3 volumes of H_2O and 2 volumes of 100% ethanol and then centrifuged at 10,000 rpm 20 minutes at 4 °C. The pellet was washed in 70% ethanol and resuspended in sterile H_2O.

2.5. PCR amplification from genomic DNA

The PCR reaction has been performed in a total volume of 50 µl, using about 10-50 ng of genomic DNA as template, 0.2 mM of dNTP mix (dATP, dTTP, dCTP, dGTP), 1X PCR Buffer (Roche), 0.05 U/µl of Taq DNA Polymerase (Roche) and 2 pmol/µl of each

forward and reverse suitable oligonucleotides. The PCR amplification program has been set as follows: First step (one cycle): Denaturation 5 minutes at 95°C.

Second step (repeated for 35 cycles):

DNA denaturation: 1 minute at 95°C.

Oligonucleotides annealing: 2 minutes at suitable temperature (the temperature used in this step has been set at least 8-10°C below the melting temperature of the oligonucleotides).

Polymerization: 72°C for a suitable time (the polymerization time has been calculated considering the desired amplified fragment length.

Final elongation step: 10 minutes at 72°C.

The amplified fragments were separated from the genomic DNA and from the dNTPs and oligonucleotide excess, by gel electrophoresis, using, as fragment length marker, 1X GeneRuler™ 1Kb DNA Ladder (Fermentas). The fragments were then isolated and purified by gel extraction (QIAquick Gel Extraction Kit, QIAGEN; GenElute™ Gel Extraction Kit, Sigma). The concentration of the gel extraction DNA was evaluated by gel electrophoresis, using, as concentration marker, 1X Lambda DNA/Hind III Marker,2 (Fermentas).

2.6. *In silico* analysis of putative *trans*-acting factors

Four putative ETS binding sites were identified in the promoter region of construct *pTCF0.4>GFP* using Transfac software tools (http://www.biobase-international.com/pages/index.php?id=transfac). This is a relational database of transcription factor from many organisms, their genomic binding sites and DNA-binding profiles. Genomatics (http://www.genomatix.de/)and JASPER (http://jaspar.cgb.ki.se/) softwares were used to cross check the analysis

2.7. Site Directed Mutagenesis

Site directed substitution was done to change the ETS binding site from GGAA to AGAA (Bertrand et al., 2003), in the promoter region of construct *pTCF0.4>GFP* following the Quick change site-directed mutagenesis kit (Stratagene) instructions. Primers were designed using the available software tool provided by Stratagene (http://www.stratagene.com/qcprimergesign). Each Ets binding site was mutated individually more over, starting from the 5'end the last three sites were also mutated in a single construct. The PCR reaction was carried out using following cycling parameters: after a single denaturation step at 95°C for 30 seconds, 18 amplification cycles were performed as follows: denaturation 95°C 30 seconds, annealing 55°C 1 minute, extension 72°C 7 minutes. The presence of amplified product has been checked loading 10 µl of the reaction on 1% agarose gel. To eliminate the template plasmid *pTCF0.4>GFP*, the PCR product was digested with 1 µl of the *Dpn*I restriction enzyme (10 U/µl) for 1hr at 37°C. This enzyme digests only the methylated supercoiled dsDNA used as template but not the newly synthesized mutated and unmethylated DNA. After the digestion, 1 µl of the reaction was transformed and grown as previously described.

Ten clones have been selected and after growth, the isolated plasmid DNAs were sequenced to check the presence of the desired mutation.

Following primers were used for mutagenesis purpose:

Table 2.1: Primer for mutatagenesis:

Name of primer	Sequence of primer 5'-3'
M1S	GCA GTC ACA TTG CAT TAA ATT CTG GCT TAA AAG AAA CAG TAT TAA C
M1A	G TTA ATA CTG TTT CTT TTA AGC CAG AAT TTA ATG CAA TGT GAC TGC
M2A	ACC AGC TAG CCA ACC AGA AAA CGA AAT CTG
M2S	CAG ATT TCG TTT TCT GGT TGG CTA GCT GGT
M3A	GCG TTT ATT CTT TCT TAT TTG CAA TAT TGC
M3S	GCA ATA TTG CAA ATA AGA AAG AAT AAA CGC
M4A	GAC TGA TGA CCC CAA TTC TGT GCG AAT AAA GCC AAT A
M4S	TAT TGG CTT TAT TCG CAC AGA ATT GGG GTC ATC AGT C

2.8. Embryo treatment with U0126

The U0126 (1,4-diamino-2,3-dicyano-1,4-bis[2-aminophenylthio]butadiene) is a chemically synthesized organic compound that inhibits the kinase activity of MAP kinase, MEK. It is able to block both the active (phosphorylated) and inactive (not phosphorylated) forms of MEK. Treatments with this compound give the possibility to block the MAP Kinase signaling pathway downstream of MEK, obtaining an inhibition of its direct targets, that cannot be phosphorylated, hence remain inactive.

For this experiment embryos were grown in MFSW at R.T. until the desired stage. Then, they were treated with U0126 (4 μM in MFSW) (Sigma) for 20 minutes and then washed with MFSW to remove the compound. The embryos have been grown till the desired stage and then fixed for WMISH or directly observed under the microscope.

2.9 Whole Mount In Situ Hybridization (WMISH)

2.9.1. Embryo fixation and storage

Embryos of the desired developmental stages were collected and fixed overnight at 4°C/ 1 hour at RT in the Fixing solution (4% formaldehyde, 0.1 M MOPS pH 7.5, 0.5 M NaCl.). The embryos were washed three times in 1XPBT (Phosphate Buffered Saline, 0.1% Tween-20) and immediately used or dehydrated with a series of 30%, 50% and 70% Ethanol and stored in 70% ethanol at -20°C. These fixed embryos were further used for WMISH or Immunohystochemistry.

2.9.2. Plasmid linearization

To synthesise sense and antisense mRNA corresponding to the cDNA fragments isolated from the *C. intestinalis* cDNA library, the plasmid containing the promoters T3 and T7 respectively upstream and downstream of the cloning sites was first linearised by digestion with suitable restriction enzyme. When the plasmid was digested with an enzyme cutting at the 3' end of the insert, RNA polymerase recognised T3 promoter and a sense mRNA was obtained, whereas, if an enzyme cuts the 5'end the T7 promoter was recognised and an antisense mRNA was synthesised.

2.9.3. Linearized plasmid purification

In order to eliminate protein contamination, the linearised plasmid was treated with Proteinase K (0.2 µg/µl), Tris 1M pH 7.4 (0.1), SDS (0.5%), in a total volume of 200 µl, using DiEthylPyroCarbonate (DEPC) treated H_2O. The reaction was then incubated for 30 minutes at 50°C. Purification was done by adding 1 volume of phenol:chloroform:isoamylic alcohol (25:24:1), vortexed vigorously and centrifuged at 14000 rpm for 10 minutes at 4°C. The aqueous phase was collected and 1 volume of

chloroform:isoamylic alcohol (24:1) was added; the sample was vortexed vigorously and centrifuged at 14000 rpm for 10 minutes, at 4°C. The aqueous phase was recovered and the DNA was precipitated adding 3 volumes of ethanol 100%, 1µl of glycogen (20 mg/ml), and 1/10 volume of Sodium acetate 3M pH 5.2, stored over night at -20°C or 1 hour at -80°C. Then, it was centrifuged at 14000 rpm for 15 minutes, at 4°C. The precipitated DNA was washed with ethanol 70% (DEPC-treated), centrifuging at 14000 rpm for 15 minutes at 4°C. The ethanol has been removed and the DNA pellet was air-dried at R.T. At the end, the DNA pellet was resuspended in a suitable volume of H_2O (DEPC-treated). Aliquots were analysed on 1 % agarose in TBE 1x and quantified in Nanodrop (1000, Thermo Scientific).

2.9.4. Synthesis of riboprobe

Both sense and antisense mRNAs were obtained by using a Digoxygenin RNA labeling kit (Roche) in the following reaction mixture: 1µg linearized plasmid DNA, 10xNTP mix, 2 µl; 10xTranscription buffer 2 µl, 20 U/µl RNase inhibitor 1 µl, 20 U/µl T3 /T7 RNA polymerase 2 µl, DEPC H_2O up to 20 µl. Synthesis reaction was conducted at 37 °C for 2 hours. To remove DNA template, 2 µl of 10 U/µl DNase I RNase free were added and incubated at 37 °C for 10 minutes. The reaction was stopped by adding EDTA pH 8 to a final concentration of 25 mM. The unincorporated nucleotides were removed from the RNA probes using the Mini Quick Spin RNA Columns G-50 Sephadex (Roche), following manufacturer's instructions. To check the quality and the quantity of the synthesized riboprobe gel electrophoresis and Dot Blot analysis were done respectively. The riboprobe was immediately stored at -80 °C until use.

2.9.5. Quantification of riboprobe

For each newly made Dig-labelled riboprobe, the concentration was evaluated by dot-blot immunostaining with anti-Dig antibody AP conjugated (Roche) against a known standard, Dig-labelled RNA control (Roche). RNA dilutions were prepared using the dilution buffer [DEPC H2O: 20X SSC: formaldehyde (5:3:2)]. Typically, dilutions of the Dig-labelled riboprobes were blotted to Hybond N membrane (Amersham) along with serial dilutions of standard Dig-labelled RNA (Roche) and UV-crosslinked to the membrane, with Stratalinker for 30 seconds. The filter was first incubated for 30 minutes in blocking solution (5% BSA in 0.1 M maleic acid pH 7.5) and then incubated, 1 hour at RT, in the same solution containing the anti-Dig alkaline phosphatise (AP) antibody (0.15 U/ml). To remove unbound antibodies, two washes in a solution containing 0.1 M maleic acid pH 7.5 and 0.15 M NaCl were done. The filter was equilibrated in the detection solution (100 mM Tris-HCl pH 9.5; 100 mM NaCl; 50 mM MgCl2) and then incubated in dark in the same solution in which 5-bromo-4-chloro-3-indolyl-phosphate (BCIP) (50 mg/ml) and nitroblue tetrazolium (NBT) (50 mg/ml) were added. The AP enzyme produces an insoluble blue precipitate in the presence of these 2 enzymatic substrates. The colored compound starts to precipitate in few minutes. The reaction was blocked after 10 minutes by washing the filter with H_20. The concentrations of experimental riboprobes were making serial dilutions 1:1, 1:4, 1:16, 1:64, 1:256, of the sample ribonucleic probes and comparing with the same dilutions of a control RNA of reference (1:1 100 ng/µl; 1:4 25 ng/µl; 1:16 6.25 ng/µl; 1:64 1.56 ng/µl; 1:256 0.39 ng/µl) (Roche),

Table 2.2: Genes of which ribonucleic probes have been synthesized.

Gene's name	Corresponding clone in N. Satoh gene collection 1
Arrestin	cibd069f14 (R1CiGC28m09)
Bmp5/7	ciad42d16 (R1CiGC04j07)
Mitf	cilv041b12 (R1CiGC28k08)
Opsin-1	cilv41m16 (R1CiGC28m24)
TCF	ciad10f19 (R1CiGC02c03)
Tyrosinase	citb41l04 (R1CiGC33c19)
Ets1/2	ciad08k16 (R1CiGC01h16)

4.9.6. Whole Mount In situ Hybridzation

In situ hybridization was done on fixed *C. intestinalis* embryos at different developmental stages. In case of dehydrated stored embryos, it was necessary first of all to rehydrate them in different strengths of ethanol for certain time period then the embryos were washed 2x10 minutes in PBS and, when necessary, dechorionated by hand with subtle platinum needle. The samples were washed 3x15 minutes in 1 ml PBT (PBS + 0.1% tween 20) at RT and incubated 30 minutes at 37 °C in 1 ml PBT containing 4 µg/ml protease K to increase the permeability to the cells and accessibility to mRNA target. After this treatment, samples were washed 3x15 minutes in PBT and post-fixed 1 hour at RT in 1 ml 4% paraformaldehyde in PBS. Embryos were again washed 3x5 minutes at RT in PBT, placed 10 minutes at same temperature in the hybridization solution (50% formammide, 5xSSC, 50 µg/ml tRNA, 5xDenhardt's solution, 0.1% tween 20, 50 µg/ml heparin) and PBT (1:1), 10 minutes in the hybridization solution and finally 1 hour at 55 °C. Riboprobe was added up to a final concentration of 0.3-0.5 ng/µl and the hybridization occurred overnight at the same temperature. It was necessary to keep all the working solution and materials RNAase free on the first day of WMISH.

The following day a series of washing was conducted at different temperatures and salinity to avoid unspecific interactions. Embryos were washed 2x15 minutes in 4xSSC, 50% formamide, 0.1% tween 20 and again 2x15 minutes in 2xSSC, 50% formamide, 0.1% tween 20. Successively, embryos were treated 3x10 minutes at 37 °C with 1 ml of solution A (0.5 M NaCl, 10 mM Tris-HCl pH 8.0, 5 mM EDTA, 0.1% tween 20), containing RNase A (20 µg/ml), then washed again 15 minutes with 1 ml of solution A(-RNAse A) at the same temperature. Another series of washing was performed 20 minutes in 2xSSC, 50% formammide, 0.1% tween 20, and 2x15 minutes in 1xSSC, 50% formammide, 0.1% Tween 20 at 45 °C, then 15 minutes in SSC:PBT (1:1), and 4x5 minutes in PBT.

Before the anti-DIG antibody addition, embryos were incubated 30 minutes at RT in PBT containing 5% sheep serum. The anti-DIG antibody (750 U/ml) is diluted 1:2000 in an equal solution. 500 µl of this solution were added to each sample incubated at 4 °C over night on a shaker. The samples were washed at RT 4x10 minutes in PBT, 2x5 minutes in AP buffer (100 mM NaCl, 60 mM $MgCl_2$, 100 mM Tris-HCl pH 9.5, 0.1% Tween 20). In order to localize the DIG-labeled RNA bound to anti-DIG antibodies conjugated with alkaline phosphatase, two substrates were added which were converted by the phosphatase into a blue coloured precipitate. The two substrates were Nitro Blue Tetrazolium (NBT) and 5-bromo-4-chloro-3-indoxyl phosphate (BCIP) and in particular, each sample was incubated in 1 ml of AP buffer containing 4.5 µl of NBT and 3.5 µl of BCIP. Timing of precipitate formation depended on the amount of bound antibodies. When a signal was found the staining reaction was stopped in PBT.

2.10. Immunohistochemistry

Immunohystochemistry was done on fixed electroporated and control larvae. In case of stored embryos, they were rehydrated and then washed with phosphate- buffered

saline (PBS, pH 7.4) containing 0.2% Triton X100 (PBST). Larvae were then incubated with 20% heat treated (65° C for 30 min) sheep serum (blocking buffer) overnight at 4°C. Next day pre-absorbed Rabbit anti-*Ciona* βγ-crystalline antibody (kindly provided by Sebastian M. Shimeld) diluted 1:2000 in blocking buffer was added and the embryos were incubated at 4° C overnight

After 6 hours washing with PBST, the larvae were incubated overnight at 4°C with pre-absorbed Alexa Fluorescence 594 donkey anti-rabbit IgG (Invitrogen) diluted 1:200 in blocking buffer, then washed 6 hours with PBST (rocking on ice), mounted on slides and examined under a confocal microscope at 594 nm (LSM510 META, ZEISS).

2.11. Electrophoretic mobility shift assay (EMSA)

2.11.1. Radiolabeling of oligonucleotide by 5' phosphorylation

6 pmol single-strand of both wild type and mutant Oligonucleotides were radiolabeled at 5' end by Polynucleotide kinase (PNK). This enzyme catalyses transfer of γ-phosphate residues from [γ-^{32}P]ATP to the 5'-hydroxyl terminal of dephosphorylated oligonucleotide. The reaction mixture contained: 6 pmol oligonucleotide, 10xPNK buffer 1 µl, 30 µCi [γ-^{32}P] ATP (3,000 Ci/mmol), 10 units T4 PNK, H_2O up to 10 µl. The reaction was incubated at 37 °C for 40 minutes. After addition of 0.66M NaCl, the labelled oligonucleotides were purified by gel-filtration on a Sephadex G-25 (Pharmacia) column to remove excess unincorporated nucleotide. 150 µl fractions were collected and 1 µl from each was counted by LS1701 Beckman scintillation counter, using 5 ml of Insta-Gel (Packard). The fraction containing the radioactivity peak was utilized for further use. The radiolabeled single-stranded oligonucleotides were then annealed with its cold complementary strand by boiling 5 minutes and slowly chilled overnight at room temperature.

2.11.2. *In vitro* transcription and translation

In vitro transcription and translation of the DNA binding domain (DBD) of *Ci-Ets1/2*, in PBS the vector, was carried out using the Kit (PROMEGA) "TNT Coupled Reticulocyte Lysate System". The reaction mixture contained: 25µl Reticulocyte Lysate, 1µg of *Ci-Ets1/2* plasmid, 2 µl 10X TNT buffer, 1µl T7 RNA Polymerase, 1µl of Aminoacid mix without Methionine (1mM), 2µl Methionine, H_2O DEPC up to 50 µl final volume. As positive control the cDNA of the Luciferase (500 ng/µl) has been used. The reaction was performed at 30°C for 90 minutes.

2.11.3. Band-shift assay

Band shift assay was performed in a mixture containing 10 mM Hepes pH 7.9, 60 mM KCl, 1 mM EDTA pH 8.0, 1 mM DTT, 20% glycerol and 6 pmol poly (dIdC). The mixture was incubated 10 minutes on ice with 2.5 µl of CiEts1/2 DBD (*in vitro* translated protein) before the addition of radiolabeled DNA probe (10^5 cpm) in a final volume of 20 µl in the presence or absence of specific or random double strand cold competitor oligonucleotides corresponding to a 200x molar excess. The sequence of the double strand random oligonucleotide (R) was: 5' -atagagtaagccgattattg-3'. After addition of the labeled DNA, the samples were placed 20 minutes on ice and successively separated by electrophoresis at 200 mV 2-3 hours on 5% polyacrylamide/0.5x TBE gel. Run was stopped when bromophenol blue ran out of the gel. After 2 hour drying at 70° C by means of a Bio-Rad 583 gel dryer, the gel was analyzed by autoradiography by exposing overnight on a Biomax MS film or by Tyfoon Phosphor-imager.

Table 2.3: Primers used for EMSA.

Name of primer	Sequence of primer 5'-3'
M2A	ACC AGC TAG CCA ACC AGA AAA CGA AAT CTG
M2S	CAG ATT TCG TTT TCT GGT TGG CTA GCT GGT
WT2A	ACC AGC TAG CCA ACC GGA AAA CGA AAT CTG
WT2S	CAG ATT TCG TTT TCC GGT TGG CTA GCT GGT
M4A	GAC TGA TGA CCC CAA TTC TGT GCG AAT AAA GCC AAT A
M4S	TAT TGG CTT TAT TCG CAC AGA ATT GGG GTC ATC AGT C
WT4A	GAC TGA TGA CCC CAA TTC CGT GCG AAT AAA GCC AAT A
WT4S	TAT TGG CTT TAT TCG CAC GGA ATT GGG GTC ATC AGT C

2.12. Quantitative PCR

2.12.1. Total RNA extraction from *Ciona intestinalis* embryos

All the procedures were carried out in a dust free environment, using clean gloves and RNAase free plastic instruments to prevent RNAase contamination.

Total RNA was extracted using ready-to-use reagent Trizol (Invitrogen and Roche). Tailbud stage of *Ciona intestinalis* was used for RNA extraction. In briefly, 200 to 400 embryos were collected in a 2 ml tube in 50 µl of fresh filtered seawater. Then 0.8-1 ml of Trizol has been added, in case of lower number of embryos, 5-10 µg of glycogen was also added to get a better yield. The samples were homogenized with a Tissue Lyser (Qiagen) in a continuous agitation for 2 minutes twice with a frequency of 20 Hz in presence of sterile steel spheres (3mm) to facilitate destruction and homogenization of the samples. Subsequently the samples were centrifuged at 12000 rpm for 10 minutes at 4°C. At this point the supernatants have been collected in new tubes of 1.5 ml. Prior to chloroform addition the specimens were incubated for 5 minutes at RT to facilitate the

complete dissociation of nucleoprotein complexes. After the addition of 160-200 µl chloroform the samples were mixed vigorously by hand and again incubated for 15 minutes at room temperature, following by centrifugation for 15 minutes at 12000 rpm. Then the upper colourless aqueous phase containing the RNA was recovered. In order to better eliminate the residues of phenol, two more centrifugations were done using chloroform in a 1:1 ratio with the recovered aqueous phase. The RNA contained in the aqueous phase was then precipitated by adding 0.5 ml of isopropyl alcohol followed by an incubation of 10 minutes at RT and centrifuged for 10 minutes at 12000 rpm. The RNA pellet was washed twice with 1 ml of chilled ethanol 75%. Finally, the RNA pellet was briefly air dried and dissolved with 10 µl of DEPC water.

To eliminate possible genomic DNA contamination, the RNA was treated with DNase I (Invitrogen). In brief, 1µl of DNase and 1µl of reaction buffer 10x was added to the dissolved RNA and incubated for 15 minutes at 25°C. The reaction was inactivated in the presence of 1µl of EDTA 25 mM and incubated for 10 minutes at 65°C.

The RNA has been then quantified using Nanodrop 1000 (Thermo Scientific) as Spectrophotometer. The quality of the extracted RNA was verified by loading on 1% Agarose gel in TBE (DEPC) to check for the presence of 28S and 18S ribosomal RNA.

2.12.2. cDNA synthesis:

Single strand cDNA synthesis from total RNA was obtained by SuperScript™ III First-Strand Synthesis System KIT (Invitrogen).

A mixture was prepared containing:

Total RNA	from 100 ng to 1 µg
Oligo $(dT)_{20}$ (50 µM)	1µl
dNTP mix (10mM)	1µl
H_2O DEPC	up to 10 µl

This mixture was heated at 65°C for 5 minutes and cooled on ice for 1 minute. Subsequently 10 µl of the following solution was added: 2µl of 10X RT Buffer, 4µl $MgCl_2$ (25 mM), 2µl DTT (0.1 mM) , 1µl RNase OUT™ (40U/µl) and 1µl Super Script™ III RT (200U/µl).

The cDNA was then prepared by a series of incubations of the above mentioned reaction mixtures:

25°C for 10 minutes,

50°C for 50 minutes

and finally at 85°C for 5 minutes.

To eliminate the RNA template 1 µl of RNaseH was added and incubated at 37°C for 20 minutes. The resulted cDNA was used for the Real Time PCR experiments.

2.12.3. Quantitative Real-time PCR (qPCR)

qPCR is a powerful and widely used method for measuring gene expression. The fluorescence of intercalating DNA dye is monitored at each cycle during the amplification. This is proportional to the amount of amplicon production. During the exponential phase the amount of product increases linearly (on a log plot). Therefore, PCRs from different samples can be compared to determine which among them contains the higher amount of a specific sequence. This is done by setting a threshold in the linear phase of amplification and assessing how many cycles are necessary to reach the same level of product amplification in the different samples. The number of cycle is called Ct {reviewed in (Wong and Medrano, 2005)}. Because of the chemistry used, when the difference in the amount of a specific sequence between two samples (a "control" and an "experimental" one) is assessed, this is given by $2^{\Delta Ct}$, where 2 is the multiplier for amplification per cycle, and ΔCt is the difference in the Ct between the two samples.

All qPCR reactions were conducted using an MJ Research-Biorad Chromo 4 machine, equipped with "Opticon Monitor" analysis software. The dye used was "Fast Start Sybr Green Master" (Qiagen), which binds to double stranded DNA (dsDNA). SYBR green dye can not distinguish between the amplicon and contamination products from mispairing or primer-dimer artifacts. To overcome this, not only DNA synthesis is monitored, but also the melting point of the PCR products is measured at the end of the amplification reaction. The melting temperature of a DNA double helix depends on its base composition and its length. Therefore, qPCR products can be distinguished from mispairing or primer-dimer artifacts. For each gene qPCR primers were designed to generate products of 100-200 bp, by using online based "Primer 3, v.0.4.0" software (http://fokker.wi.mit.edu/primer3/input.htm).

This method requires a known reference gene as internal control with constant expression in all tested samples and whose expression is not changed by the treatment under study. A pair of primers for Rps27 ribosomal gene has been used as standard reference. The number of cycles needed for the standard to reach a specified Ct is used to normalize the Ct for the selected genes. A higher Ct for the gene of interest implies a lower initial material in the sample, and vice versa.

To capture intra-assay variability all RT-qPCR reactions were carried out in triplicate and the average Ct value was taken into account for further calculations. The efficiency of each pair of primers was calculated according to standard method curves using the equation $E=10^{(-1)/slope}$. Five serial dilutions were set up to determine the Ct value and the efficiency of reaction of all pairs of primers. Standard curves were generated for each oligonucleotides pair using the Ct value versus the logarithm of each dilution factor. Diluted cDNA was used as template in a reaction containing a final concentration of 0.3 μM for each primer and 1X FastStart SYBR Green master mix (total volume of 25 μl). PCR amplifications were performed in triplicate in a Chromo4TM Real-Time

Detector (Biorad) thermal cycler using the following thermal profile: 95°C for 10 min, one cycle for cDNA denaturation; 95°C for 15 sec and 60°C for 1 min, 40 cycles for amplification; 72°C for 5 min, one cycle for final elongation; one cycle for melting curve analysis (from 60°C to 95°C) to verify the presence of a single product. Each assay included a no-template control for each primer pair. Fluorescence was measured using Opticon Monitor 3.1 (Biorad).

Real time PCR has been carried out in order to analyze expression changes between embryos with interfering endogesnous *Ci-TCF* expression versus wild type (Wt) embryos. To determine the expression ratio between the sample and control embryos, Pfaffl Method for relative quantification in real-time PCR has been used. In this method, the relative quantification of target gene transcripts is obtained in comparison to a reference gene transcript. This calculation is based on the following equation (Fleige *et al.*, 2006):

$$\text{Ratio} = \frac{E\,(\text{Target})^{\Delta Ct\ \text{target(Control-Treated)}}}{E\,(\text{Reference})^{\Delta Ct\ \text{reference(Control-Treated)}}}$$

In the above equation, E target and E reference are the amplification efficiencies of the target and reference genes, respectively. ΔCt, target (Control–Treated) = Ct of the target gene in the control sample minus the Ct of the target gene in the treated sample, and ΔCt, reference (Control–Treated) is the Ct of the reference gene in the control sample minus the Ct of the reference gene in the treated sample. Data for each gene were normalized against Rps27. A ratio above 1 indicates an increase in the transcript for that particular marker gene in the experimental sample compared to the control while, a value ranging from 0 to 1 indicates a decrease, it means that that gene is down regulated. To obtain a negative value for the down regulated gene, the following formula can be used.

$$IF(E_{target}^{(Ct_{mean-wt}-Ct_{mean-mut})} > E_{reference}^{(Ct_{mean-wt}-Ct_{mean-mut})};$$

$$\frac{E_{target}^{(Ct_{mean-wt}-Ct_{mean-mut})}}{E_{reference}^{(Ct_{mean-wt}-Ct_{mean-mut})}};\frac{1}{E_{target}^{(Ct_{mean-wt}-Ct_{mean-mut})}/E_{reference}^{(Ct_{mean-wt}-Ct_{mean-mut})}})*(-1))$$

Alternatively a simplified version of this formula can be used too:

$$\left(\frac{1}{Ratio}\right)*(-1)$$

Since qPCR on tailbud stage was performed in three replicates and at least 3 times, the variation was evaluated statistically by standard deviation (STDEV) using "Microsoft Excel Worksheet". The standard deviation is a measure of how widely values are dispersed from the average value, the mean. STDEV uses the following formula:

$$\sqrt{\frac{\sum(x-\bar{x})^2}{(n-1)}}$$

Here "x" is the sample mean AVERAGE (number1,number2,...) and "n" is the sample size.

qPCR primers used in this study are listed in table 2.3.

Table 2.4: qPCR primers:

Name of qPCR primer	Sequence (5'-3')
Arrestin F	5'CAAGTGTCCTGTTGCCTTCA3'
Arrestin R	5'CCAGACCTCGCTTATCCTTG3'
Bmp F	5'TCC AGA GAG TTG CGG AGA AT 3
Bmp R	5'GCA TTG CTT GGT ACA CGT TG 3
Gapdh F	5'GCACTCGTACACTGCTACCCAGAAGAC3'
Gapdh R	5'GCTGTATCCAAATTCATTGTCGTACCAG3'
Mitf F	5'ATTGAGCGGAGACGAAGGTA3'
Mitf R	5'TGCACGATGTTTCTGTTGT3'
Opsin1 F	5'TTCGTTGGCGGGTTTATTAG3'
Opsin1 R	5'CAGCAATTGAGAGCAAACCA3'
Pax6 F	5'ACCGCGTTCTTCGAAACTTA3'
Pax6 R	5'GGCAACCAACCGTTACAAGT3'
Rps27 F	5'AAT CCA CCC TTC ACC TTG TG 3
Rps R	5'GGG AGA TCT TGC CAT TTT CA 3
Rx F	5'CCTCGAACGAAGATCAAAGC3'
Rx R	5'ACATCCGGGTAGTGAGATCG3'
TCF F	5'CCAACTAGCCCAACACCATT3'
TCF R	5'TGGCAGGGTGTGGTATCAT3'
Tyrosinase F	5'AGT GTT GCC CAA CTT TCA CC 3
Tyrosinase R	5'GAC ACG CAC GAT CGT AAA AA 3

2.13. Preparation of construct

Different constructs were prepared during this PhD study, the cloning strategies of them are explained below:

2.13.1. Reporter constructs for electroporation

Reporter construct for *pTCF2.0>GFP* was prepared from *C. intestinalis* genomic DNA by PCR amplification using specific oligonucleotides. The primers were designed based on the genome sequence available at the JGI *Ciona* genome project database consisting of SmaI site at their 5' end. The amplification was done for a region of almost 2 kb upstream from the *Ci-TCF* translation start site. (from -2000 to -35) The PCR product was then phosphorylated and cloned upstream from GFP in a vector already linearized by SmaI (*pTCF2.0>GFP)*. The basic vector used for this purpose was pBluescript II KS containing GFP (Green Fluorescence Protein) as a reporter gene together with SV40 polyadenylation sequences REF. This 2 kb and all the subsequent PCR fragments were inserted in 5'-3' orientation.

The primers used for this 2 kb region:

pTCF1 (5'-CTTAAACCTGTATTAGTGTATCAACCA-3') and

pTCF9r (5'-GCGCTGTTATGCGATCAAAACTATCTACCG-3').

Subsequently other TCF *cis*-regulatory constructs (*pTCF0.4* {cF-cR}, *pTCF 0.100* {cF-c1r}, *pTCF 0.170* {c3-cR}, *pTCF 0.210* {cF-c2r} and *pTCF 0.220* {c2-cR}) were generated by PCR amplification with appropriate primers from *pTCF 2.0.* In all cases the primers were designed with EcoRI site at their 5' ends. After digestion they were purified by columns. Since all these short promoter regions were lacking the TATA box, the purified fragments were inserted in a vector containing Epstain Barr Virus basal promoter sequence *E1bTATA* upstream from GFP which was already available in the laboratory.

Table 2.5: Oligo for different TCF enhancer fragments:

Name of primer	Sequence of primer 5'-3'
cF	AAT TCC GGC TTA AAA GAA ACA G
c3	CTT TGT TCT ATC CGT TAA
c1r	CAA CCG GAA AAC GAA ATC
c2r	CTT TCC TCT TTG CAA TAT
cR	CAG TCT AGA ATT CTG TAC ACT GAA ACA GCT C

2.13.2. Construct for *in vitro* protein translation

In order to prepare Ets 1/2 protein for band shift assay, it was necessary to clone Ets downstream to T7 promoter for *in vitro* translation by "TNT Coupled Reticulocyte Lysate System". The original construct used for this purpose was *T7>TCF-SV40*, which was prepared in the laboratory previously for *Ci-TCF* riboprobe. The vector was prepared by removing the coding sequence of *Ci-TCF* by digesting with *Not I* and *Spe I* since TCF contained *Not I* and *Spe I* site at 5' and 3' ends respectively. Then after dephosphorylation the digested plasmid was purified by gel elution.

Ets 1/2 DNA binding domain was obtained by double digestion of another construct *pTyr>EtsVP16* (a kind gift from Filomena Ristoratore) with *SpeI* and *Not I. Not I* site was present at the 5'of Ets DBD while VP16 was linked with ETS DBD by *Spe I.* After digestion the fragment was inserted in the previously prepared vector by ligation.

2.13.3. *pTyr>ΔN Ci-TCF*

The vector (*pPans>Sv*) used to prepare *pTyr>ΔN Ci-TCF* was already available in the Laboratory. *pPans>Sv* contains a polylinker (*Sac*I, *Bst*XI, *Sac*II, *Not*I, *Eag*I), *Ci-Pans* promoter (Alfano et al., 2007), a second polylynker (*BamH*I, *Sma*I, *Sal*I, *Sac*I, *Spe*I, *BamH*I, *EcoR*I) and the *SV40* intron in pBluescript vector..

The dominant negative form of *Ci-TCF* coding sequence (*ΔN TCF*), lacking N-terminal β-catenin binding domain, was prepared by PCR from a construct containing the full coding sequence of *Ci-TCF* using two oligonucleotides containing *Spe*I site at 5' end; *N1F* (5'-AGAACTAGTCACC**ATG**TACGATGTTCCGGCAAAAGTA-3') and *N1R* (5'-AGAACTAGTTCAGGATTTTCCTTCTAATGCTGATG-3').Oligo *N1F* corresponds to the TCF sequence 198-221 and contains at the 5' end the *Spe*I site, a Kozac consensus and an *ATG* (in bold) respectively; oligo *N1R* corresponds to the sequence 2038-2064. After *Spe*I digestion, the PCR fragment (*ΔN Ci-TCF)* was eluted from gel and was inserted into linearized vector, *pPans>SV* (digested with SpeI). The resulted vector was named *pPans>*ΔN *Ci-TCF/SV*. The final clone was made by replacing *pPans* with *pTyr* from *pPans> ΔN Ci-TCF/SV*. *pTyr* promoter was amplified from a construct kindly provided by Dr. Fimolena Ristoratore, with the oligos *pTyrF* (5'-ATGAGCTCGCGGCCGCTGCCTTTTGAGAATTACC-3') and *pTyrR* (5'-ATGAGCTCGCGGCCGCGCTCTGCTTCTGGAAGGC-3') containing *Sac*I and *Not*I at the 5' ends. The PCR product, *pTyr*, as well as the vector *pPans>ΔN Ci-TCF/SV* were digested with *Sac*I and purified by gel extraction. Ligation was performed (T4 DNA Ligase, New England Biolabs) and thus the resultant construct, *pTyr> ΔN Ci-TCF* was prepared.

2.13.4. *pTyr>ΔN Ci-TCF mChe*

Construct *pTyr>ΔN Ci-TCF-mChe* was prepared by replacing Dn FGFR with *ΔN TCF* in *pTyr> FGFR^{DN} mChe*. The construct was kindly provided by F. Ristoratore (unpublished). The insert was generated by PCR (Expand High Fidelity from Roche) with suitable oligos. The forward primer (TCF-B NotI: 5'ATA GCG GCC GCA GGG TCT ATA ATC ACC ATG TAC GAT GTT CC 3') contained a *Not I* site at its 5'end followed by E1BTATA, Kozac consensus and an *ATG* respectively. The reverse oligo (TCF end

BamHI: 5'ATG GAT CCG CTG ATG TTG CAC GGC GG 3') contained a *BamHI* site at its 5'end. The sequence amplified by PCR with these specific oligos spans a region of 1847 bp (+169-+2015) coding sequence of *Ci-TCF* lacking the stop codon because, the primers were designed to have mCherry in frame which lacks the initial Methionine. After PCR the fragment was double digested with *NotI* and *BamHI*, followed by column purification. The vector was also double digested with the same enzymes and dephosphorylated with CIAP. Then after gel elusion the ligation was performed.

2.14 Diagram, graphs and drawings

Figures were made using Adobe Photoshop and Microsoft Power Point. Graphs and calculations were prepared by Microsoft Excel.

2.15 Alignments and phylogenetic analysis

A phylogenetic tree comparing *Ciona intestinalis* TCF protein and homologues from other species was constructed to understand its evolutionary position.

Protein sequences for human, *Ciona savignyi*, and *Drosophila melanogaster*, zebra fish, chicken and sea urchin family members were obtained using the NCBI Entrez Protein Database (http://www.ncbi.nlm.nih.gov/entrez/query.fcgi?db=Protein). CiTCF protein sequence used in multiple alignment and phylogenetic tree construction was deduced from the Nucleaic acid sequence of *Ci-TCF*.

Protein domains were identified using SMART (Letunic et al., 2006; Schultz et al., 1998) (http://smart.embl-heidelberg.de/) and Pfam (Bateman et al., 2004) (http://pfam.sanger.ac.uk/) databases.

To obtain a simpler phylogenetic tree, each member of vertebrate TCF protein family was individually aligned with *Ciona* TCF protein. Then the closest homolog was chosen for the final alignment and phylogenetic tree construction.

Multiple sequence alignment was done with CLUSTAL -W (Thompson et al., 1994) presented in Jalview (Clamp et al., 2004). Phylogenetic reconstruction was carried out using the neighbor-joining method (Saitou and Nei, 1987), and bootstrap values determined by 1000 replicates. The tree was also generated using maximum parsimony method with bootstrap replicates of 1000. The final output of the phylogenetic tree was obtained using MEGA-4 software version 1.6.6 (http://taxonomy.zoology.gla.ac.uk/rod/treeview.html). Accession numbers for TCF proteins used in these analyses are listed in table 2.6.

Table 2.6: Accession numbers of TCF proteins used in phylogenetic analyses:

Species	**Database**	**Acc Code/Reference**	**Gene**
C. savignyi	NCBI	BAB68354.1	Cs-TCF
S. purpuratus	NCBI	NP_999640.1	TCF/LEF
D. melanogaster	NCBI	NP_726522.1	Pangolin/dTCF
H. sapiens	NCBI	NP_001128323.1	TCF1/TCF7
H. sapiens	NCBI	NP_112573.1	TCF3/TCF7L1
H. sapiens	NCBI	NP_110383.2	TCF4/TCF7L2
H. sapiens	NCBI	NP_057353.1	LEF1
G. gallus	NCBI	NP_989878.1	TCF1/TCF7
G. gallus	NCBI	AAM73850.1	TCF3
G. gallus	NCBI	BAA92881.1	TCF4
X .laevis	NCBI	NP_001082691.1	TCF1/TCF7
X. laevis	NCBI	NP_001080938.1	TCF3
X. laevis	NCBI	NP_001083866.1	TCF4
X. laevis	NCBI	NP_001082124.1	LEF1
D. rerio	NCBI	NP_001012389.1	TCF1/TCF-7
D. rerio	NCBI	NP_571344.1	TCF3a/TCF7L1a
D. rerio	NCBI	NP_571371.1	TCF3b/TCF7L1b
D. rerio	NCBI	NP_571334.1	TCF4/TCF7L2
D. rerio	NCBI	NP_571501.1	LEF1

CHAPTER 3

THE *Ciona intestinalis TCF* GENE FAMILY

Genes belonging to the TCF (T cell factor)/LEF (Lymphoid enhancer factor) family have been identified in a variety of organisms from fly to mammals analysed to date. Vertebrate genomes contain four members of this family while in invertebrate as well as in non-chordate genomes one member is reported {reviewed in (Arce et al., 2006)}. The whole genome of *Ciona intestinalis* has been sequenced and published in 2002. By annotating the sequenced genome, a single member of the LEF/TCF gene family has been reported in this tunicate model species which is called *Ci-TCF* (Arce et al., 2006). In this chapter, analysis of conserved domains and phylogenetic comparison of the Ci-TCF protein is described.

3. Phylogenetic analysis and domain structure of TCF gene:

In order to analyze the phylogenetic relationship of Ci-TCF protein with the vertebrate members of its family, the amino acid sequence of *Ci-TCF* was blasted in NCBI, Pfam and SMART data bases.

3.1 Domains:

SMART and Pfam databases recognized two conserved domains in Ci-TCF deduced protein sequence: β-catenin binding domain, also known as CTNNB1 binding domain, and High mobility group domain (HMG), which is the DNA binding domain of this transcription factor.

The alignment done with CLUSTAL-W permitted to verify the conservation of Ci-TCF amino acid sequence with other chordate and non chordate species. Conservation is noticeable in two domains β–catenin binding domain {from 1-50 aa (Yi and Merrill, 2007)}and HMG domain {from 277-350 aa (Pfam database)}. HMG shows the highest conservation in alignment, which is very logical since it recognizes and interacts with the target DNA sequence. Conservation is also observed in E-tail which is located between 370-400 aa (Atcha et al., 2007).

In Fig. 3.1 CLUSTAL-W alignments of deduced Ci-TCF aa with other vertebrate and non-vertebrate members are shown. This alignment is done by comparing TCF protein sequences of three representative vertebrate TCF family members; two tunicate species; two non-chordate species, the deuterostome sea urchin *Strongylocentrotus purpuratus* and the fly *Drosophila melanogaster.*

The vertebrate organisms included here are the two widely used model species, Chicken (*Gallus gallus*) and Zebra fish (*Danio rerio*). The other vertebrate species is human (*Homo sapiens*). The tunicate species included here is *C. intestinalis* itself and its' sister species *C. savignyi.* Although, the vertebrate species included in this analysis each contain at least 4 TCF/LEF family proteins (except zebra fish which contains 5), one member from each organism was used. To this end I first aligned *Ciona* TCF protein sequence with each member of vertebrate TCF/LEF family individually. Then I chose the closest vertebrate member for further alignment and phylogenetic tree construction.

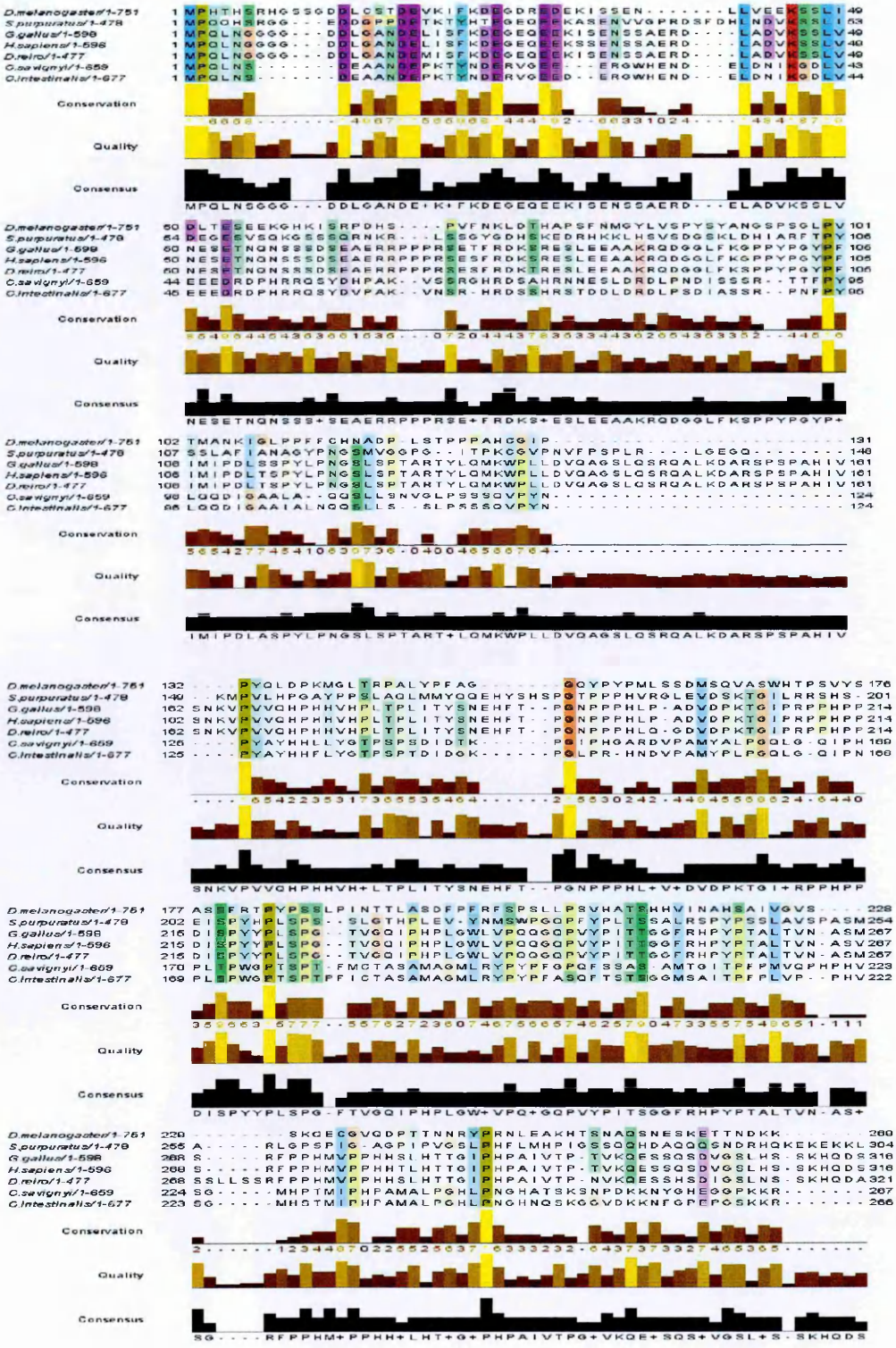
D.melanogaster/1-751
S.purpuratus/1-478
G.gallus/1-598
H.sapiens/1-596
D.reiro/1-477
C.savignyi/1-659
C.intestinalis/1-677
Conservation
Quality
Consensus

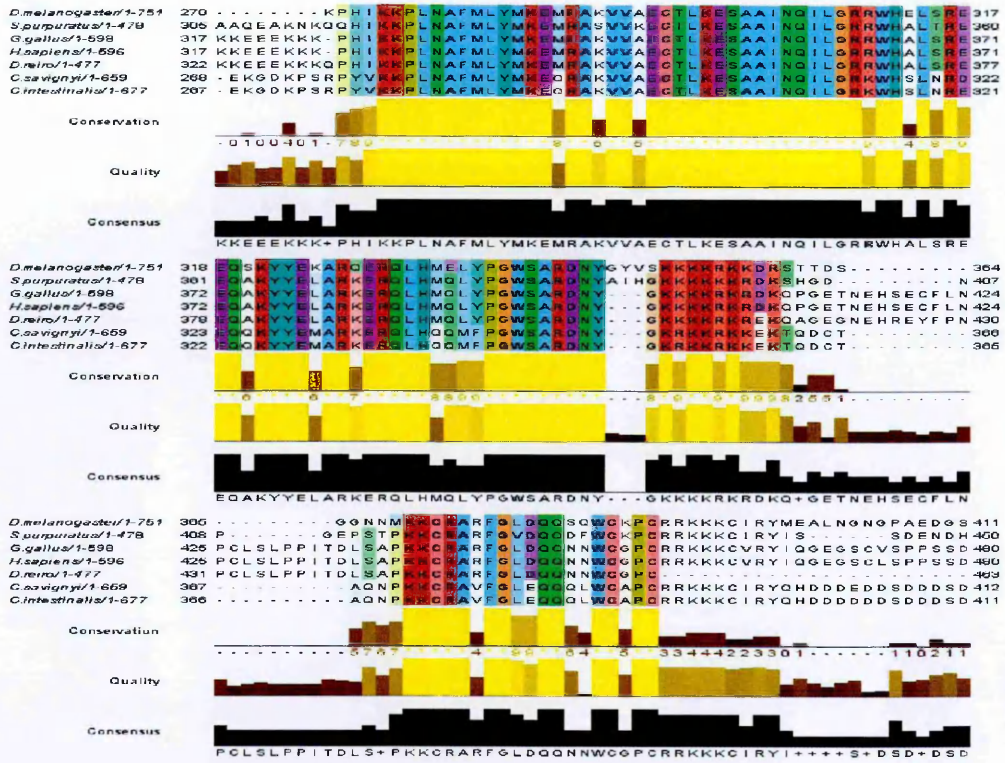

Figure 3.1: CLUSTAL-W alignment of protein sequence of the LEF/TCF family members.

The alignment shown here includes one member of the LEF/TCF family from vertebrate species; TCF3. For each residue, the level of conservation between all Tcf family members and the quality of the alignment are indicated by the yellow-brown bar. The high level of amino acid conservation in the HMG domain of all Tcf proteins is noticeable.

3.2 Phylogenetic tree:

The phylogenetic study of gene families provides insight into the evolution and function of genes, as well as contributes to the understanding of genome evolution. Ascidians occupy a unique position in the chordate branch since they belong to the phylum Urochordata, a sister group of vertebrates. Thus, they represent a starting point to understand the evolution and origin of chordate-and vertebrate-specific features. The *TCF* gene family has an extremely ancient origin. A *TCF* gene is present in one of the simplest multicellular organisms such as Hydra (Plickert et al., 2006). Moreover, this gene is a

component of the canonical Wnt signaling cascade which is involved in various aspects of embryonic development. Thus, the members of the TCF protein family are subject of particular interest because their functions and their modifications could be linked to many developmental processes during evolution.

To understand the relationship of TCF protein family members among chordate and non chordate representatives, in particular with the aim to clarify the position of the Ci-TCF member, a phylogenetic tree was constructed. The tree showed that Ci-TCF is more closely related to the vertebrate TCF-4 than to non-vertebrate TCF members. At first glance it is easily visible that all chordate TCF members have a common branch where Ci-TCF and Cs-TCF were grouped together and branched out from a common root of the vertebrate TCF-4. While TCF from the two non-chordate representatives grouped together and branched out separately from the common chordate branch (Fig.3.2).

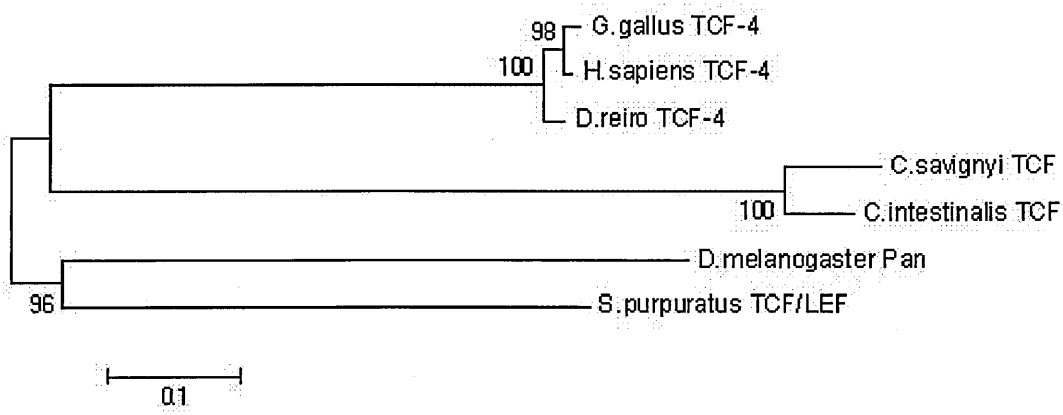

Figure 3.2: Phylogenetic tree relating TCF protein sequences.

Neighbor Joining tree of TCF proteins. The tree was generated from the alignment of the amino acid sequences of the TCF proteins using CLUSTAL W and Mega 4 (see Materials and methods for details). Validation of the tree using maximum parsimony methods confirmed all group nodes. Numbers at nodes are percentage of 1000 bootstrap replicates that support the branches. Groups are appended with the species designation (one letter for the genus with complete species names; beside the member of the TCF family; see Table 2.5 for complete names and sequence accession numbers). The scale bar indicates 10% replacement of amino acid per site.

CHAPTER 4

RESULTS

4.1. Interfering endogenous *Ci-TCF* activity by the dominant negative form of *TCF*

The first approach with *Ci-TCF* was to better define its involvement in pigment cell differentiation.

4.1.1 *pTyr>ΔN Ci-TCF* phenotype

Loss of function experiments using a *Ci-TCF* morpholino oligonucleotide were used, as first approach, to study the role of *Ci-TCF* in pigment cell differentiation. We faced many difficulties to obtain a reproducible phenotype despite of the huge number of experiments done. The problem is mostly related to the presence of *Ci-TCF* maternal transcript that is involved in the regulatory network which patterns the early ascidian - ectoderm (Rothbacher et al., 2007). Given this important function early in embryogenesis, it revealed to be very difficult to inject the right dose of morpholino able to interfere with the zygotic transcript without affecting the maternal transcript. To circumvent these problems I exploited an approach based on transgenesis experiments. In the laboratory, a *Tyrosinase* enhancer able to drive reporter expression in pigment cell precursors since the late neurula stage was already identified. A dominant negative form of *Ci-TCF* coding sequence, deprived of the N-terminal armadillo repeats responsible for the interaction with β-catenin (*ΔN Ci-TCF)*, was fused downstream from the pigment cell promoter, pTyr. The aim was to interfere with zygotic *Ci-TCF* function, specifically in pigment cells, almost at

the time when the endogenous gene is activated. The resulting fusion construct, *pTyr>ΔN Ci-TCF,* was introduced into *Ciona* fertilized eggs via electroporation and embryos were scored at the larval stage for the presence of pigment cells in the brain. As control, *pTyr>GFP* was used.

The phenotype obtained with this construct, *pTyr>ΔN Ci-TCF* can be classified into two categories, according to the number of pigment cells. Among them, almost 35% of larvae contained only one pigment cell, that at the morphological level appears to be either otolith or ocellus,. In few cases, around 5% the pigment cells were absent completely and 60% showed normal phenotype containing both pigment cells (Fig. 4.1.1).

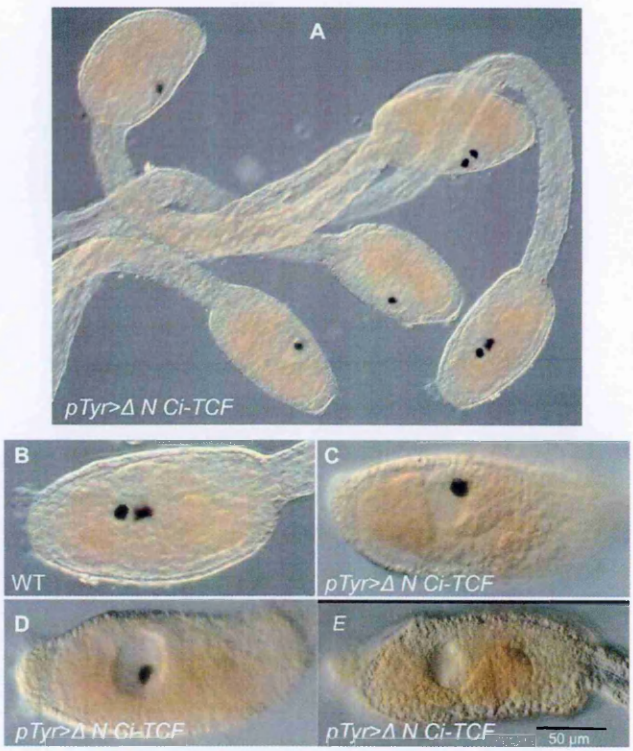

Figure 4.1.1. Interference with *Ci-TCF* function by *pTyr>ΔN Ci-TCF* electroporation. A: Group, B: control (wild type) and C&D: two representative larvae showing a single pigmented cell in the sensory vesicle. E: sensory vesicle without any pigmented cell. Wt-Wild type, Anterior is at the Left.

The phenotype seems very specific since no other evident aberration in development was detected.

Table 4.1: Phenotypes obtained in *pTyr>ΔN Ci-TCF* electroporated embryos:

Phenotypes	Phenotype in percentage	Phenotype in total screened larvae
No pigment cell	5%	23/457
1 pigment cell	35%	160/457
2 pigment cells (Wt)	60%	274/457

A co-electroporation, with *pTyr>ΔN Ci-TCF* and *pTyr>GFP*, was used to label with GFP the cells where endogenous *Ci-TCF* activity was perturbed by *pTyr>ΔN Ci-TCF* (Fig. 4.1.2).

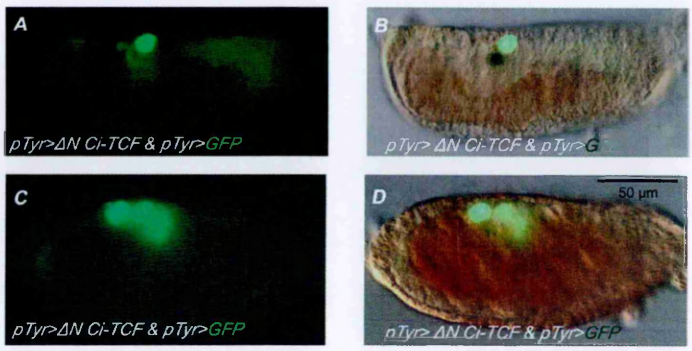

Figure 4.1.2. Transgenic larvae, co-electroporation with *pTYR>ΔN Ci-TCF & pTYR>GFP*.
A &B: GFP is localized in a cell different from the pigmented one or C &D: in two cells in the brain region lacking any pigmented cell.

To follow more precisely the fate of pigment precursor cells in endogenous *TCF* perturbed larvae, I prepared a transgene in which *ΔN Ci-TCF* was fused in frame with the coding sequence for the red fluorescence protein mCherry, under the control of the *pTyr* enhancer.

Transgenic embryos with this *pTyr>ΔN Ci-TCF-mChe* construct allowed me to detect, *in vivo*, the cells expressing *ΔN Ci-TCF*, through mChe fluorescence. The use of

this transgene caused no more variations, in comparison with phenotype alterations previously obtained. Fig. 4.1.3 shows larvae expressing this construct.

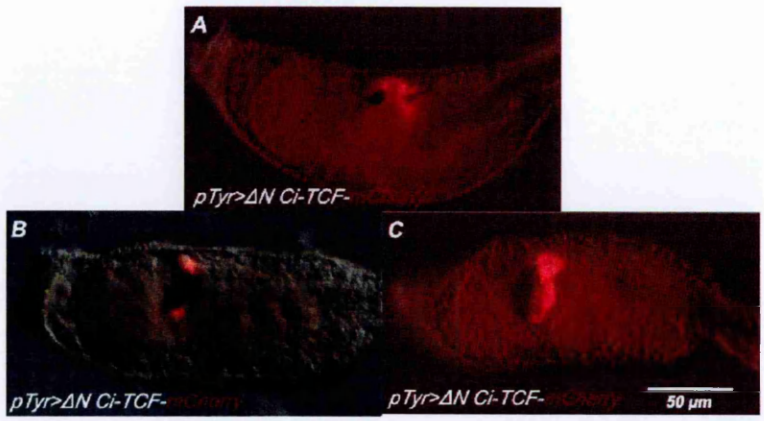

Figure 4.1.3. ***pTyr>ΔN Ci-TCF-mChe*** **transgenic larvae.** A: showing mCherry expression in larva containig both pigment cells in the sensory vesicle. B: larvae with single pigment cell but expressing red fluorescence in two cells and C: larvae lacking both pigment cells: the presence of red fluorescent-ΔN Ci-TCF-mChe, is observed in the sensory vesicle. Lateral view, anterior is at the Left

mCherry expression also permitted to trace back *ΔN Ci-TCF* expression in embryos at the tailbud stage (Fig. 4.1.4).

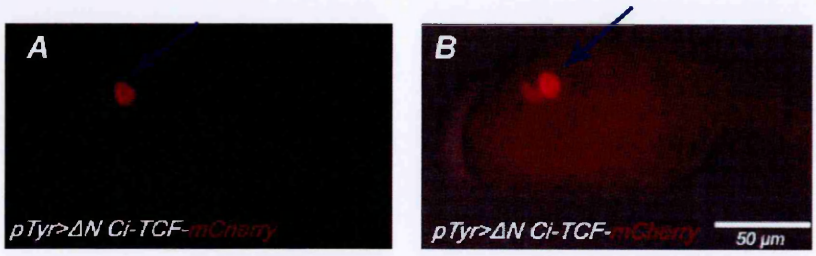

Figure 4.1.4. ***pTyr>ΔN Ci-TCF-mChe*** **transgenic embryo, tailbud stage.** A & B: Red fluorescence is visible in two cells in the trunk region, blue arrow. Tailbud, lateral view, anterior at the Left.

4.1.2 Immunohystochemistry with βγ-crystallin on *pTyr>ΔN Ci-TCF* electroporated larvae

It was necessary to define the pigment cell type in the 35% larvae containing single pigment cell obtained in previous experiment with *pTyr>ΔN Ci-TCF*. From morphological

analysis it seemed that in 50% of them the otolith developed whereas, in the other half, the pigment cell appeared to be of the ocellus type.

To this end I did immunohistochemistry experiments, using an otolith specific marker, the βγ-crystallin antibody that recently has been identified as a marker for otolith development in ascidians, as well as palps (Shimeld et al., 2005).

Fig. 4.1.5 exhibits the results of imunohistochemistry, where the fluorescence is visible in the palps of all larvae. In 50% of the single pigment cell containing larvae the signal was found in the pigment cell of the brain, indicating the development of the otolith. The remaining 50% embryos did not show any fluorescence in the sensory vesicle which suggests that the single pigment cell has the ocellus characteristics.

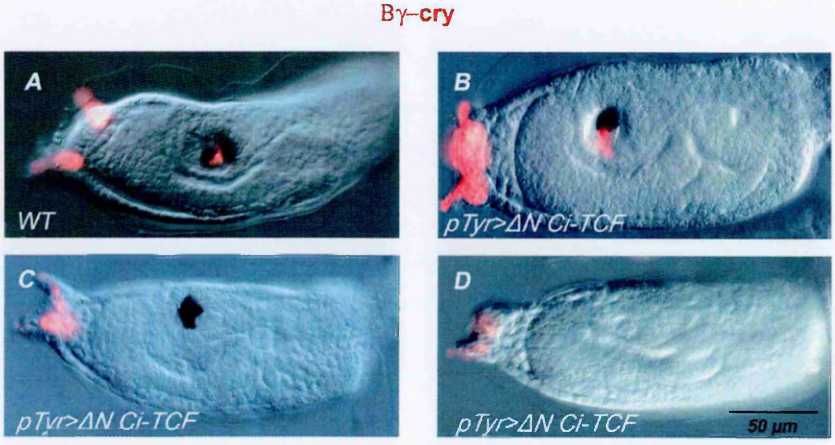

Figure 4.1.5. Immunohistochemical detection of βγ-crystallin on *pTyr>ΔN Ci-TCF* transgenic larvae. A: wild type specimens. B, C: 35% of the larvae showed only one pigment cell in the sensory vesicle, resembling, morphologically, the one of the otolith (B), presence of βγ-crystallin expression in the sensory vesicle is detectable, around the pigment cell. Or the one of the ocellus sensory organ (C) lacking βγ-crystallin fluorescence. D: 5% of the total screened larvae showed complete absence of pigment cells and no βγ-crystallin expression in the sensory vesicle otolith region. Anterior is at the left; w.t., wild type; βγ cry, βγ-crystallin.

4.1.3 In situ hybridization on *pTyr>ΔN Ci-TCF* electroporated embryos

in situ hybridization experiments, on endogenous *Ci-TCF* perturbed tailbud and larval stage embryos, were used to better define the *pTyr>ΔN Ci-TCF* phenotype and compare with the same stages of wild type embryos. The probes were chosen according to

the expression pattern in pigment organ territories, by screening the ascidian literature and ANISEED database (Ascidian Network for *In Situ* Expression and Embryological Data) (http://aniseed-ibdm.univ-mrs.fr/). *in situ* experiments done on tailbud stage with probe *Ci-Tyrosinase* (Caracciolo et al., 1997) *Ci-Mitf* and *Ci-Bmp 5/7* (unpublished), of the perturbed embryos did not yeild any significant differences in the signal, compared with the control.

On the contrary, a strongly reduced signal for *Ci-Tyrosinase* was found in larvae with one and no pigment cell compared to wild type larvae indicating the involvement of *Ci-TCF* in *Ci-Tyrosinase* gene expression regulation (Fig.4.1.6). However, in situ of larval stage with *Ci-opsin* and *Ci-Arrestin* (Kusakabe et al., 2001) probe did not show any detectable variation in the staining between control and electroporated embryos.

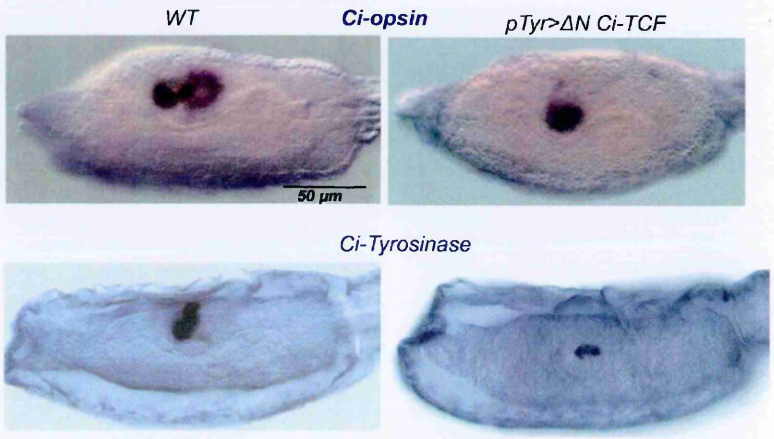

Figure 4.1.6. *in situ* hybridization on *pTyr>ΔN Ci-TCF* transgenic larvae.
(A&B) with *Ci-Opsin* probe, A: Wt larvae *Ci-opsin* staining around the ocellus, B transgenic larvae with a reduced staining in the brain vesicle. (C& D) with *Ci-Tyr* probe Tyrosinase signal in the pigment cells of control larvae (C) and in the brain vesicle of transgenic larvae (D).

4.1.4 Real time quantitative PCR with *pTyr>ΔN Ci-TCF* electroporated embryos

Tailbud stage of *pTyr>ΔN Ci-TCF* electroporated embryos were chosen to investigate possible changes in the expression levels of some selected genes and compared with wild type embryos. Phenotype of the transgenic larvae from this construct mimics the

phenotype of *Ci-TCF* morpholino injected larvae in terms of loss of *Ci-TCF* function (Fig. 4.1.1).

Various genes expressed in the sensory vesicle and involved in the pathway of eye and/or of pigment cells formation in Vertebrates and/or *Ciona* have been analyzed: *Ci-Opsin1*; *Ci-Arrestin*; *Ci-Mitf*; *Ci-TCF*; *Ci-Pax6*; *Ci-Tyrosinase*; *Ci-BMP; Ci-Rx. Ci-opsin1* and *Ci-Arrestin* are specifically expressed in the photoreceptor cells of the ocellus and are both involved in the transduction of the light signal (Kusakabe *et al.*, 2001; Nakagawa *et al.*, 2002). *Mitf* is an essential factor in the pathway of development and function of all melanin-producing pigment cells in vertebrates. In ascidian *Halocynthia roretzi Mitf* (Yajima *et al.*, 2003) is expressed in the pigment cells and activates the promoter of *Tyrosinase,* a key gene responsible for melanogenesis in all types of pigment cell. In *Ciona intestinalis Ci-Mitf* expression has been observed in pigment precursor cells (unpublished). *Ci-Tyr* has been found to be expressed in pigment precursor cells at tailbud stage (Caracciolo et al., 1997). *Pax6* plays an important role in the development of eyes and central nervous system (CNS) in many animal groups. In *Ciona* it is expressed in the caudal nerve cord and in the anterior brain associated to the photoreceptive ocellus (Irvine *et al.*, 2008). BMPs are multifunctional growth factor involved in various aspects of embryonic development including that of the vertebrate eye (Sehgal et al., 2009). In *Halocynthia roretzi* BMP/CHORDIN antagonism determines the terminal differentiation of ocellus and otolith in a dose-dependent manner (Darras and Nishida, 2001). *Rx* gene belongs to the paired-like class of homeobox-containing genes, which has a critical role in the development of the eye in several vertebrate species including *Xenopus*, mouse, chicken, medaka, zebrafish and human. *Rx* has been suggested to be involved in ocellus formation in *Ciona* because loss of *Ci-Rx* expression produces ocellus less phenotype (D'Aniello et al., 2006).

All the Real Time PCR experiments have been done in triplicate, on three different batches of embryos, and the data have been normalized using *Ci-Rps27*as reference gene. In Fig. 4.1.7, the fold differences in transcript levels of these genes between Wt and *pTyr>ΔN Ci-TCF* electroporated embryos were shown. Only those genes showing a fold difference greater than 2 were considered significant. Real Time PCR data in Fig. 4.1.7 clearly showed that *Ci-TCF* increased significantly compared to the wt embryos. The other genes did not show any significant variation in fold difference of the transcript level although *tyrosinase* showed a trend to be down regulated but the change was too little to be considered as repression.

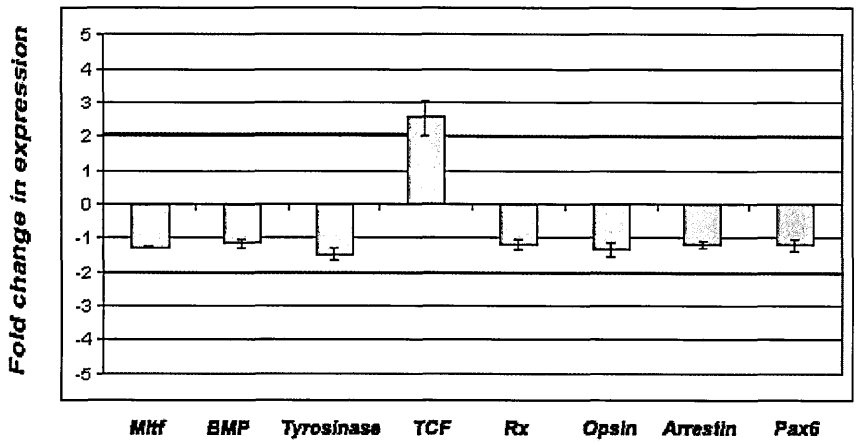

Figure 4.1.7. Changes in gene expression levels assessed by qPCR on *pTyr>ΔN Ci-TCF* transgenic embryos when compared with levels in control unelectroporated embryos. Diagram of *Ci-Mitf* (Mitf), *Ci-BMP* (Bmp1), *Ci-Tyrosinase* (Tyrosianse) *Ci-TCF* (TCF), *Ci-Rx* (RX), *Ci-Opsin1* (Opsin), *Ci-Arrestin* (Arrestin) and *Ci-Pax6* (PAX6) expression levels in embryos electroporated with *pTyr>ΔN Ci-TCF* construct. Data are expressed as a fold difference in transcript levels with respect to control tailbud embryos. For all data, the cycle threshold (Ct) was first normalized to the Rps27 expression levels in each sample. An amplification efficiency of 2.0 is assumed, and all samples varied from one another by no more than 0.3 cycles. Fold difference is calculated as 2ΔCt; thus, fold differences greater that ± 2 (indicated by red lines) are considered significantly different. No differences in transcript levels have been found in all the genes analyzed except for *Ci-TCF* (TCF) in the endogenous *Ci-TCF* perturbed larvae compared to the control.

Table 4.2: Primary data of qPCR analysis from which the above graph was obtained:

Name of the Gene	Average Ct value (Wt)	Average Ct value (Treated)	Primer efficie-ncy	Ratio (calculated by Pfaffl method)	1/Ratio * (-1) of data set 1	1/Ratio * (-1) of data set 2	1/Ratio * (-1) of data set 3	Average of data set 1, 2 & 3	Standard Deviation
Rps27	16.223	16.406	2	1	1	1	1	1	0
Mitf	21.15	21.63	2	0.814131	-1.228	-1.29	-1.2339	-1.2506	0.0341
Bmp	20.443	20.746	2	0.920188	-1.09	-1.33	-1.0867	-1.1689	0.1395
Tyr	19.32	20.06	2	0.679871	-1.47	-1.675	-1.307	-1.4841	0.1842
Tcf	18.38	17.456	2	2.153475	2.1534	2.4004	3.1238	2.5592	0.5043
Rx	22.776	23.433	2	0.720298	-1.38	-1.133	-1.062	-1.1916	0.1669
Opsin	23.82	24.25333	2	0.840896	-1.19	-1.467	00	-1.3285	0.1958
Arrestin	19.853	20.31	2	0.827406	-1.2	-1.263	-1.0594	-1.1741	0.1042
Pax6	21.153	21.363	2	0.981686	-1	-1.259	-1.3271	-1.1953	0.1726

4.2 *Ci-TCF* gene promoter

The principal aim of my thesis was to study the regulatory mechanisms underlying the expression of *Ci-TCF* during *Ciona intestinalis* embryonic development.

4.2.1 *In vivo Ci-TCF* promoter analysis:

The loss of function data, through *Ci-TCF* morpholino injection and through transgenesis, collectively point to a role for *Ci-TCF* in pigment cell development. As a first step toward understanding the tissue-specific expression of *Ci-TCF*, in particular related to pigment cells, I started an analysis of the 5' genomic region upstream of the gene, in order to identify the *cis*-acting elements required for *Ci-TCF* tissue specific expression

As an initial step, a 2.0 kb genomic region (from-2000 to -35) upstream of *Ci-TCF* transcription initiation site was amplified by PCR from the genomic DNA, using the most suitable oligonucleotides designed on the basis of the genomic sequence available on JGI2 (http://genome.jgi-psf.org/Cioin2/Cioin2.home.html). The amplified fragment was inserted upstream from GFP reporter gene (construct; *pTCF 2.0>GFP*). The transgene was introduced into *C. intestinalis* fertilized eggs via electroporation and the embryos were checked, under fluorescent microscopy, during their development. Almost 70% of the electroporated embryos started to show transgene expression at the tailbud stage. As shown in Fig. 4.2.1 the fluorescence was present in the dorsal side of brain vesicle, where GFP expression was strongly visible in one or two cells corresponding most probably, to precursor cells of otolith and/ or ocellus,. GFP expression was also observed in the ventral side of brain vesicle as well as in mesenchyme. This expression pattern was quite comparable with the endogenous *Ci-TCF* expression (Fig. 1.9). Later in the larval stage, the transgene expression persisted in the same territory, *i.e.*, ocellus, otolith ventral part of brain vesicle and mesenchyme, although this pattern was not observable with endogenous *Ci-TCF* expression, probably due to the stability of GFP protein.

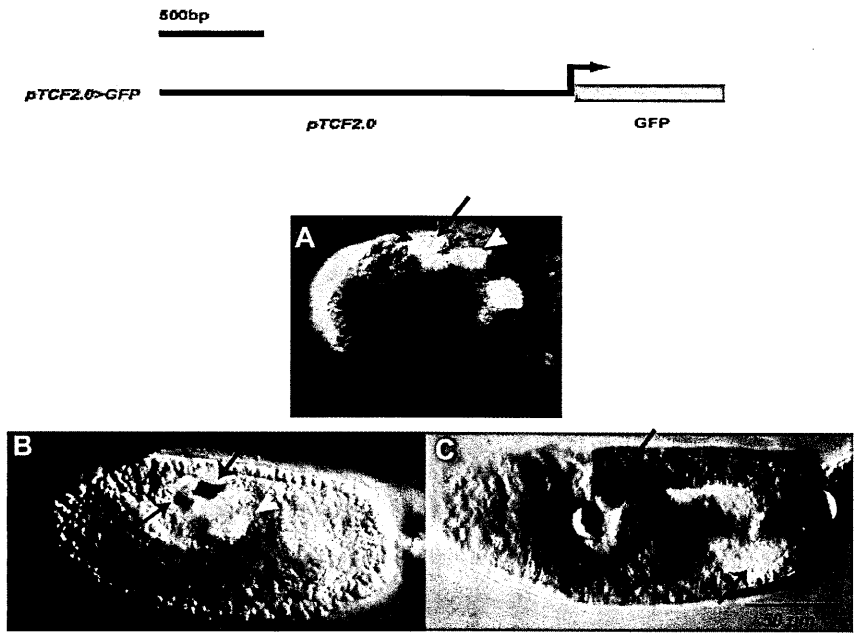

Figure 4.2.1. Isolation of a cis-element required for *Ci-TCF* activation in the endogenous territories. GFP expression in *pTCF 2.0>GFP* transgenic embryos. The diagrammatic view of the construct *pTCF 2.0>GFP* is given in the top. A 2.0 kb upstream reproduce the zygotic expression of *Ci-TCF*. A: tailbud and B,C: larvae showing GFP expression driven by the *pTCF2.0* enhancer with bright green fluorescence All the embryos are in lateral view, anterior is at the Left. *pTCF 2.0* enhancer directs reporter gene expression in the otolith and/or ocellus pigment cells (blue and indigo arrow), in the mesenchyme (purple arrow) and in the ventral region of the brain vesicle (yellow arrowhead).

Regarding the earlier stages, as neurula, it was not possible to find any GFP expression most probably because of the low amount of accumulated GFP protein. *in situ* Hybridization experiments were thus done with GFP mRNA probe on neurula stage and the signal was found localized in the neural plate and mesenchyme. There was also a signal present in the anterior region of the embryo, probably in the palp precursor cells. These expression patterns match with the endougenous *Ci-TCF* pattern of the same stage. Moreover, in some embryos an ectopic signal was also visible along the neural edges.

4.2.2 *Ciona intestinalis* vs *Ciona savignyi* *cis*-regulatory region comparison

To narrow down the regulatory region of *Ci-TCF* I took advantage from the genome sequence of another closely related species *Ciona savignyi.* For this analysis I exploited the version2 of *C. intestinalis* genome sequence (http://genome.jgi-psf.org/Cioin2/Cioin2.home.html). This version provides information about the two *Ciona* species genomes and it is possible to make genetic comparison of all annotated genes as well as their upstream and downstream regions. These genomic comparisons have been obtained using the mVISTA comparative genomic tool (Mayor et al., 2000) and are very useful to find conserved regulatory sequences functionally relevant.

Figure 4.2.2 depicts the genomic comparison of the *Ci-TCF* sequences of *C. intestinalis* and *C. savignyi* where a conserved non-coding region is represented by a yellow peak in the plot corresponding to a region of 250 base pairs.

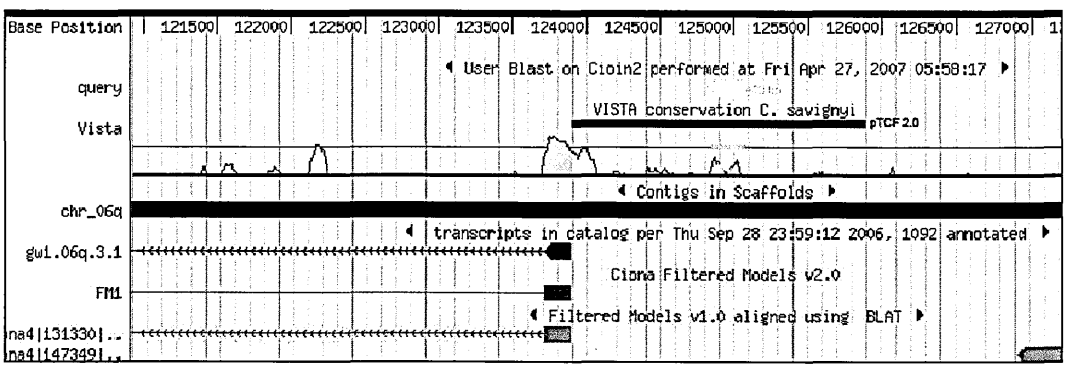

Figure 4.2.2. Comparison of *C. intestinalis and C. savignyi TCF* 5' region.
Visual representation of the alignment and conserved regions identified with the mVista comparative genomic tool. The conserved block between *C. intestinalis and C. savignyi* is shown as yellow peak. Base positions are written on top.

4.2.3 *In vivo* analysis *Ci-TCF* minimal enhancer

The conserved block of 250 bp extends from position -1099 to -854 within that 2.0 kb promoter. My next strategy was to amplify a wider region of 400 bp, extending from position -1173 to -771, by PCR with specific oligos. Since this 0.4 kb sequence lacked a TATA box, it was cloned in a vector upstream from GFP which already contained the Epstain Barr Virus (E1bTATA) basal promoter (Leong et al., 1988; Parks et al., 1988). This is transcriptionally inactive *per se* but works finely in *Ciona* and it was previously tested in our laboratory (data not published). E1bTATA sequence is able to amplify the signal driven by the elements cloned upstream from it.

Fig. 4.2.3 and Fig. 4.2.4 represents embryos electroporated with the resulting transgene construct *pTCF0.4>GFP*. At the late tailbud stage the transgene was able to drive GFP expression in one or two cells in the dorsal side of the trunk, in almost 50%-60% embryos, which can be considered as otolith and ocellus precursor blastomeres as confirmed by the analysis at the larval stage. In some embryos a faint fluorescence was observed in trunk mesenchyme in both tailbud and larvae and also in the sensory vesicle of larvae. Very rarely an ectopic signal was localized in the photoreceptors. This construct has also been analyzed at earlier stages of development such as early tailbud and neurula but no fluorescence has ever been detected.

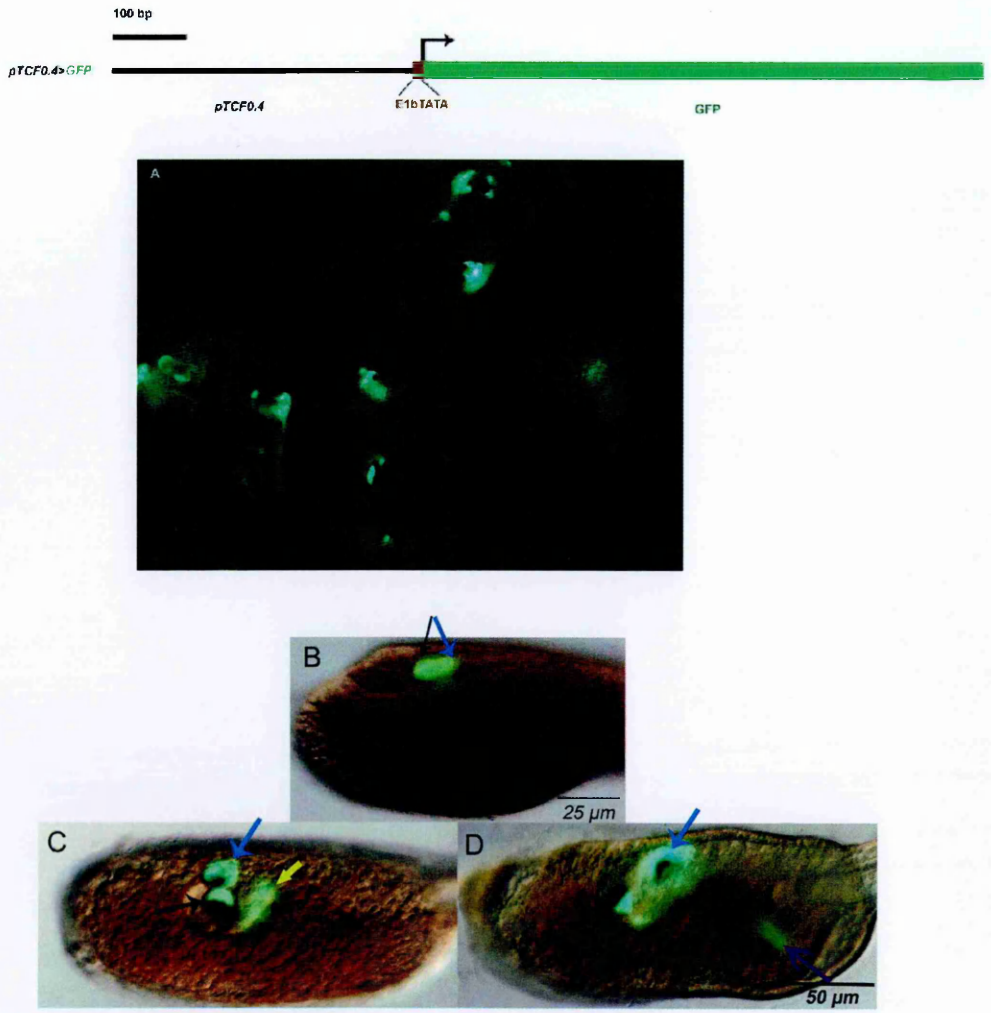

Figure 4.2.3. Identification of a minimal *Ci-TCF* enhancer. A 0.4 kb fragment (*pTCF0.4>GFP*), containing a region of 250 kb conserved between *Ciona intestinalis/Ciona savignyi* controls *Ci-TCF* activation in pigment cells. A: a group of larvae showing GFP expression driven by pTCF0.4 promoter. B: tailbud stage showing two fluorescent cells, precursor of otolith and ocellus pigment cells (blue and indigo arrow respectively). C and D: larvae with GFP fluorescence. Otolith: blue arrow, ocellus: indigo arrow, a low percentage of embryos showing signal in brain vesicle: yellow arrow and rarely a faint signal is observed in mesenchyme: purple arrow. All the embryos are in lateral view, anterior is at the Left.

in situ hybridization experiments were therefore done, using GFP mRNA as probe, to detect any possible signal at earlier stages of development. As depicted in Fig. 4.2.4, in neurula and early taibud stage the signal was found in the mesenchyme and in one or two cells in the neural plate. These results permitted the identification of a minimal *cis-*

regulatory element of 400 bp, which was able and sufficient to drive the reporter expression in the territories of the endogenous gene.

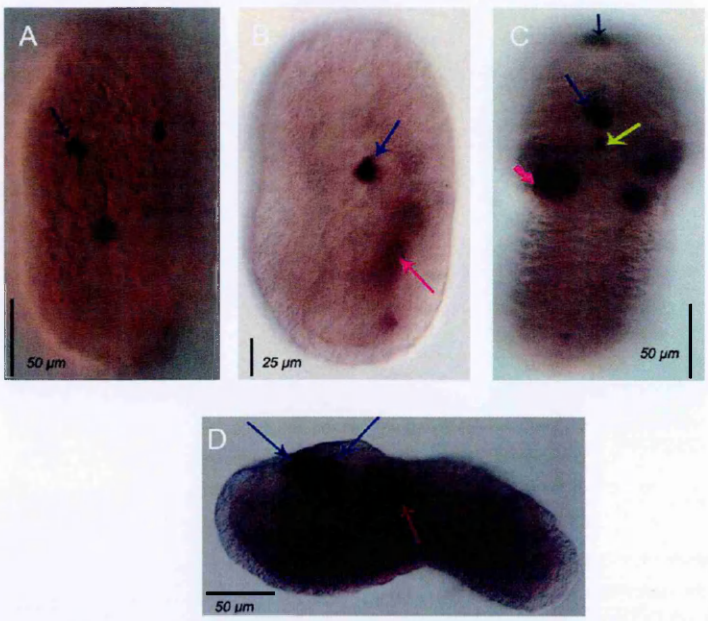

Figure 4.2.4. WMISH with GFP probe on *pTCF 0.4>GFP* transgenic embryos.
GFP RNA has been detected by *in situ* hybridization. A & B: Neurula stage, dorsal view. C & D: Tailbud stage C: dorsal view and D: lateral view Anterior is up (A,B and C). Anterioir is at the Left (D). *pTCF 0.4* enhancer directed reporter gene expression mostly in the otolith and/or ocellus pigment cells (blue arrow). A low percentage of embryos showed a staining in the mesenchyme (pink arrow) and in brain vesicle (yellow arrow).

Based on these results, summarized in figure 4.2.3 and 4.2.4 I focused my attention on this 0.4 kb sequence extending from position -844 to -1228.

For further analysis, I prepared 4 constructs by PCR with specific primer pairs. Two of them contained almost half of 0.4 kb sequence *pTCF 0.210* and *pTCF 0.220,* 210 bp and 220 bp respectively overlapping. Other two, *pTCF 0.100* and *pTCF 0.170* contained part of construct *pTCF 0.210*, and *pTCF 0.220* respectively. After electroporation the reporter expressions were analysed directly in larvae since at this stage the pigment cells can be immediately identified.

Introduction of the two smaller constructs *pTCF 0.100* and *pTCF 0.170* containing the promoter sequences from -1127 to -1228 and -844 to -1013 respectively were not able to induce transgene expression at all. With *pTCF 0.210* (-1022 to -1228) and *pTCF 0.220* (-844 to -1060) GFP expression was observed in the right place i.e. in ocellus and/or otolith cells but in a lower percentage of embryos (20-25%) compared to *pTCF0.4>GFP* (50-60%). These constructs and the expression profiles are reported in Fig. 4.2.5. These results suggest that the core region, in the *pTCF0.4* promoter fragment is included between -996 and -1166, which corresponds almost perfectly to the region shared with *Ciona savigny*, most probably contains elements that cooperate to an efficient expression of the transgene in the pigment cells at the larval stage.

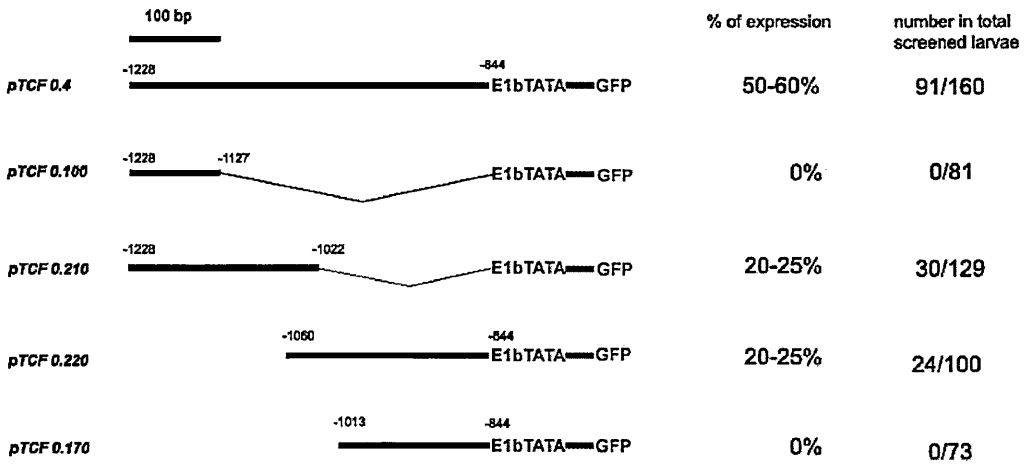

Figure 4.2.5. Summarizing scheme of the results obtained from the *Ci-TCF* minimal enhancer region analysis. The GFP expression obtained in transgenic larvea is presented as percentage at the right. While the corresponding constructs are shown on the left. The topmost is the basic construct containing a promoter region *Ci-TCF* of 400 bp. Below, the subsequent analysed fragments (dark black line), with the respective length and position on the genomic sequences are shown.

4.3 *Ci-TCF* trans-acting factor

4.3.1. Searching for putative transcription factor binding sites in *Ci-TCF* minimal *cis*-regulatory region

In order to identify putative transcription factors that can efficiently regulate *Ci-TCF* expression, TRANSFAC, Genomatix and JASPAR database were used with the promoter sequence *pTCF 0.4*. These analyses revealed the presence of four consensus ETS binding sites in this region. Among the four Ets binding site, the first one was located outside the region conserved with *C. savignyi*. These four sites were named 1, 2, 3 and 4 respectively and their positions are shown in Fig. 4.3.1 in respect to *pTCF 0.4* promoter site and in comparison with *C. savignyi*.

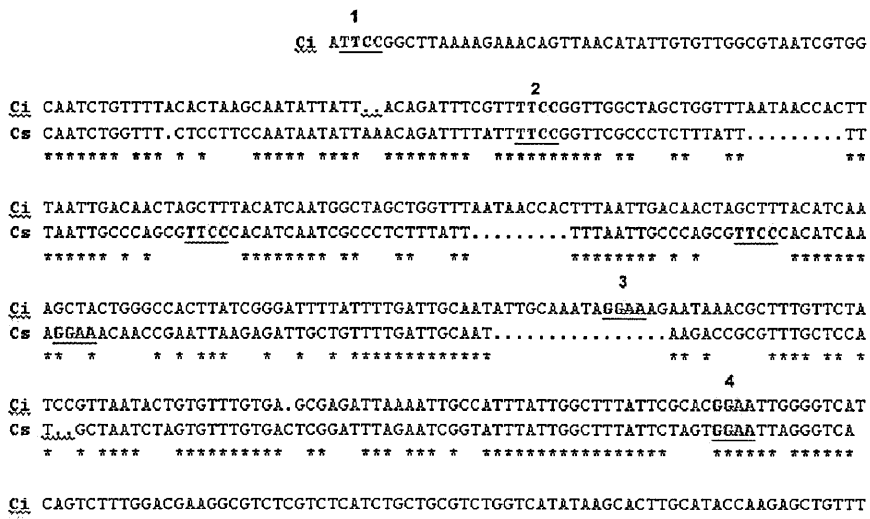

Figure 4.3.1. Phylogenetic footprinting of the Ets-element between *C. intestinalis* (Ci) and *C. savignyi* (Cs). Ets binding sites (EBS) in *C. intestinalis* cis-regulatory element are shown in orange color with number on top while the EBS unique to *C. savignyi* are shown in indigo color. Stars indicate conserved nucleotides.

4.3.2. *Ci-Ets 1/2* spatial expression pattern

It has been suggested in the genome wide survey study of Yagi et al (2003) that 15 members of the ETS transcription factor family are present in the *C. intestinalis* genome.

In order to find out the candidate member of the ETS family controlling *Ci-TCF* expression in pigment cell, the expression pattern of different members of this gene family was analyzed in the ANISEED database (ANISEED-Ascidian Network for In Situ Expression and Embryological Data- http://aniseed-ibdm.univ-mrs.fr/). In this database expression pattern of some ETS genes were characterized among which *Ci-Ets1/2* is found widely expressed in neural plate territories. By WIMSH assay *Ci-Ets1/2* signal was obtained in a-line neural territories including pigment cell precursor blastomeres at late gsstrula stage, while, at early neurula stage the signal gets more confined to a9.49 blastomeres at the time in which their specification occurs. (personal communication, Filomena Ristoratore unpublished data). This expression pattern also emphasizes the possibility of its involvement in *CiTCF* transcriptional activation in pigment cells.

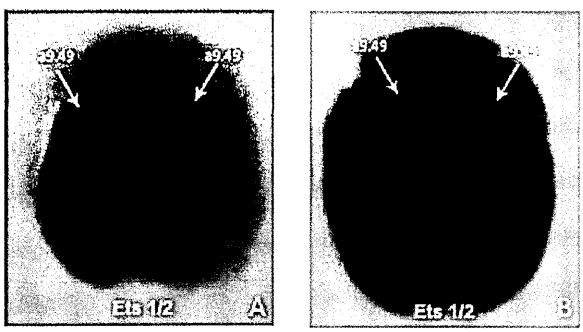

Figure 4.3.2. *Ci-Ets1/2* expression at the late gastrula and early neurula stage embryos.
In both the stages, *Ci-Ets1/2* is broadly expressed in the neural plate region, including pigment cell precursors (a9.49) (white arrows). A: late gastrula stage embryo. B: early neurula stage embryo. Anterior is up, vegetal view (personal communication, Paola Squarzoni).

4.3.3. Site specific mutagenesis of *Ci-Ets1/2* binding site:

To demonstrate the role *Ci-Ets1/2* transcription factor in regulating *Ci-TCF* transcription, I adopted a mutational approach. It is already reported that all Ets members recognize a DNA sequence, approximately 10bp long, containing a central core GGAA/T referred to as Ets binding site (EBS) (Woods et al., 1992) Hence, all 4 Ets binding sites

were mutated separately by point mutation changing **GGAA** to **AGAA** in *pTCF 0.4>GFP* construct (Bertrand et al., 2003).

I performed at least 2 individual experiments for each of the mutant construct M1, M2, M3 and M4 corresponding to the position of the Ets binding sites mentioned above with two different batches of eggs. Since the pigment cells are immediately visible at larval stage, the electroporation embryos (with mutant constructs) were analyzed for GFP expression directly at this stage. As positive control, wild type construct *pTCF0.4>GFP* was also electroporated. The analysis revealed that site 1 is not involved in transgene expression because the mutation in M1 could not affect GFP expression at all, in comparison to *pTCF0.4>/GFP*. The other three mutant constructs, M2, M3 and M4 were able to reduce GFP expression significantly. The constructs M3 and M4 reduced the transgene expression from 50% to 20-25%, on the other hand with M2, GFP expression was found only in 10-15% larvae.

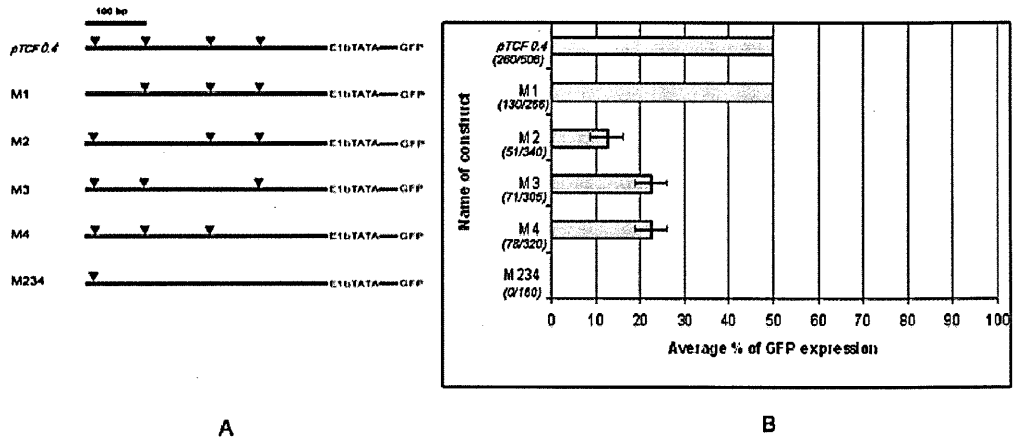

Figure 4.3.3. Mutational analysis. A: The triangles represent the EBS site in the minimal enhancer element of *Ci-TCF*. The absence of triangle indicates the mutant EBS in the construct. B: The histogram displays the percentage of embryos showing GFP expression in the X axis and Y axis the corresponding mutation construct. The number of embryos expressing GFP fluorescence among the total number of larvae screened is depicted in parenthesis under the corresponding construct.

Moreover, the intensity of the GFP fluorescence was also lower in most of the mutant construct expressing larvae compared to the control. As with the previous experiments WMISH approach was taken once againto compare between control embryos with mutant ones. In this case the signal for the GFP mRNA, in embryos electroporated with Ets mutant constructs, was obtained almost at the same percentage observed in the larvae. Furthermore, signal given by GFP probe was much stronger in the controls, compared with the electroporated tailbuds.

Inspired by these results I decided to mutate all three sites in the same construct by three single point mutations, named M234. These mutations were able to abolish the trancrptional activity of the enhancer completely, thus no GFP expression was observed by electroporating M234. These results are summarized in Figure 4.3.3 and 4.3.4.

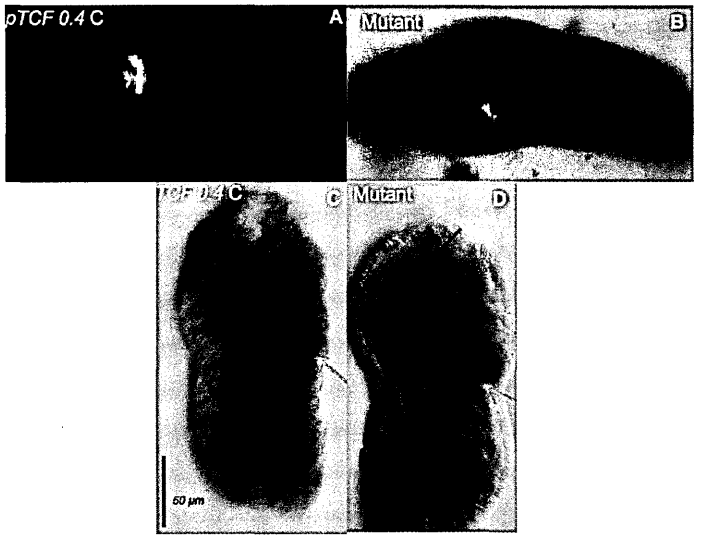

Figure 4.3.4. GFP expression (A, B) and WMISH with GFP probe (C,D) in transgenic embryos: mutant *vs* control. A: GFP expression in *pTCF0.4>GFP* electroporated (Control) larvae B: GFP expression in mutant construct electroporated larvae in lower intensity. C: Control tailbud showing GFP mRNA signal in pigment precursor cells (blue arrow) and in mesenchyme (pink arrow). D: Tailbud from mutant construct showing faint GFP signal in the same territories.

These data strongly support that *Ci-Ets* is involved in the activation of *Ci-TCF* expression. These also suggest that putative Ets binding sites 2, 3, and 4 are necessary and cooperate to achieve full expression of the transgene in the pigment cells.

Results obtained by different fractions of promoter *pTCF 0.4* also confirm these mutation assays (Fig. 4.3.5)

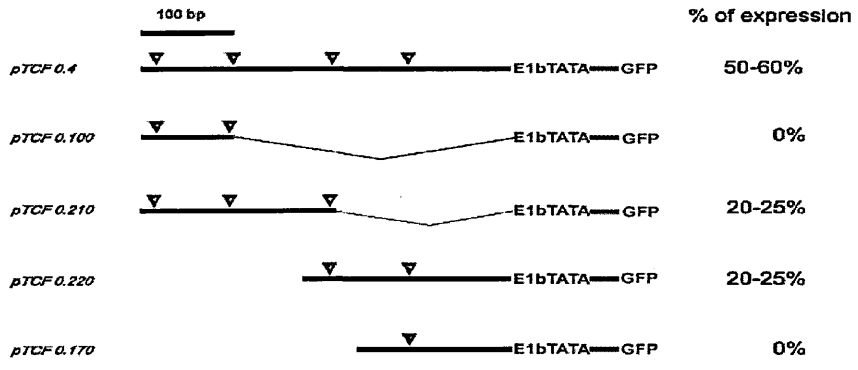

Figure 4.3.5. Fragments of *pTCF 0.4* enhancer element showing Ets binding sites. Construct containing different fragments of *pTCF 0.4* used in transgenic assay. The Ets binding sites in each construct are indicated by blue triangles. The percentage of GFP expression obtained with each construct is given at the left site.

4.3.4. Analyses of the interaction between *Ci-Ets1/2* and *Ci-TCF* enhancer

To demonstrate that *Ci-Ets1/2* is the protein which recognizes the Ets binding site (EBS) in *pTCF0.4*and is responsible for *Ci-TCF* enhancer activation, I decided to perform an EMSA (electrophoretic mobility shift assay). For this purpose, the *Ci-Ets 1/2* DNA binding domain (DBD) cDNA sequence (kindly provided by Davidson, B., Davidson et al., 2006) has been used to synthesize the corresponding protein *in vitro*. The protein was produced using the "TNT Coupled Reticulocyte Lysate System" (Promega) as described in material and methods. I started this analysis focusing my attention on the site 2. To this end, two complementary oligonucleotides of the *Ci-TCF* enhancer were designed which contains the 2nd EBS (Fig. 4.3.1.). The WT 2 oligonucleotide contains the intact Ets binding site (GGAA) while in the M2 oligonucleotide the first **G** is replaced by **A,** thus interrupting Ets binding in this oligo. In figure 4.3.6 it is possible to observe in lane 1 a shifted band corresponding to a DNA-protein complex as the results of the interaction of the labeled WT 2 oligonucleotide with the *Ci-Ets1/2* protein. This interaction appears very

specific given that, in the lane 2, the retardation band disappears when the reaction is carried out in presence of an excess (200x) of the same unlabeled WT2 oligonucleotide. To demonstrate the specificity of the binding, the reaction was carried out in presence of an excess (200x) of a random oligonucleotide (lane 4). As shown in lane 4, the random oligonucleotide does not affect the formation of the complex and a shifted band is clearly visible. For competition, oligonucleotide corresponding to another Ets binding site in the promoter *i.e.* EBS 4 was also included in this experiment in lane 3 where another retardation band is visible due to interaction between hot WT2 oligo and Ets 1/2 protein. This band, however, shows lower intensity compared to the band present in lane 1 and 4. In the same way, labeled mutant oligo for M2 was also loaded in the next four lanes (6, 7, 8, 9) together with Ets 1/2 protein where no bands were observed indicating that Ets 1/2 did not interact with the mutant sites.

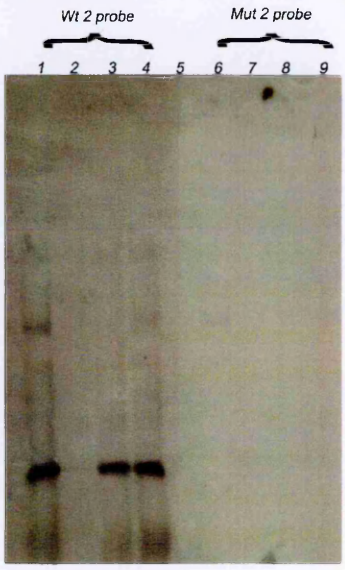

Figure 4.3.6. EMSA with wild-type (Wt2) and mutated (Mut2) oligonucleotides and in vitro translated Ci-Ets1/2 (DBD) protein. A shifted band is observed in lane 1 were Ci-Ets1/2 (DBD) protein was incubated with the labeled Wt2 oligonucleotide. DNA protein complex formation was inhibited by incubation with 200-fold molar excess of Wt2 unlabeled oligonucleotide (lane 2) but not with random oligonucleotide (lane 3). Incubation with 200-fold molar excess of Wt4 unlabeled oligo was not able to completely replace labelled WT2 to interact with the protein, thus a band with lower intensity is visible in lane 3. On the

contrary, DNA- protein interaction is completely absent in the lanes where the corresponding mutant oligos (Mut2) were used in the same condition (lane 6-9).

To test whether or not the *pTCF0.4* element is sensitive to the blockage of Ets factor, I exploited co-electroporation experiments using *pTCF 0.4>GFP* and the construct *pTyr>EtsWRPW* (a kind gift of F. Ristoratore). *pTyr>EtsWRPW* contains *Ciona* Ets1/2 DNA binding domain fused in frame with WRPW domain, to create a constitutive repressor form of Ets (EtsWRPW) (a kind gift of B. Davidson) (Beh et al., 2007). EtsWRPW is specifically targeted to be expressed in pigment precursor cells through Tyrosinase promoter. Interference with Ets activity in pigmented cell precursors decreased the GFP fluorescence enhanced by *pTCF 0.4* element (15%) compared to the control larvae (50%). The GFP expression found in 15% of embryos could be due to the early activation of the transgene, by the endogenous Ets protein already present in the pigment cell precursor before the exogenous repressor protein (Ets WRPW) was synthesized. This possibility was checked with in situ experiments on late tailbud/early larval stage where the absence of hybridization signal confirms the failure of newly synthesized GFP mRNA (Fig.4.3.7).

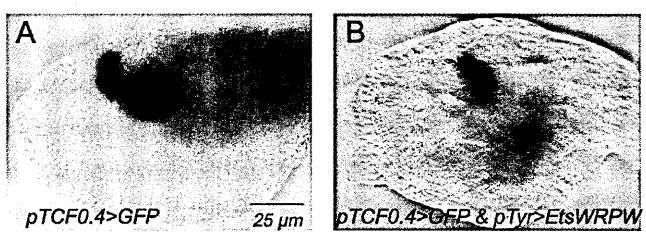

Figure 4.3.7. Coelectroporation of *pTyr>EtsWRPW* together with *pTCF0.4>GFP*.
pTCF 0.4 element is sensitive to the block of Ets factor (A) Control embryo showing a strong GFP mRNA expression in the pigment cells. (B) The absence of newly synthesized GFP mRNA has been assessed by in situ hybridization experiments using GFP mRNA as probe.

4.3.5. Suppression of *pTCF* transgene expression was induced by treatment with MEK inhibitor

Ets transcription factors are mediators of the FGF signalling pathway (Yordy and Muise-Helmericks, 2000). Upon binding to its receptor, FGF activates the Ras-, MEK-, ERK signalling cascade through a receptor tyrosine kinase, FGFR {reviewed by (Szebenyi and Fallon, 1999)}. Members of the Ets1/2 subfamily can be directly phosphorylated and activated by Erk (Yordy and Muise-Helmericks, 2000) thus acting as downstream effector of FGF signalling. In *Ciona* embryos, FGF signaling is essential for early neural and mesodermal patterning events (Bertrand et al., 2003; Miya and Nishida, 2003; Pasini et al., 2006). These studies have involved the use of a pharmaceutical inhibitor of MEK activity, U0126 (Bertrand et al., 2003; Hudson et al., 2003; Kim and Nishida, 2001).

The effect of MEK signalling regulated phosphorylation of Ets transcription factor during pigment cell development was verified by treating the wild type embryos with MEK inhibitor U0126 at the early gastrula stage, for 20 minutes at R.T. (about 25°C). Larvae obtained from this experiment showed quite usual morphology regarding the overall body plan and tail motility, but the whole brain vesicle differentiation was affected and lacked pigment cells completely (Fig. 4.3.8). To better define the time window in which the MEK signalling is required for pigment cells specification another student (Paola Squarzoni) in our laboratory performed this experiment in the later stages of development at different time points. With her treatment she observed that treatment with U0126 from the early tailbud stage produces fairly normal larvae. Incubation with U0126 for 20 and 10 minutes, starting from the late gastrula stage and from the neurula stage produced larvae containing, a narrow sensory vesicle deprived of pigment cells in both cases.This indicates the necessity of Ets transcription factor as well as the MEK governed phosphorylation of Ets for pigment cell formation in the sensory vesicle of *Ciona.*

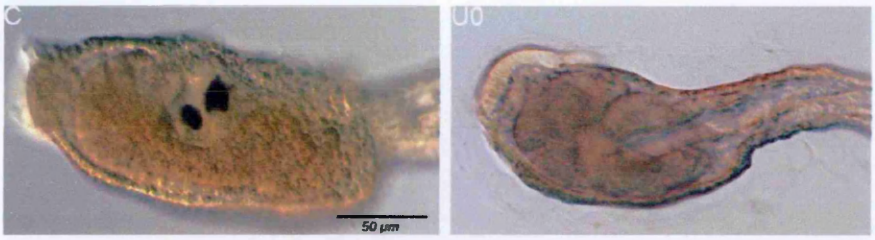

Figure 4.3.8 U0126 MEK inhibitor treatment. On the left: fixed time treatments with U0126, on developing gastrula stage embryos, gave rise to larvae without pigment cells and altered sensory vesicle. C,control; U0, U0126-treated larvae.

To check if a MEK signaling interferes with *pTCF* transgene expression, *Ciona* embryos electroporated with *pTCF2.0>GFP* or *pTCF 0.4>GFP*, were treated with U0126 at the gastrula stage and then the larvae were observed for the GFP expression. With both constructs the GFP expression was almost absent in U0126 treated larvae, they also lack the pigment cells where as, the control larvae showed GFP expression in their pigment cells (Fig. 4.3.9).

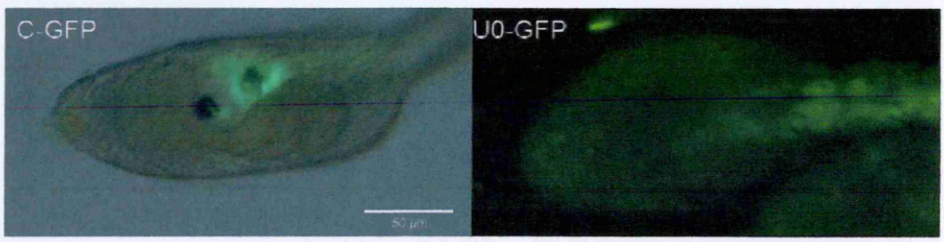

Figure 4.3.9. U0126 MEK inhibitor treatment in *pTCF0.4>GFP* transgenic embryos: The GFP expression driven by *pTCF 0.4* enhancer element is completely abolished with U0126 treatment. C-GFP: *pTCF0.4>GFP* electroporated larvae without U0126 treatment. U0-GFP: *pTCF0.4>GFP* electroporated larvae treated with U0126 at gastrula stage.

TCF probe was used for in situ on U0126 treated and Wt embryos to check for endogenous *TCF* mRNA whose transcription was found under control of Ets transcription factor so, I was expecting to visualize a decreased signal for *Ci-TCF* due to the interference with Ets site specific phosphorylation. From the result achieved with this *in situ* (Fig. 4.3.10) it is very definite that in U0126 treated tailbud stage there was no

positive signal for *TCF* in pigment precursor cells in comparison with Wt where 2 cells corresponding to a10.97 showed very strong signal.

in situ against GFP mRNA was performed to asses the transgene expression driven by *TCF* 0.4 enhancer in U0126 treated embryos. In the control electroporated embryos the GFP expression was obtained in palp and pigment cell precursors and in mesenchyme. While, no GFP expression was observed in the treated electroporated embryos.

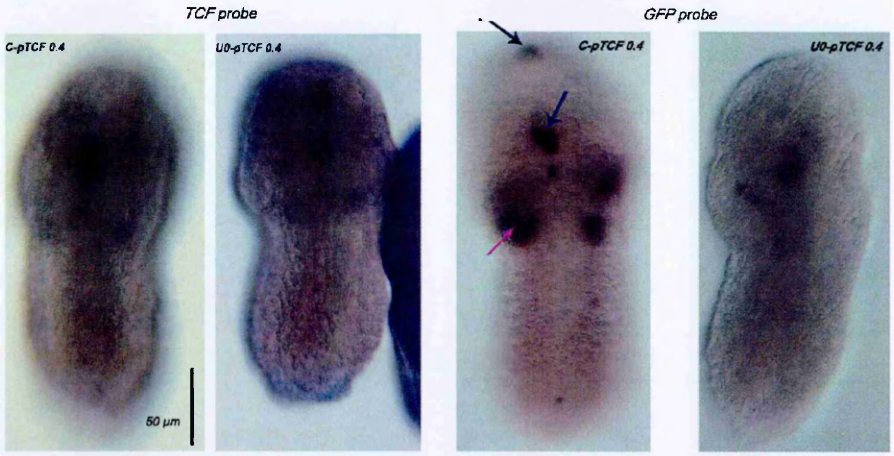

Figure 4.3.10. in situ on *pTCF0.4>GFP* transgenic embryos treated with MEK inhibitor: *in situ* with both *TCF* and GFP probes. C-*pTCF0.4*: electroporated untreated embryo and UO-*pTCF0.4*: electroporated treated embryo. With *TCF* probe no signal is detectable in the treated embryo (B) while strong signal is present in two cells corresponding to a10.97 pair in the control embryo (A) (blue arrow). With GFP probe, signal was obtained in control transgenic embryo (C) in palp precursor (black arrow), pigment cell precursor (blue arrow) and in mesenchyme (pink arrow) in treated embryo (D) no signal was detected. Tailbud stage, dorsal view, anterior to the top.

These data further confirm a regulation of *TCF* expression through a mechanism that involves a MEK signaling via Ets transcriptional regulation.

CHAPTER 5

DISCUSSION

5.1 *Ci-TCF* function in *Ciona intestinalis* pigment cells

The presence of *Ci-TCF* mRNA in sensory vesicles' pigment cell lineage indicates a possible involvement of this gene in pigment cell development (Fig. 1.9). The *Ci-TCF* function during pigment cell formation was studied by injecting morpholino antisense oligonucleotide before I started my PhD study. As a powerful tool, morpholinos are used in reverse genetics to knock down a gene function through which function of a protein can be studied. With this approach some fruitful phenotypes were obtained concerning the presence as well as the number of pigment cell in the sensory vesicle (Fig. 1.10). The phenotypic variations among the endogenous *Ci-TCF* disrupted embryos also included disrupted brain vesicle and palps. Moreover, in some cases the entire head development was altered. The reason behind this is the presence of zygotic *Ci-TCF* mRNA, which was not only confined to the pigment precursor cells rather it was also localized in the palp precursor cells as well as in some cells that take part in brain vesicle formation (figure 1.10). Furthermore, maternal *Ci-TCF* mRNA is present in the unfertilized eggs and broadly expressed in the very early stages of development (Fig. 1.9 A &B) where it plays a fundamental role in the regulatory network which patterns the early ascidian ectoderm (Rothbacher et al., 2007). Therefore, it is quite critical to calibrate the right dose of *Ci-TCF* morpholino injection, because a slight increase is able to perturb the patterning of early ectoderm resulting in very severe phenotypes. Given these remarks, I exploited a different approach to interfere with the zygotic *Ci-TCF* function particularly in pigment

cells. As mentioned before (Section 1.3.2.1) all LEF/TCF family proteins contain two major domains to exert their function; DNA binding domain and β-catenin binding domain. The later one is responsible for interaction with the co-factor β-catenin which is a prerequisite for mediating Wnt signal by TCF via its transcriptional activator property. A truncated protein lacking the β-catenin binding domain must not be able to contribute as a transcriptional activator. So, I prepared a construct coding for TCF lacking this domain, thus producing a dominant negative form of *Ci-TCF* (*ΔN Ci-TCF*). This approach has been proven very efficient to interfere with the endogenous *TCF* expression in *Xenopus* and zebrafish embryos (Lewis et al., 2004b; Lewis and Eisen, 2004; Molenaar et al., 1996) and permitted to analyze the biological role played by *TCF* genes in these model systems. For targeted expression of this construct in pigment cell precursors I used the Tyrosinase enhancer (*pTyr*) identified by another group of my laboratory (unpublished). *Ci-Tyrosinase* is one of the few known *C. intestinalis* genes whose expression is very specific to the pigment cell precursor lineage, during the embryonic development (Caracciolo et al., 1997). Thus, this particular approach restricts the interference to pigment cell lineage, without affecting any other developmental process in which *TCF* might be involved, as differentiation of palps, mesenchyme and brain vesicle, where endogenous *Ci-TCF* is also present. Larvae obtained by electroporation of this construct show overall normal morphology, including the structure of head, tail, palp and sensory vesicle except the number of pigment cells in the brain vesicle. Among them almost 35% larvae contain only one pigment cell, morphologically some of them are similar to otolith and others are like ocellus. While, in about 5% larvae no pigment cell is visible and the rest (60%) of the larvae show no morphological alteration, appearing similar to the wild type specimens (Fig.4.1.1). The phenotypic alteration by transgenesis, via electroporation method, actually depends on several factors. Among them the quality of the eggs is fundamental and unfortunately it varies largely which may affect the transgenic incorporation. The strength of the promoter used for the targeted expression of transgene also contributes to the

penetrance. In this case I used the *Tyrosinase* promoter which is expressed at late neurula stage in a9.49 blastomeres simultaneously with the activation of endogenous *Ci-TCF* in the same cells. Reporter gene fused with *pTyr* has been found to be expressed almost at the same stage in one or two of the pigment precursor cells (personal communication Ristoratore, unpublished). Moreover, mosaic incorporation is also a major factor during electroporation technique which can affect in perturbation by the transgenic truncated TCF protein. Above all, there is a competition between the mutant proteins with the endogenous protein for binding with the target DNA sequence. Furthermore, the amount of transgenic protein is also important since it has to be enough to compete with the endogenous TCF to block its function, which is another possible reason for this lower percentage of altered phenotype.

Results obtained from these electroporation experiments indicate that *ΔN Ci-TCF* protein is able to interfere with the endogenous *Ci-TCF* function at a certain level and can alter the pigment cell developmental program. The reason behind the absence of pigment cells in the sensory vesicle can be explained as failure in melanin biosynthesis. However, this possibility is excluded by immunohistochemistry done with βγ crystallin antibody because with this experiment the complete absence of otolith in the sensory vesicle is ensured by the absence of βγ crystallin fluorescence, which is a marker of otolith cell body and stalk (Shimeld et al., 2005) (Fig. 4.1.5). These observations suggest that the *Ci-TCF* is, in such a way, involved in the appropriate development of these pigment cell structures.

In order to identify cells where the endogenous *Ci-TCF* activity is perturbed by *pTyr>ΔN Ci-TCF* I used co-electroporation technique because this technique has been already established as a mean of labelling particular tissues with a reporter gene and at the same time altering target genes' expression or function. For this purpose, *pTyr>ΔN Ci-TCF* and *pTyr>GFP* constructs are used by which the cells where the mutant protein is manufactured are labeled with GFP fluorescence.

Another strategy is taken to clarify the fate of the endogenous *TCF* perturbed cells. Using another construct capable to produce ΔN TCF protein, fused in frame with mCherry reporter protein, downstream to *pTyr* enhancer, it has been possible to visualize the perturbed cells in the larval sensory vesicle.

With both these strategies it was possible to deduce that no apoptotic events have occurred during development and the perturbed cells, although unable to produce sensory pigment cells, still remained in the sensory vesicle (Fig. 4.1.2. & Fig. 4.1.3). This suggests that, interference of endogenous *Ci-TCF* function is able to interrupt with the proper differentiation of pigment cell precursors. The rationale behind this is the activation of the zygotic *Ci-TCF* starts at neurula stage when the neural plate is already formed and the pigment precursor cells are already fate restricted to be a part of the CNS.

in situ hybridization with different probes (*Ci-Tyrosinase, Ci-Opsin* and *Ci-arrestin*) is done with this perturbed larvae to check for the specificity of the interference in pigment cell precursors. Riboprobe for *Ci-arrestin* and *Ci-Opsin* mRNA do not produce any difference in the signal between control and perturbed larvae. On the contrary, a strongly reduced signal iis obtained in the perturbed larvae for *Ci-Tyrosinase* probe (Fig.4.1.6). This result is completely in accordance with my expectation since tyrosinase is the key enzyme for melanin biosynthesis; the absence of pigment cells in the sensory vesicle thus reflects the failure in tyrosinase mRNA transcription. *Ci-Opsin* and *Ci-Arrestin* are the markers for photoreceptor cells which share a totally different cell lineage than pigment cells (Fig. 1.8). Moreover, the ΔNTCF protein is targeted to be manufactured in pigment precursor cells, through *pTyr* enhancer element, so the transgenic protein production is confined to this territory.

In order to identify genes whose expression might be altered, due to the interference of endogenous Ci-TCF by transgenic ΔNTCF, qPCR approach was adopted. Since *TCF* gene family produces proteins that act as transcription factor, other gene's expression can be interrupted by the altered function of TCF in transgenic embryos. The

selection of the genes for qPCR analysis was done on the basis of their expression pattern *i.e* the genes that are expressed in pigment cell precursors and the neighboring cells for example, photoreceptor cells. For this purpose, I took advantage of online *in situ* expression pattern from Ascidian database ANISEED and previously published literature. The selected genes were: *Ci-Mitf, Ci-Bmp5/7, Ci-Tyrosinase* (pigment precursor cells), *Ci-Rx, Ci-Opsin, Ci-Arrestin* (photoreceptor cells) and *Ci-Pax6* (sensory vesicle including photoreceptor cells). I started quantitave PCR with embryos at early tailbud stage in order to look for genes differentially expressed in perturbed embryos with respect to Wt embryos (control).

qPCR experiments done on endogenous *Ci-TCF* perturbed embryos and Wt embryos do not show variation at a significant level in any of the transcripts tested in this experiment, except *Ci-TCF* which shows almost 2.5 times higher transcription in interfered embryos than in Wt (Fig.4.1.7). The reason behind this is the over expression of *TCF* mRNA through the incorporation of *pTyr>ΔN Ci-TCF* construct. Moreover, the oligos used for qPCR are designed downstream to β-catenin binding domain. The qPCR data mirrors the result of WMISH, performed on perturbed and Wt tailbud embryos, because with probe for *Ci-Tyrosinase, Ci-Bmp5/7* and *Ci-Mitf* no significant differences were obtained in the staining. However, in all performed qPCR a trend of downregualtion in the transcript level of tyrosinase gene has been observed in the perturbed embryos comparing to the Wt and that trend was quite stable.

Moreover, *in situ* hybridization with *Ci-Tyrosinase* probe, a very strong reduction in hybridization signal is obtained in larval stage (Fig.4.1.6) which hints about a regulation of *Tyrosinase* gene expression by *Ci-TCF*.

The possible reason could be the stage I used for qPCR *i.e.* the early tailbud stage which might be quite early to allow the detection of any difference in the amount of transcript of genes potentially regulated by *Ci-TCF* activity. Another important factor is that the analysis has been done on the whole embryo that, at the tailbud stage, is made of around

1000 cells. The number of pigment cell in *Ciona* is only two so the change in the transcript levels of a gene in two cells, out of 1000, may be very little, under threshold, to make a significant level of difference in the data analysis. The embryo collection for qPCR is also very tricky because up to late-tailbud stage the pigmentation does not start and I can not sort out the embryos based on the phenotype. The collection, therefore, remains random, with a high chance of picking up wild type embryos, given the 35-40% penetrance of the phenotype. Unfortunately I could not continue with qPCR using further developmental stages due to the limitation of time. Moreover, the animal supply was also not sufficient at that season. In all the performed qPCR experiments the transcript levels of *Ci-Tyrosinase* was observed to be decreased by around 1.5 fold in perturbed embryo compared to the control embryo which indicates a possible downregulation of *Ci-Tyrosinase* in endogenous *Ci-TCF* perturbed embryos. Although this pattern was obtained in all performed experiments, producing more biological replicates might help to justify the significance of these results.

As explained earlier, several factors might be involved in the qPCR results I obtained. So, we are planning to perform qPCR with other advanced stages including late tailbud and larval stages to overcome with the possible problem of using an early stage of development. To improve the sample collection procedure we are organizing FACS (Fluorescence activated cell sorter) through which it is possible to mark target cells on the basis of transgenic fluorescence from the large number of embryonic cells. In this way we hope to fish the right cells and to reduce the sampling error which will provide us with better and more reliable results from qPCR analysis.

5.2 Analysis of *Ci-TCF* gene regulatory region

I started my study with an aim to characterize the factors potentially involved in regulating *Ci-TCF* expression. Due to the compact genome and the close proximity of the *cis*-regulatory region to the genes they control, *Ciona intestinalis* provides itself as a

suitable model system for studies of transcriptional regulation. c*is*-regulatory region of a gene holds the binding sites for transcription factors which regulate its expression (Howard and Davidson, 2004). Therefore, to identify the factors activating *Ci-TCF* expression in pigment precursor cells, the prerequisite is to isolate the minimal *cis*-regulatory elements of *Ci-TCF*. I started with a 5'genomic region of 2kb (*pTCF2.0>GFP*) which is able to recapitulate the endogenous *Ci-TCF* at tailbud stage. The GFP fluorescence also persists up to the larval stage (Fig. 4.2.1) where the signal for endogenous transcript is usually not visible. This is because of the stability of GFP protein compared with TCF protein. On the contrary, I can not detect any fluorescent GFP at the neurula stage, most probably because the amount of GFP protein manufactured by this time is probably not enough to produce a visible effect. *in situ* hybridization experiments revealed the presence of the GFP mRNA in the pigment cell lineage and in the mesenchyme, mirroring the territories of the endogenous *TCF* mRNA. The data therefore indicate that the 2.0 kb fragment contains the element necessary to drive the expression of endogenous *TCF* both spatially and temporally.

To identify the minimal enhancer element I decided to narrow down the promoter region. To this end I took advantage of the published genome sequence of *Ciona intestinalis* and its sister species, *Ciona savignyi*, since these two species show a high degree of conservation sufficient to identify conserved regulatory sequence (Alfano et al., 2007; Satoh et al., 2003) (figure 4.2.2). Moreover, non-coding DNA with regulatory functions has a higher tendency to be more conserved than other non-coding DNA region (Satoh et al., 2003). So, prediction of *cis*-regulatory DNA sequences is facilitated by phylogenetic footprinting between these two genome sequences.

Alignment of the 5' upstream region of *Ci-TCF* with the corresponding region of C. *savignyi* revealed a high degree of conservation in a 250 bp region.

I cloned a wider region of 400 bp, containing this 250 bp conserved block, into a pBS plasmid containing, upstream from GFP, the Epstein Barr virus (E1bTATA) minimal

promoter, because this 400 bp region lacks a basal promoter. E1bTATA box is transcriptionally inactive *per se*, but works finely in *Ciona* (data from the Laboratory not published). Electroporation assay of this construct (*pTCF0.4>GFP*) is able to drive the transgene expression, in an average 50% of embryos, in otolith and ocellus pigment precursor cells at late tailbud stage and in pigment cells in larvae. Faint signal in trunk mesenchyme at both stages is rarely obtained which indicates that this shorter promoter region lacks the enhancer responsible for mesenchyme specific expression (figure 4.2.3). GFP fluorescence driven by this construct is not visible at earlier stages for example early tailbud, neurula as observed also with the 2.0 kb enhancer element. However, the presence of GFP transcript is obatained by *in situ* hybridization with GFP probe in pigment precursor cells (a10.98) also sometimes in mesenchyme at both neurula and early tailbud stage. Very often the signal is located in one of the pigment precursor cell because of the mosaic incorporation of the transgene (Figure 4.2.4).

For further deletion of this 400 bp region I produced 4 shorter regions, cloned them using the same strategy and assayed GFP expression directly at the larval stage, given the regular projection of the fluorescence from tailbud to larva, obtained with *pTCF0.4-E1b>GFP*, and the immediate identification of pigment cells in the larvae. Among these, the two constructs containing the shorter promoter (*pTCF0.170* and *pTCF0.100*) completely failed to drive any GFP fluorescence at larval stage. The other two (*pTCF 0.210* and *pTCF 0.220*) although able to produce the fluorescence in the right territories, revealed to be active in a lower percentage of larvae, compared to *pTCF0.4>GFP* (Fig. 4.2.5). These expression patterns indicate that the binding sites for putative transcription factors, potentially involved in regulating *TCF* expression, are located in the two larger fragments and that the shorter promoter regions might lack some of them. However, the two larger promoters can not drive the GFP expression at the same level of *pTCF0.4>GFP*, which suggests that these two larger enhancer elements co-operate to fully induce the endogenous *TCF* expression.

Form these analyses it is clear that the construct *pTCF0.4>GFP* is the most suitable one containing the minimal *cis*-regulatory region, since only this construct is able to produce pigment cell specific GFP expression and in a significant level. So, this region must contain the necessary regulatory elements which are efficiently involved in expressing endogenous *Ci-TCF* in pigment cell territories. For this reason, I selected this 400 bp promoter region to further carry my study forward.

5.3 Characterization of *Ci-TCF* upstream regulators

The expression pattern and function of the TCF protein family have been studied in a variety of model organisms including mouse, zebra fish, chicken, *Xenopus* mostly as a mediator of the canonical Wnt signaling pathways. Until now, no study has been carried out to deduce the upstream regulators of *TCF* gene expression in order to elucidate the mechanism controlling its expression in the right territories at the right time to function as downstream effectors of the Wnt signaling cascade. So, my attention was focused just in this direction that is in the detection of trans-acting factors potentially involved in *Ci-TCF* expression.

During scanning for putative transcription factor binding site I noticed four ETS binding sites (1, 2, 3 and 4) in this 400 bp promoter region having an organized pattern in their distribution, with a distance of around 100 bp in between.

Four ETS binding sites were also identified in the corresponding region of *C. savignyi,* two of which were located in the same position as in *C. intestinalis* (Fig. 4.3.1).

The Ets family of transcription factors

Ets transcription factors constitute an evolutionarily conserved gene family, characterized by the presence of a DNA-binding domain, termed ETS domain which is highly conserved from lower metazoans to humans. The founding member of this family,

v-ets (E twenty six), was originally discovered in 1983 (Hollenhorst et al., 2004; Klempnauer and Bishop, 1984; Leprince et al., 1983). The ets gene family is noted for its wide distribution among metazoans comprising more than 30 members (Degnan et al., 1993; Remy and Baltzinger, 2000). In *C. intestinalis* the presence of 15 members of ETS family have been reported by genome wide survey (Yagi et al., 2003).

All Ets members recognize a target DNA sequence, approximately 10 bp long, containing a central core GGAA/T, referred to as the Ets binding site (EBS). Sequences flanking the core EBS are variable and contribute to the specificity of individual Ets transcription factors (Woods et al., 1992). Some members of the family also contain an amino-terminal conserved domain called Pointed (PNT), which is required for protein-protein interaction.

Functionally most ETS proteins are transcriptional activators while, some work as a repressors, and others both as an activator and repressor in a context dependant manner (Mavrothalassitis and Ghysdael, 2000; Oikawa and Yamada, 2003; Sharrocks, 2001).

Ets genes play crucial roles in the regulation of a variety of cellular functions, including development, growth, differentiation, apoptosis and oncogenic transformation (Bassuk and Leiden, 1997; Dittmer and Nordheim, 1998; Graves and Petersen, 1998; Wasylyk et al., 1998). Their function and specificity is controlled at several levels. Their transcriptional activity often depends on protein-protein interactions (Li et al., 2000).

Many Ets family proteins are downstream nuclear targets of signal transduction cascades and are activated in response to a wide array of extracellular stimuli. Specificity can be achieved through modifications of specific family members by distinct signal transduction pathways (Oikawa and Yamada, 2003; Yordy and Muise-Helmericks, 2000).

Among the several Ets family members present in *Ciona* genome, expression pattern of some of them have been analyzed and collected in the gene expression pattern database, ANISEED (Ascidian Network for *In Situ* Expression and Embryological Data)

(http://aniseed-ibdm.univ-mrs.fr/). The interesting outcome of this analysis is the expression pattern of Ets 1/2, one member of Ets protein family present in *Ciona* genome. *Ci-ETS 1/2* is expressed widely in the neural plate territories at late gastrula stage and the expression persists up to tailbud stage in the nervous system and in epidermis. Ci-Ets1/2, which is also known as ets/pointed2 is the only *Ciona* orthologue of the vertebrate Ets1 and Ets2 transcription factors (Yagi et al., 2003). Both the Ets DNA-binding domain and pointed domain are present in Ci-Ets1/2. *Ci-Ets 1/2* have been demonstrated previously in early nervous system induction in *Ciona* (Bertrand et al., 2003). The potential *Ets1/2* involvement is also evident in heart specification of *C. intestinalis* (Davidson et al., 2006).

Better characterization of *Ci-ETS 1/2* expression has been done by WMISH in my laboratory by another group which suggests that *Ci-ETS1/2* is expressed broadly in the neural plate region at both late gastrula and neurula stage where the expression is stronger in pigment precursor cells. So, the expression of *Ci-Ets 1/2* starts prior to the expression of *Ci-TCF* in pigment precursor cells and the expression of both genes merges at neurula stage. This expression pattern gives a good indication for Ets1/2 governed regulation of *Ci-TCF* expression in pigment cell precursors.

From this expression profile I decided to continue my study to understand the involvement of *Ci-ETS1/2* in regulating *Ci-TCF* enhancer element by both *in-vivo* and *in-vitro* strategies.

Therefore, I took a site specific mutagenesis approach and performed substitution mutation for each of the Ets binding site individually in *pTCF0.4>GFP* construct. Transgenic assays were performed by electroporating these mutant constructs, M1, M2, M3 and M 4 (named according to the mutant Ets site they contained). After analyzing the electroporation data it is found that with M1 there is no change in GFP expression compared to the control. With M2, M3 and M4, individually, significant decrease in reporter gene activation is achieved compared to the control (*pTCF0.4>GFP)* and the reduction is highest with M2 than with the M3 or M4. These results strongly suggest a role

for Ets in *Ci-TCF* activation although none of the three constructs was able to completely abolish GFP expression (figure 4.3.3). A fifth construct, M234 containing mutation in all three sites together, except 1, seems really promising since a complete absence of GFP expression is observed after electroporation. These results indicate that all three sites are individually necessary but not sufficient for the full tissue specific expression of *Ci-TCF.* These three sites participate and co-operate to contribute in the full tissue specific expression of *Ci-TCF.*

These data also coincide with the previous analysis of promoter deletion (Fig. 4.2.5) where four different deletion constructs were electroporated and significant reporter gene expression was observed in two of them, *pTCF 0.210* and *pTc f0.220.* Another interesting observation is that the core region containing the three significant Ets binding sites (2, 3 and 4) resides in the 250 bp sequence conserved with *C. savignyi.* After a detailed analysis of the promoter sequence of these four constructs I observed that the smaller constructs *pTCF 0.100* and *pTCF 0.170* contain EBS 2 and 4 respectively, on the contrary, *pTCF 0.210* and *pTCF 0.220* contain at least two necessary EBS; 2, 3 and 3, 4 respectively (Fig.4.3.5). Although each of the construct *pTCF 0.100* and *pTCF 0.170* contain at least one Ets binding site still they are not able to produce any significant transgene expression. These results indicate that a single Ets site is not sufficient, per se, two Ets sites are able to switch on the reporter, but is only thank to the co-operation of the three Ets sites for which a full tissue specific activation of *Ci-TCF* is accomplished. I cannot exclude the co-participation of other factors aiding Ets in transgene expression.

Potential involvement of Ets transcription factor in the activation of *Ci-TCF* was also confirmed, *in vivo*, by a co electroporation experiment done with a fusion construct *pTyr>EtsWRPW*, containing Ets1/2 DNA binding domain linked to the WRPW repressor domain, and *pTCF 0.4>GFP.* This constitutive repressor form of Ets DBD decreases the GFP expression driven by *pTCF0.4* from 50% to 15%. The 15% of fluorescent embryos can be related to an early activation of the transgene, by the endogenous Ets protein

already present in the pigment cell precursors before the exogenous repressor protein (Ets WRPW) is synthesized. This hypothesis is confirmed by *in situ* hybridization experiments using GFP probe. With this hybridization no signal is obtained at late tailbud/early larval stage which confirms the absence of newly synthesized GFP mRNA (Fig.4.3.7). Thus, the GFP fluorescence signal observed in the larvae (15%) is most probably due to the stable GFP protein that was produced at earlier stage by endogenous Ets but persisted up to the larval stage.

In order to study the direct interaction between *Ci-TCF* enhancer element and Ets transcription factor I adopted Electrophoretic Mobility Shift Assay (EMSA). Probe containing entire Ets binding site as well as a substitution mutation were used for experiment and control respectively. Instead of whole Ets1/2 protein, Ets1/2 DNA binding domain (DBD) was used. For EMSA I decided to start my experiment with probe Wt2 since *in vivo* experiment with mutation of this Ets binding site (EBS 2) reduced the reporter gene expression more than the other two (EBS 3& 4). The Ets binding site1 was not taken into account as it was not able to decrease the GFP expression at all.

EMSA analysis clearly demonstrates the direct interaction between the Ets binding site in Wt2 with Ets 1/2 DBD, by the formation of a DNA-protein complex visible on the gel as a retardation band (Fig. 4.3.5: lane 1, 4). No DNA-protein complex is visible on gel when the same reaction is carried out in the presence of Mut 2 probe containing the substitution mutation with Ets 1/2 DBD (Fig. 4.3.5: lane6, and 9). This result strongly indicates the interaction of Ets 1/2 protein with *Ci-TCF* enhancer which further confirms a role for Ets transcription factor in regulating endogenous TCF gene expression.

For a competition, cold probe Wt 4 is also used to check if EBS site 4 is able to compete with EBS 2 for interacting with Ets 1/2 DBD. The expectation was to find no DNA-protein complex on gel. Surprisingly a retardation band is also observed in this lane (figure 4.3.5: lane 3) but in a much lower intensity which indicates that EBS 4 can not completely replace EBS 2. Notably, there are 15 members of Ets gene family found in

Ciona genome and ANISEED database does not cover the expression pattern of all these family members. In the present study EMSA is done only with DNA binding domain of ETS 1/2 given its expression profile in the neural plate territories. I cannot exclude that EBS4 might be specific for a different member of the ETS family other than ETS1/2. During physical interaction with DNA most Ets factors recognize and bind to a core region containing the same sequence; the specificity of individual Ets transcription factors resides in the sequences flanking the core EBS. Given these remarks, I can postulate that the core sequence of EBS 4 is recognized by Ets 1/2 DBD and that, given the low specificity, it is displaced, at some levels, by hot EBS 2. Due to time constrain it was not possible for me to analyze other Ets binding sites (EBS 3 and 4) by EMSA during this study which I hope to continue. Furthermore, in my present study I investigated the involvement of Ci-Ets1/2, one of the 15 members of *Ciona* Ets protein family but the possibility of involvement of other members in activating *Ci-TCF* expression still remains. So, further study is necessary to deeply investigate the possible involvement of other Ets family members in *Ci-TCF* expression. To explore the full scenario concerning the factors regulating *Ci-TCF* expression in pigment precursor cells it is necessary to continue the present study and investigate the remaining Ets binding sites *in vitro* as well as the participation of other Ets family members in controlling *Ci-TCF* expression.

Like most other members of Ets protein family in other organisms, it has been reported that in *Ciona*, Ets1/2 also contains a conserved ERK docking site and mitogen activated protein kinase (MAPK) phosphorylation site (Davidson et al., 2006). A very interesting data related to that is the effect of U0126, an inhibitor of MAPK cascade, on the *pTCF0.4>GFP* transgene expression. Treatment with U0126 of Wt embryos at gastrula stage produce larvae with an altered phenotype showing complete absence of pigment cells and highly reduced sensory vesicle, sometimes with no palps as well (Fig.4.3.8). Treatment of *pTCF0.4>GFP* transgenic embryos with U0126 resulted in larvae having the same phenotype and without any GFP protein expression. Moreover, *in*

situ hybridization experiments on these embryos, using GFP and TCF as probes, show complete absence of TCF as well as GFP message synthesis. The results indicate that inhibition of MAPK cascade blocks endogenous TCF and transgenic GFP switch on (Fig.4.3.10). The data thus strongly link TCF expression-Ets activation-MAPK signalling cascade.

5.4 Conclusions and Future Directions

My PhD study permits me to draw some conclusions concerning the activity of *Ci-TCF* in pigment cells development in *Ciona intestinalis*. *Ci-TCF* is not the sole gene bringing to switch on the final differentiation of pigment cells. *Ci-TCF* functions as a fine tuner to aid in this process, given that it does not behave as a classical transcription factor working rather in a context dependent manner. TCFs are therefore important players in the assembling of the correct transcriptional machinery that in turn might be involved in regulating other pigment cell specific genes' expression. Interference with endogenous *Ci-TCF* activity disturbs this program but do not bring the cells to death. Actually, the presence of *Ci-TCF* perturbed cells in the sensory vesicle confirms that these cells were not victim of apoptosis; rather they took other fate than pigment cells. Similar findings are also reported by Dorskey and his co-workers who observed that by injecting mRNA coding for a truncated form of *TCF3* promotes neuronal fates at the expense of pigment cell in zebra fish neural crest cells (Dorsky et al., 2000). Currently studies are going on in my lab to identify markers for different territories of *Ciona* embryos to clarify the fate of the purterbed cells in *pTyr>ΔN TCF* transgenic larvae which were supposed to be pigment cells.

A further interesting outcome of this study is the identification of the upstream regulator of *Ci-TCF* gene, which effectively controls *Ci-TCF* expression at the right time in the right place to exert its function. The direct regulation of *TCF* expression has never

been explored, since until now *TCF* functions has been studied and the importance has been given to this protein family mostly as downstream effector of canonical Wnt signaling. From my study I was able to identify one of the potential transcription factors ruling over *Ci-TCF* expression, *Ci-Ets 1/2*. The involvement of Ets factors in early neural induction in *Ciona* has already been demonstrated previously (Bertrand et al., 2003). My results suggest a potential role for Ets family member in further CNS differentiation step in *Ciona*, which is accomplished by activating *Ci-TCF*, most probably together with other factors, in the pigment cell precursors at the right time to bring about the final differentiation of pigment cells. Ets family of transcription factor thus represents the first upstream regulator of *TCF* identified so far.

However, the probability of different members of the Ets family involved in *Ci-TCF* expression still needs to be elucidated. This basic finding, although very preliminary, can be instrumental for future studies.

From my results regarding the activation of Ets by specific phosphorylation, controlled by MAP kinase pathway, indicates a possible upstream signal able to turn on and regulate the phophorylation. Involvement of FGF signaling, via the MAP kinase pathway, in the activation of Ets factors through phophorylation has been already demonstrated in various ascidian developmental processes, including the early specification of anterior neural presumptive territories that will form the anterior part of CNS (Bertrand et al., 2003; Hudson et al., 2003).

In our group of "Cellular and Developmental Biology Laboratory" another PhD student, Paola Squarzoni, working with Dr. Filomena Ristoratore was investigating the role of FGF signaling during pigment cell development of *Ciona*. From their study they have concluded that pigment cell specification induction is mediated by FGF signaling pathway via the MAP Kinases downstream effector *Ci-Ets1/2*. Thus, the cascade continues as follow: FGF signaling activates MAP kinases, which phosphorylates and

activates *Ci-Ets* 1/2 which in turn activates *Ci-TCF* expression. This *Ci-TCF* participates in terminal differentiation of pigment cells in the sensory vesicle.

To continue with the present study some experiments have been already organized.

First of all, I am preparing more riboprobes for new genes with an aim to identify more genes expressed in pigment cell precursors and their neighboring cells (photoreceptor and brain vesicle precursor cells) by WMISH. Once identified, this information will help me to pick up more genes for further analysis by qPCR to verify their relation with *Ci-TCF*.

From my present study the possible involvement of the Wnt signaling cascade for inducing TCF activation in pigment precursor cells can be predicted but has not been demonstrated so far. To this end it would be interesting to clarify the specific member of the Wnt family morphogen involved in this process. So, analysis of the expression pattern of different members of Wnt family, during *Ciona* development, would be very useful as first step to verify the presence of any particular member of Wnt family in cells around pigment cell precursors. Simultaneously, I am preparing constructs for targeted expression of a stabilized form of β-catenin in nervous system territories wider than pigment cell precursors. This will help me to study the contribution of this co-activator in pigment cell differentiation, given that TCF exerts its function by physically interacting with β-catenin.

Chromatin Immuno Precipitation (ChIP) is a powerful tool for the spatial and temporal mapping of chromatin bound factors *in vivo*. This technique allows one to determine whether and where in the genome a protein is bound. Thus, with this method the enhancer region where a transcription factor interacts can be identified. So, to identify TCF target gene one possibility could be to adopt ChIP protocol. The prerequisite of this method is to have a specific antibody against the protein of my interest. For this purpose I already obtained antibody against *Ci-TCF* from a commercial company (PRIMM; www.primm.it) which I have tested with Western blot. ChIP method, however, could

reveal to be time consuming, since a protocol for ascidian model organism has not been established yet.

In order to identify genes whose expression might be regulated by *Ci-TCF*, we have decided to use FACS (Fluorescence activated cell sorter) to fish out our target cells. As in *Ciona* larvae there are only two pigment cells, it is difficult to get, by qPCR, a significant level of change in differentially expressed gene during data analysis. The little change given by the altered embryos may be masked by the huge number of cells in the whole larvae (~2600) compared to the interfered cells (2/4). Thus, FACS may help to isolate directly the perturbed cells and subsequently facilitate qPCR analysis. Sorting out cells by FACS can also be very effective to understand the molecular mechanisms involved in the early differentiation of pigment cells. At present a project is being organized with another group of our laboratory, Filomena Ristoratore, to fish pigment cell precursors perturbed earlier than *Ci-TCF* activation, in order to identify more factors that may participate in the genetic cascade controlling pigment cell differentiation.

REFERENCES

Adams, M. D., et al., 2000. The genome sequence of Drosophila melanogaster. Science. 287, 2185-2195.

Ahmed, Y., et al., 2002. Drosophila Apc1 and Apc2 regulate Wingless transduction throughout development. Development. 129, 1751-62.

Aksan, I., Goding, C. R., 1998. Targeting the microphthalmia basic helix-loop-helix-leucine zipper transcription factor to a subset of E-box elements in vitro and in vivo. Mol Cell Biol. 18, 6930-8.

Alfano, C., et al., 2007. Developmental expression and transcriptional regulation of Ci-Pans, a novel neural marker gene of the ascidian, Ciona intestinalis. Gene. 406, 36-41.

Arce, L., et al., 2006. Diversity of LEF/TCF action in development and disease. Oncogene. 25, 7492-504.

Atcha, F. A., et al., 2003. A new beta-catenin-dependent activation domain in T cell factor. J Biol Chem. 278, 16169-75.

Atcha, F. A., et al., 2007. A unique DNA binding domain converts T-cell factors into strong Wnt effectors. Mol Cell Biol. 27, 8352-63.

Barker, N., Clevers, H., 2000. Catenins, Wnt signaling and cancer. Bioessays. 22, 961-5.

Bassuk, A. G., Leiden, J. M., 1997. The role of Ets transcription factors in the development and function of the mammalian immune system. Adv Immunol. 64, 65-104.

Bateman, A., et al., 2004. The Pfam protein families database. Nucleic Acids Res. 32, D138-41.

Behrens, J., et al., 1996. Functional interaction of beta-catenin with the transcription factor LEF-1. Nature. 382, 638-42.

Bertrand, V., et al., 2003. Neural tissue in ascidian embryos is induced by FGF9/16/20, acting via a combination of maternal GATA and Ets transcription factors. Cell. 115, 615-27.

Brantjes, H., et al., 2001. All Tcf HMG box transcription factors interact with Groucho-related co-repressors. Nucleic Acids Res. 29, 1410-9.

Brinkmeier, M. L., et al., 2003. TCF and Groucho-related genes influence pituitary growth and development. Mol Endocrinol. 17, 2152-61.

Bruhn, L., et al., 1997. ALY, a context-dependent coactivator of LEF-1 and AML-1, is required for TCRalpha enhancer function. Genes Dev. 11, 640-53.

Budd, P. S., Jackson, I. J., 1995. Structure of the mouse tyrosinase-related protein-2/dopachrome tautomerase (Tyrp2/Dct) gene and sequence of two novel slaty alleles. Genomics. 29, 35-43.

Cadigan, K. M., Nusse, R., 1997. Wnt signaling: a common theme in animal development. Genes Dev. 11, 3286-305.

Caracciolo, A., et al., 1997. Specific cellular localization of tyrosinase mRNA during Ciona intestinalis larval development. Dev Growth Differ. 39, 437-44.

Carlsson, P., et al., 1993. The hLEF/TCF-1 alpha HMG protein contains a context-dependent transcriptional activation domain that induces the TCR alpha enhancer in T cells. Genes Dev. 7, 2418-30.

Chen, G., et al., 1999. A functional interaction between the histone deacetylase Rpd3 and the corepressor groucho in Drosophila development. Genes Dev. 13, 2218-30.

Clamp, M., et al., 2004. The Jalview Java alignment editor. Bioinformatics. 20, 426-7.

Cole, A. G., Meinertzhagen, I. A., 2004. The central nervous system of the ascidian larva: mitotic history of cells forming the neural tube in late embryonic Ciona intestinalis. Dev Biol. 271, 239-62.

Corbo, J. C., et al., 1997. Characterization of a notochord-specific enhancer from the Brachyury promoter region of the ascidian, Ciona intestinalis. Development. 124, 589-602.

D'Aniello, S., et al., 2006. The ascidian homolog of the vertebrate homeobox gene Rx is essential for ocellus development and function. Differentiation. 74, 222-34.

Daniels, D. L., Weis, W. I., 2005. Beta-catenin directly displaces Groucho/TLE repressors from Tcf/Lef in Wnt-mediated transcription activation. Nat Struct Mol Biol. 12, 364-71.

Darras, S., Nishida, H., 2001. The BMP/CHORDIN antagonism controls sensory pigment cell specification and differentiation in the ascidian embryo. Dev Biol. 236, 271-88.

Davidson, B., et al., 2006. FGF signaling delineates the cardiac progenitor field in the simple chordate, Ciona intestinalis. Genes Dev. 20, 2728-38.

Davidson, E. H., 1989. Lineage-specific gene expression and the regulative capacities of the sea urchin embryo: a proposed mechanism. Development. 105, 421-45.

Deb, D. K., et al., 2008. Wingless signaling directly regulates cyclin E expression in proliferating embryonic PNS precursor cells. Mech Dev. 125, 857-64.

Degnan, B. M., et al., 1993. The ets multigene family is conserved throughout the Metazoa. Nucleic Acids Res. 21, 3479-84.

Dehal, P., et al., 2002. The draft genome of Ciona intestinalis: insights into chordate and vertebrate origins. Science. 298, 2157-67.

Delsuc, F., et al., 2006. Tunicates and not cephalochordates are the closest living relatives of vertebrates. Nature. 439, 965-8.

Di Gregorio, A., Levine, M., 1998. Ascidian embryogenesis and the origins of the chordate body plan. Curr Opin Genet Dev. 8, 457-63.

Di Gregorio, A., Levine, M., 2002. Analyzing gene regulation in ascidian embryos: new tools for new perspectives. Differentiation. 70, 132-9.

Dittmer, J., Nordheim, A., 1998. Ets transcription factors and human disease. Biochim Biophys Acta. 1377, F1-11.

Dorsky, R. I., et al., 2003. Two tcf3 genes cooperate to pattern the zebrafish brain. Development. 130, 1937-47.

Dorsky, R. I., et al., 1998. Control of neural crest cell fate by the Wnt signalling pathway. Nature. 396, 370-3.

Dorsky, R. I., et al., 2000. Direct regulation of nacre, a zebrafish MITF homolog required for pigment cell formation, by the Wnt pathway. Genes Dev. 14, 158-62.

Dunn, K. J., et al., 2005. WNT1 and WNT3a promote expansion of melanocytes through distinct modes of action. Pigment Cell Res. 18, 167-80.

Eakin, R. M., Kuda, A., 1971. Ultrastructure of sensory receptors in Ascidian tadpoles. Z Zellforsch Mikrosk Anat. 112, 287-312.

Faro, A., et al., 2009. T-cell factor 4 (tcf7l2) is the main effector of Wnt signaling during zebrafish intestine organogenesis. Zebrafish. 6, 59-68.

Fleige, S., et al., 2006. Comparison of relative mRNA quantification models and the impact of RNA integrity in quantitative real-time RT-PCR. Biotechnol Lett. 28, 1601-1613.

Galceran, J., et al., 1999. Wnt3a-/--like phenotype and limb deficiency in Lef1(-/-)Tcf1(-/-) mice. Genes Dev. 13, 709-17.

Galceran, J., et al., 2000. Hippocampus development and generation of dentate gyrus granule cells is regulated by LEF1. Development. 127, 469-82.

Galibert, M. D., et al., 1999. Pax3 and regulation of the melanocyte-specific tyrosinase-related protein-1 promoter. J Biol Chem. 274, 26894-900.

Gordon, M. D., Nusse, R., 2006. Wnt signaling: multiple pathways, multiple receptors, and multiple transcription factors. J Biol Chem. 281, 22429-33.

Gorman, A. L., et al., 1971. Photoreceptors in primitive chordates: fine structure, hyperpolarizing receptor potentials, and evolution. Science. 172, 1052-4.

Graves, B. J., Petersen, J. M., 1998. Specificity within the ets family of transcription factors. Adv Cancer Res. 75, 1-55.

Gribble, S. L., et al., 2009. Tcf3 inhibits spinal cord neurogenesis by regulating sox4a expression. Development. 136, 781-9.

Habas, R., Dawid, I. B., 2005. Dishevelled and Wnt signaling: is the nucleus the final frontier? J Biol. 4, 2.

Habas, R., et al., 2003. Coactivation of Rac and Rho by Wnt/Frizzled signaling is required for vertebrate gastrulation. Genes Dev. 17, 295-309.

Hamann, S., et al., 1998. Aquaporins in complex tissues: distribution of aquaporins 1-5 in human and rat eye. Am J Physiol. 274, C1332-45.

Hari, L., et al., 2002. Lineage-specific requirements of beta-catenin in neural crest development. J Cell Biol. 159, 867-80.

He, X., et al., 2004. LDL receptor-related proteins 5 and 6 in Wnt/beta-catenin signaling: arrows point the way. Development. 131, 1663-77.

Hecht, A., et al., 2000. The p300/CBP acetyltransferases function as transcriptional coactivators of beta-catenin in vertebrates. EMBO J. 19, 1839-50.

Hoekstra, H. E., 2006. Genetics, development and evolution of adaptive pigmentation in vertebrates. Heredity. 97, 222-34.

Holland, L. Z., Gibson-Brown, J. J., 2003. The Ciona intestinalis genome: when the constraints are off. Bioessays. 25, 529-32.

Holland, P. W., et al., 1994. Gene duplications and the origins of vertebrate development. Dev Suppl. 125-33.

Hollenhorst, P. C., et al., 2004. Expression profiles frame the promoter specificity dilemma of the ETS family of transcription factors. Nucleic Acids Res. 32, 5693-702.

Horie, T., et al., 2005. Structure of ocellus photoreceptors in the ascidian Ciona intestinalis larva as revealed by an anti-arrestin antibody. J Neurobiol. 65, 241-50.

Horie, T., et al., 2008. Pigmented and nonpigmented ocelli in the brain vesicle of the ascidian larva. J Comp Neurol. 509, 88-102.

Hou, L., et al., 2000. Signaling and transcriptional regulation in the neural crest-derived melanocyte lineage: interactions between KIT and MITF. Development. 127, 5379-89.

Houston, D. W., et al., 2002. Repression of organizer genes in dorsal and ventral Xenopus cells mediated by maternal XTcf3. Development. 129, 4015-25.

Howard, M. L., Davidson, E. H., 2004. cis-Regulatory control circuits in development. Dev Biol. 271, 109-18.

Huang, L., et al., 2000. Involvement of Tcf/Lef in establishing cell types along the animal-vegetal axis of sea urchins. Dev Genes Evol. 210, 73-81.

Hudson, C., et al., 2003. A conserved role for the MEK signalling pathway in neural tissue specification and posteriorisation in the invertebrate chordate, the ascidian Ciona intestinalis. Development. 130, 147-59.

Hurlstone, A., Clevers, H., 2002. T-cell factors: turn-ons and turn-offs. EMBO J. 21, 2303-11.

Imai, K. S., et al., 2004. Gene expression profiles of transcription factors and signaling molecules in the ascidian embryo: towards a comprehensive understanding of gene networks. Development. 131, 4047-58.

Imai, K. S., et al., 2002. An essential role of a FoxD gene in notochord induction in Ciona embryos. Development. 129, 3441-53.

Irvine, S. Q., et al., 2008. Cis-regulatory organization of the Pax6 gene in the ascidian Ciona intestinalis. Dev Biol. 317, 649-659.

Jeffery, G., 1997. The albino retina: an abnormality that provides insight into normal retinal development. Trends Neurosci. 20, 165-9.

Jiao, Z., et al., 2004. Direct interaction of Sox10 with the promoter of murine Dopachrome Tautomerase (Dct) and synergistic activation of Dct expression with Mitf. Pigment Cell Res. 17, 352-62.

Jin, E. J., et al., 2001a. Wnt and BMP Signaling Govern Lineage Segregation of Melanocytes in the Avian Embryo. Dev. Biol. 233, 22–37.

Jin, Z., et al., 2001b. Adenomatous polyposis coli (APC) gene promoter hypermethylation in primary breast cancers. Br J Cancer. 85, 69-73.

Kim, C. H., et al., 2000. Repressor activity of Headless/Tcf3 is essential for vertebrate head formation. Nature. 407, 913-6.

Kim, G. J., Nishida, H., 2001. Role of the FGF and MEK signaling pathway in the ascidian embryo. Dev Growth Differ. 43, 521-33.

Klempnauer, K. H., Bishop, J. M., 1984. Neoplastic transformation by E26 leukemia virus is mediated by a single protein containing domains of gag and myb genes. J Virol. 50, 280-3.

Kuhl, M., et al., 2000. The Wnt/Ca2+ pathway: a new vertebrate Wnt signaling pathway takes shape. Trends Genet. 16, 279-83.

Kunz, M., et al., 2004. Autoregulation of canonical Wnt signaling controls midbrain development. Dev Biol. 273, 390-401.

Kusakabe, T., et al., 2001. Ci-opsin1, a vertebrate-type opsin gene, expressed in the larval ocellus of the ascidian Ciona intestinalis. FEBS Lett. 506, 69-72.

Kusakabe, T., Tsuda, M., 2007. Photoreceptive systems in ascidians. Photochem Photobiol. 83, 248-52.

Lang, D., et al., 2005. Pax3 functions at a nodal point in melanocyte stem cell differentiation. Nature. 433, 884-887.

Lemaire, P., 2009. Unfolding a chordate developmental program, one cell at a time: invariant cell lineages, short-range inductions and evolutionary plasticity in ascidians. Dev Biol. 332, 48-60.

Lemaire, P., et al., 2008. Ascidians and the plasticity of the chordate developmental program. Curr Biol. 18, R620-31.

Leong, K., et al., 1988. Factors responsible for the higher transcriptional activity of extracts of adenovirus-infected cells fractionate with the TATA box transcription factor. Mol Cell Biol. 8, 1765-74.

Leprince, D., et al., 1983. A putative second cell-derived oncogene of the avian leukaemia retrovirus E26. Nature. 306, 395-7.

Letunic, I., et al., 2006. SMART 5: domains in the context of genomes and networks. Nucleic Acids Res. 34, D257-60.

Lewis, J. L., et al., 2004a. Reiterated Wnt signaling during zebrafish neural crest development. Development. 131, 1299-1308.

Lewis, J. L., et al., 2004b. Reiterated Wnt signaling during zebrafish neural crest development. Development. 131, 1299-308.

Lewis, K. E., Eisen, J. S., 2004. Paraxial mesoderm specifies zebrafish primary motoneuron subtype identity. Development. 131, 891-902.

Li, L., et al., 1999a. Axin and Fratl interact with dvl and GSK, bridging Dvl to GSK in Wnt-mediated regulation of LEF-1. EMBO J. 18, 4233-40.

Li, L., et al., 1999b. Dishevelled proteins lead to two signaling pathways. Regulation of LEF-1 and c-Jun N-terminal kinase in mammalian cells. J Biol Chem. 274, 129-34.

Li, R., et al., 2000. Regulation of Ets function by protein - protein interactions. Oncogene. 19, 6514-23.

Liu, C., et al., 2002. Control of beta-catenin phosphorylation/degradation by a dual-kinase mechanism. Cell. 108, 837-47.

Liu, F., et al., 2005. Distinct roles for Xenopus Tcf/Lef genes in mediating specific responses to Wnt/beta-catenin signalling in mesoderm development. Development. 132, 5375-85.

Liu, H., et al., 2006. Mapping canonical Wnt signaling in the developing and adult retina. Invest Ophthalmol Vis Sci. 47, 5088-97.

Ludwig, A., et al., 2004. Melanocyte-specific expression of dopachrome tautomerase is dependent on synergistic gene activation by the Sox10 and Mitf transcription factors. FEBS Lett. 556, 236-44.

Marks, M. S., Seabra, M. C., 2001. The melanosome: membrane dynamics in black and white. Nat Rev Mol Cell Biol. 2, 738-48.

Marmor, M. F., 1999. Mechanisms of fluid accumulation in retinal edema. Doc Ophthalmol. 97, 239-49.

Martinez-Morales, J. R., et al., 2004. Eye development: a view from the retina pigmented epithelium. Bioessays. 26, 766-77.

Mavrothalassitis, G., Ghysdael, J., 2000. Proteins of the ETS family with transcriptional repressor activity. Oncogene. 19, 6524-32.

Mayor, C., et al., 2000. VISTA : visualizing global DNA sequence alignments of arbitrary length. Bioinformatics. 16, 1046-7.

Meneghini, M. D., et al., 1999. MAP kinase and Wnt pathways converge to downregulate an HMG-domain repressor in Caenorhabditis elegans. Nature. 399, 793-7.

Merrill, B. J., et al., 2004. Tcf3: a transcriptional regulator of axis induction in the early embryo. Development. 131, 263-74.

Miller, J. R., et al., 1999. Mechanism and function of signal transduction by the Wnt/beta-catenin and Wnt/Ca2+ pathways. Oncogene. 18, 7860-72.

Miller, S. S., Edelman, J. L., 1990. Active ion transport pathways in the bovine retinal pigment epithelium. J Physiol. 424, 283-300.

Minokawa, T., et al., 2005. cis-Regulatory inputs of the wnt8 gene in the sea urchin endomesoderm network. Dev Biol. 288, 545-58.

Minokawa, T., et al., 2001. Binary specification of nerve cord and notochord cell fates in ascidian embryos. Development. 128, 2007-17.

Miya, T., et al., 1997. Functional analysis of an ascidian homologue of vertebrate Bmp-2/Bmp-4 suggests its role in the inhibition of neural fate specification. Development. 124, 5149-59.

Miya, T., Nishida, H., 2003. An Ets transcription factor, HrEts, is target of FGF signaling and involved in induction of notochord, mesenchyme, and brain in ascidian embryos. Dev Biol. 261, 25-38.

Molenaar, M., et al., 1996. XTcf-3 transcription factor mediates beta-catenin-induced axis formation in Xenopus embryos. Cell. 86, 391-9.

Mollaaghababa, R., Pavan, W. J., 2003. The importance of having your SOX on: role of SOX10 in the development of neural crest-derived melanocytes and glia. Oncogene. 22, 3024-34.

Moody, R., et al., 1999. Isolation of developmental mutants of the ascidian Ciona savignyi. Mol Gen Genet. 262, 199-206.

Mosimann, C., et al., 2009. Beta-catenin hits chromatin: regulation of Wnt target gene activation. Nat Rev Mol Cell Biol. 10, 276-86.

Munro, E., et al., 2006. Cellular morphogenesis in ascidians: how to shape a simple tadpole. Curr Opin Genet Dev. 16, 399-405.

Murisier, F., Beermann, F., 2006. Genetics of pigment cells: lessons from the tyrosinase gene family. Histol Histopathol. 21, 567-78.

Nakagawa, M., et al., 2002. Ascidian arrestin (Ci-arr), the origin of the visual and nonvisual arrestins of vertebrate. Eur J Biochem. 269, 5112-5118.

Nakatani, Y., et al., 1999. Mutations affecting tail and notochord development in the ascidian Ciona savignyi. Development. 126, 3293-301.

Nicol, D., Meinertzhagen, I. A., 1988. Development of the central nervous system of the larva of the ascidian, Ciona intestinalis L. II. Neural plate morphogenesis and cell lineages during neurulation. Dev Biol. 130, 737-66.

Nishida, H., 1987. Cell lineage analysis in ascidian embryos by intracellular injection of a tracer enzyme. III. Up to the tissue restricted stage. Dev Biol. 121, 526-41.

Nishida, H., Satoh, N., 1983. Cell lineage analysis in ascidian embryos by intracellular injection of a tracer enzyme. I. Up to the eight-cell stage. Dev Biol. 99, 382-94.

Nishida, H., Satoh, N., 1985. Cell lineage analysis in ascidian embryos by intracellular injection of a tracer enzyme. II. The 16- and 32-cell stages. Dev Biol. 110, 440-54.

Nishida, H., Satoh, N., 1989. Determination and regulation in the pigment cell lineage of the ascidian embryo. Dev Biol. 132, 355-67.

Nishiyama, A., Fujiwara, S., 2008. RNA interference by expressing short hairpin RNA in the Ciona intestinalis embryo. Dev Growth Differ. 50, 521-9.

Oikawa, T., Yamada, T., 2003. Molecular biology of the Ets family of transcription factors. Gene. 303, 11-34.

Okada, T., et al., 1997. Distinct neuronal lineages of the ascidian embryo revealed by expression of a sodium channel gene. Dev Biol. 190, 257-72.

Ortolani, G., et al., 1979. Trypsin-induced cell surface changes in ascidian embryonic cells: regulation of differentiation of a tissue-specific protein. Exp Cell Res. 122, 137-47.

Parks, C. L., et al., 1988. Organization of the transcriptional control region of the E1b gene of adenovirus type 5. J Virol. 62, 54-67.

Pasini, A., et al., 2006. Formation of the ascidian epidermal sensory neurons: insights into the origin of the chordate peripheral nervous system. PLoS Biol. 4, e225.

Plickert, G., et al., 2006. Wnt signaling in hydroid development: formation of the primary body axis in embryogenesis and its subsequent patterning. Dev Biol. 298, 368-78.

Polakis, P., 2000. Wnt signaling and cancer. Genes Dev. 14, 1837-51.

Putnam, N. H., et al., 2008. The amphioxus genome and the evolution of the chordate karyotype. Nature. 453, 1064-71.

Remy, P., Baltzinger, M., 2000. The Ets-transcription factor family in embryonic development: lessons from the amphibian and bird. Oncogene. 19, 6417-31.

Reya, T., Clevers, H., 2005. Wnt signalling in stem cells and cancer. Nature. 434, 843-50.

Roel, G., et al., 2002. Lef-1 and Tcf-3 transcription factors mediate tissue-specific Wnt signaling during Xenopus development. Curr Biol. 12, 1941-5.

Rothbacher, U., et al., 2007. A combinatorial code of maternal GATA, Ets and beta-catenin-TCF transcription factors specifies and patterns the early ascidian ectoderm. Development. 134, 4023-32.

Saitou, N., Nei, M., 1987. The neighbor-joining method: a new method for reconstructing phylogenetic trees. Mol Biol Evol. 4, 406-25.

Sakurai, D., et al., 2004. The role of pigment cells in the brain of ascidian larva. J Comp Neurol. 475, 70-82.

Saneyoshi, T., et al., 2002. The Wnt/calcium pathway activates NF-AT and promotes ventral cell fate in Xenopus embryos. Nature. 417, 295-9.

Sato, S., Yamamoto, H., 2001. Development of pigment cells in the brain of ascidian tadpole larvae: insights into the origins of vertebrate pigment cells. Pigment Cell Res. 14, 428-36.

Satoh, N., 2001. Ascidian embryos as a model system to analyze expression and function of developmental genes. Differentiation. 68, 1-12.

Satoh, N., et al., 2003. Ciona intestinalis: an emerging model for whole-genome analyses. Trends Genet. 19, 376-81.

Satou, Y., Satoh, N., 1999. Developmental gene activities in ascidian embryos. Curr Opin Genet Dev. 9, 542-7.

Schmidt, C., Patel, K., 2005. Wnts and the neural crest. Anat Embryol (Berl). 209, 349-55.

Schultz, J., et al., 1998. SMART, a simple modular architecture research tool: identification of signaling domains. Proc Natl Acad Sci U S A. 95, 5857-64.

Schweizer, L., et al., 2003. Requirement for Pangolin/dTCF in Drosophila Wingless signaling. Proc Natl Acad Sci U S A. 100, 5846-51.

Sehgal, R., et al., 2009. BMP7 and SHH regulate Pax2 in mouse retinal astrocytes by relieving TLX repression. Dev Biol. 332, 429-43.

Seo, H. C., et al., 2001. Miniature genome in the marine chordate Oikopleura dioica. Science. 294, 2506.

Sharrocks, A. D., 2001. The ETS-domain transcription factor family. Nat Rev Mol Cell Biol. 2, 827-37.

Sheldahl, L. C., et al., 2003. Dishevelled activates Ca2+ flux, PKC, and CamKII in vertebrate embryos. J Cell Biol. 161, 769-77.

Shimeld, S. M., et al., 2005. Urochordate betagamma-crystallin and the evolutionary origin of the vertebrate eye lens. Curr Biol. 15, 1684-9.

Sodergren, E., et al., 2006. The genome of the sea urchin Strongylocentrotus purpuratus. Science. 314, 941-52.

Sordino, P., et al., 2008. Natural variation of model mutant phenotypes in Ciona intestinalis. PLoS One. 3, e2344.

Sordino, P., et al., 2001. Developmental genetics in primitive chordates. Philos Trans R Soc Lond B Biol Sci. 356, 1573-82.

Spagnuolo, A., et al., 2003. Unusual number and genomic organization of Hox genes in the tunicate Ciona intestinalis. Gene. 309, 71-9.

Steel, K. P., Barkway, C., 1989. Another role for melanocytes: their importance for normal stria vascularis development in the mammalian inner ear. Development. 107, 453-63.

Steinberg, R. H., 1985. Interactions between the retinal pigment epithelium and the neural retina. Doc Ophthalmol. 60, 327-46.

Sturm, R. A., et al., 1995. Chromosomal structure of the human TYRP1 and TYRP2 loci and comparison of the tyrosinase-related protein gene family. Genomics. 29, 24-34.

Szebenyi, G., Fallon, J. F., 1999. Fibroblast growth factors as multifunctional signaling factors. Int Rev Cytol. 185, 45-106.

Takada, S., et al., 1994. Wnt-3a regulates somite and tailbud formation in the mouse embryo. Genes Dev. 8, 174-89.

Takahashi, H., et al., 1999. Evolutionary alterations of the minimal promoter for notochord-specific Brachyury expression in ascidian embryos. Development. 126, 3725-34.

Takeda, K., et al., 2000. Induction of melanocyte-specific microphthalmia-associated transcription factor by Wnt-3a. J Biol Chem. 275, 14013-6.

Takemaru, K. I., Moon, R. T., 2000. The transcriptional coactivator CBP interacts with beta-catenin to activate gene expression. J Cell Biol. 149, 249-54.

Thompson, J. D., et al., 1994. CLUSTAL W: improving the sensitivity of progressive multiple sequence alignment through sequence weighting, position-specific gap penalties and weight matrix choice. Nucleic Acids Res. 22, 4673-80.

Tolwinski, N. S., et al., 2003. Wg/Wnt signal can be transmitted through arrow/LRP5,6 and Axin independently of Zw3/Gsk3beta activity. Dev Cell. 4, 407-18.

Travis, A., et al., 1991. LEF-1, a gene encoding a lymphoid-specific protein with an HMG domain, regulates T-cell receptor alpha enhancer function [corrected]. Genes Dev. 5, 880-94.

Tsuda, M., et al., 2003. Direct evidence for the role of pigment cells in the brain of ascidian larvae by laser ablation. J Exp Biol. 206, 1409-17.

van Beest, M., et al., 2000. Sequence-specific high mobility group box factors recognize 10-12-base pair minor groove motifs. J Biol Chem. 275, 27266-73.

Van de Wetering, M., et al., 1996. Extensive alternative splicing and dual promoter usage generate Tcf-1 protein isoforms with differential transcription control properties. Mol Cell Biol. 16, 745-52.

van de Wetering, M., et al., 1997. Armadillo coactivates transcription driven by the product of the Drosophila segment polarity gene dTCF. Cell. 88, 789-99.

van de Wetering, M., et al., 1991. Identification and cloning of TCF-1, a T lymphocyte-specific transcription factor containing a sequence-specific HMG box. EMBO J. 10, 123-32.

van Noort, M., Clevers, H., 2002. TCF transcription factors, mediators of Wnt-signaling in development and cancer. Dev Biol. 244, 1-8.

Vinson, J. P., et al., 2005. Assembly of polymorphic genomes: algorithms and application to Ciona savignyi. Genome Res. 15, 1127-35.

Wada, H., et al., 1998. Tripartite organization of the ancestral chordate brain and the antiquity of placodes: insights from ascidian Pax-2/5/8, Hox and Otx genes. Development. 125, 1113-22.

Wada, H., Satoh, N., 2001. Patterning the protochordate neural tube. Curr Opin Neurobiol. 11, 16-21.

Wallingford, J. B., Habas, R., 2005. The developmental biology of Dishevelled: an enigmatic protein governing cell fate and cell polarity. Development. 132, 4421-36.

Wasylyk, B., et al., 1998. Ets transcription factors: nuclear effectors of the Ras-MAP-kinase signaling pathway. Trends Biochem Sci. 23, 213-6.

Waterman, M. L., et al., 1991. A thymus-specific member of the HMG protein family regulates the human T cell receptor C alpha enhancer. Genes Dev. 5, 656-69.

Wegner, M., 2005. Secrets to a healthy Sox life: lessons for melanocytes. Pigment Cell Res. 18, 74-85.

Weiser, D. C., et al., 2007. Gravin regulates mesodermal cell behavior changes required for axis elongation during zebrafish gastrulation. Genes Dev. 21, 1559-71.

Westenskow, P., et al., 2009. Beta-catenin controls differentiation of the retinal pigment epithelium in the mouse optic cup by regulating Mitf and Otx2 expression. Development. 136, 2505-10.

Widlund, H. R., et al., 2002. Beta-catenin-induced melanoma growth requires the downstream target Microphthalmia-associated transcription factor. J Cell Biol. 158, 1079-87.

Winklbauer, R., et al., 2001. Frizzled-7 signalling controls tissue separation during Xenopus gastrulation. Nature. 413, 856-60.

Wodarz, A., Nusse, R., 1998. Mechanisms of Wnt signaling in development. Annu Rev Cell Dev Biol. 14, 59-88.

Wong, M. L., Medrano, J. F., 2005. Real-time PCR for mRNA quantitation. Biotechniques. 39, 75-85.

Woods, D. B., et al., 1992. Identification of nucleotide preferences in DNA sequences recognised specifically by c-Ets-1 protein. Nucleic Acids Res. 20, 699-704.

Yagi, K., et al., 2003. A genomewide survey of developmentally relevant genes in Ciona intestinalis. III. Genes for Fox, ETS, nuclear receptors and NFkappaB. Dev Genes Evol. 213, 235-44.

Yajima, I., et al., 2003. Cloning and functional analysis of ascidian Mitf in vivo: insights into the origin of vertebrate pigment cells. Mech Dev. 120, 1489-504.

Yasumoto, K., et al., 1997. Functional analysis of microphthalmia-associated transcription factor in pigment cell-specific transcription of the human tyrosinase family genes. J Biol Chem. 272, 503-9.

Yasuo, H., Satoh, N., 1993. Function of vertebrate T gene. Nature. 364, 582-3.

Yi, F., Merrill, B. J., 2007. Stem cells and TCF proteins: a role for beta-catenin--independent functions. Stem Cell Rev. 3, 39-48.

Yordy, J. S., Muise-Helmericks, R. C., 2000. Signal transduction and the Ets family of transcription factors. Oncogene. 19, 6503-13.

Zhang, H., Levine, M., 1999. Groucho and dCtBP mediate separate pathways of transcriptional repression in the Drosophila embryo. Proc Natl Acad Sci U S A. 96, 535-40.

Zorn, A. M., et al., 1999. Regulation of Wnt signaling by Sox proteins: XSox17 alpha/beta and XSox3 physically interact with beta-catenin. Mol Cell. 4, 487-98.

Zuasti, A., et al., 1998. The melanogenic system of Xenopus laevis. Arch Histol Cytol. 61, 305-16.

ACKNOWLEDGEMENTS

I am extremely grateful to Almighty Allah for his blessings throughout my life.

I would like to express my gratitude to my director of studies, Dr. Antonietta Spagnuolo, for her valuable advice, continuous cooperation and assistance in guiding me through out the research work.

I would like to acknowledge Dr. Detlev Arendt for his valuable discussions and suggestions during my PhD study.

I would like to thank Dr. Filomena Ristoratore for sharing some precious constructs and for her valuable advice. Special thanks to Dr. Margherita Branno, the chief of my laboratory for her help and useful discussions. I would also like to acknowledge Dr. Laura Zanetti for her suggestions and discussions.

I acknowledge Dr. Euan Brown for his continuous encouragement and support.

I acknowledge the useful technical assistance of in situ service as well as the Molecular Biology Service of Stazione Zoologica for their technical support for qPCR and Sequencing.

I would also like to thank all the past and present members of the Cellular and Developmental Biology laboratory for their friendship and stimulating discussions specially Enrico D'Aniello. I appreciate the warm friendship of Leopoldo Staiano and Rosaria Esposito. I also thank them for accompaning me during the last year of my study. I am also grateful to Luisa Berna for her help.

I would like to thank my family, psrticularly my parents for their love, encouragement and support. Finally I thank my husband for his support, help and useful discussions.